Semi-automated Ribosome Display for High-Throughput DARPin Binder Selection

Andri Häfliger, Sylvie Briand-Schumacher, Sven Furler, Birgit Dreier, Andreas Plückthun

PII: S1871-6784(26)00082-8

DOI: https://doi.org/10.1016/j.nbt.2026.06.007

Reference: NBT1734

To appear in: *New BIOTECHNOLOGY*

Received date: 15 February 2026
Revised date: 19 June 2026
Accepted date: 25 June 2026

Please cite this article as: Andri Häfliger, Sylvie Briand-Schumacher, Sven Furler, Birgit Dreier and Andreas Plückthun, Semi-automated Ribosome Display for High-Throughput DARPin Binder Selection, *New BIOTECHNOLOGY,* (2026) doi:https://doi.org/10.1016/j.nbt.2026.06.007

Semi-automated Ribosome Display for High-Throughput DARPin Binder Selection

Andri Häfliger[1], Sylvie Briand-Schumacher[1], Sven Furler, Birgit Dreier, and Andreas Plückthun*

Dept. of Biochemistry, University of Zurich, Winterthurerstr. 190, 8057 Zurich, Switzerland

*Corresponding author
Email: plueckthun@bioc.uzh.ch
Tel: +41 44 635 5570

[1]These authors contributed equally

Abstract

The combination of the Designed Ankyrin Repeat Protein (DARPin) scaffold with the selection and evolution technology of Ribosome Display has generated a wide range of specific binders to hundreds of target proteins. The binders have been used in a very diverse set of applications, from research through diagnostics to therapy. In this article, we focus on the high-throughput (HT) methods that we have developed for this purpose, which have been applied in many selections for research applications, but have never been explained in detail. We describe here the HT methods used to select for many targets in parallel, permitting the use of even different buffers and components, as well as some of the downstream characterization. To illustrate the workflow, we summarize the properties of some of the binders so obtained and their applications as well as the structures of the DARPin/target complexes. Together, these HT methods establish a robust framework for the rapid discovery and characterization of DARPins across a broad spectrum of targets.

Keywords:
Designed Ankyrin Repeat Proteins; DARPins; Ribosome Display; high-throughput, selections; high-throughput screening; protein engineering; in vitro translation; errorprone, PCR; protein libraries; synthetic libraries; scaffolds; off-rate selection

Introduction

The emergence of non-antibody scaffolds has greatly extended the options in therapy, diagnostics and research. The common goal in all of these endeavors is to generate very specific binders of high affinity. To achieve this goal, a scaffold is needed that not only equals antibodies in these properties, but also adds features that antibodies do not automatically have, such as robustness of the molecule against aggregation, rigidity to facilitate structure determination of complexes with the target, and facile engineering of fusions and chemical conjugates of all kinds. Additionally, a scaffold that can be expressed in the cytoplasm of all cells and does not carry any cysteines offers a great advantage. The Designed Ankyrin Repeat Proteins (DARPins) provide such a scaffold [1].

DARPins have been shown to work well in many applications [1-4] (cf. the Results section) and are in clinical trials [5]. Other non-antibody scaffolds have been developed as well by now, and these have been reviewed elsewhere [2, 3, 6-9]. While this article details, for the first time, the high-throughput methods with which these DARPins have been obtained and also summarizes their properties and applications, it is likely that these methods can also be applied to other scaffolds.

In addition to a suitable scaffold, the second component needed is a technology for efficiently generating specific binders against many very diverse targets. We summarize here selection and evolution from synthetic libraries. While there is great progress in generating binders de novo [10-15], at the time of writing, the de novo binders have not routinely shown picomolar equilibrium dissociation constants without subsequent experimental affinity maturation [16, 17], nor are the required high specificity and avoidance of cross-reactivity directly implemented — and this includes cross-reactivity against homologs or completely adventitious components. Briefly, generative methods output coordinates and confidence measures [18], but affinity is a free-energy difference between two solvated ensembles, i.e., the solvated complex relative to the dissociated, fully hydrated partners. Interface geometry captures, at best, the enthalpic shape- and electrostatic-complementarity of the contact surface. It is structurally blind to three quantities that dominate the entropic and desolvation terms: interfacial water reorganization [19-21], configurational (residual) entropy [22, 23], and the free energy of the unbound state. Undoubtedly, generative methods are developing rapidly, but especially method development in free energy calculations [24, 25] will have a decisive impact in this field in the future.

Therefore, the selection from synthetic libraries has remained an established method to arrive at molecules with the desired properties. Many selection systems have been developed over the years [26-28] (see Discussion). A particularly powerful one is Ribosome Display [29], as it combines several advantageous features: (i) the capacity to handle very large libraries, since

it avoids the transformation of any cells which typically restricts the library size and (ii) the natural integration with error-prone PCR. It is thus not only a selection method, but also a true in vitro directed evolution technology for proteins. A defining characteristic of Ribosome Display, in contrast to most other selection approaches [29], is the direct integration of PCR into the workflow. This feature enables straightforward diversification ("randomization") steps without the need to clone and transform a new library. As a result, Ribosome Display permits not only the refinement and affinity maturation of existing binders, but also the evolution of the entire population during selection from highly diverse and complex libraries.

The above technological components have themselves gradually evolved over almost three decades. At earlier stages, we have described the manual conduct of individual Ribosome Display rounds for individual targets in several methods papers [30-34]. In the course of these developments, an ever-increasing number of targets have been tackled for many different scientific purposes, requiring the generation of ever more specific DARPins. To permit these developments, over the last 10-15 years, we have developed a high-throughput (HT) pipeline for the generation of specific binders. While many recently published DARPin binders have already been the result of this HT pipeline [35-62], the HT methods themselves have never been published in experimental detail. Here, we summarize our technologies for the HT generation of DARPins in the Methods section. We describe in the Results section the properties and application examples of these binders, which may serve as an indication of what is possible with these technologies, which combine the DARPin framework with the high-throughput Ribosome Display technology.

Results obtained with HT-generated binders

General remarks

We summarize in this Review section examples of DARPin binders that have been obtained using the high-throughput (HT) Ribosome Display procedures that are detailed in the Methods section. We group the targets according to the main motivation in the various projects (**Figure 1**), but in almost all cases the studies had more than one objective. For example, in many cases crystal or cryo-EM structures were obtained, even though this was not the main objective.

In the course of this work, DARPins were expressed in many compartments of many cell types, illustrating the versatility of the technology and the robustness of the framework. We should point out that we limit this overview to DARPins that have been obtained by the HT workflow, and of course many different formats and/or fusion proteins of DARPins had been developed before [1]. These will not be reviewed here.

Approaches toward new therapeutic modalities

TBXT (Brachyury). DARPins can function intracellularly and in the nucleus, and they have been successfully used to counteract a tumor-causing transcription factor. TBXT (T-box transcription factor T, the product of the *brachyury* gene) is a transcription factor crucial for embryonic development, particularly the formation of the notochord and the axial skeleton. TBXT is minimally expressed in healthy adult tissues, but it appears to be a key driver of chordoma cells, a rare, slow-growing, malignant tumor that develops from remnants of the embryonic notochord, most commonly in the skull base or sacrum (lower spine). DARPins, utilizing the HT platform described here, were developed that block binding of TBXT to DNA [61], and these DARPins suppressed proliferation, impaired spheroid growth, and reduced tumor burden, while also promoting features associated with senescence and cellular differentiation. These DARPins already helped to disrupt and thereby define the regulatory network of TBXT, suggesting potential therapeutic vulnerabilities that merit further investigation in clinical settings, and the DARPins may eventually be developed into drugs themselves [61].

Fibroblast activation protein (FAP). The biological role of FAP is described further below, and it was used as a target for a gene delivery system. Systemic application of highly active therapeutic proteins is often still restricted, remains challenging, largely because toxic side effects at effective doses and unintended activity in non-target tissues often limit their clinical use. An alternative strategy with great potential is to provide the genes for the effector proteins

directly to the target cells, so the proteins can be produced locally using delivery tools such as engineered viral vectors.

In earlier work, we established a modular, protein-based platform for detargeting and retargeting adenovirus type 5 (Ad5) vectors. This system consists of two functional components. The first is a bispecific DARPin adapter that binds trivalently to the fiber knob, blocking its interaction with the coxsackievirus and adenovirus receptor (CAR) and thereby reducing native cell entry, while at the same time enabling redirection to selected cell types through the attachment of appropriate targeting domains. The second component is a trimeric shield, derived from a humanized hexon-binding single-chain variable fragment of an antibody (scFv), which limits unwanted interactions with host factors responsible for the vector's natural liver accumulation. In addition, this shield reduces immune recognition of the vector, addressing another major obstacle—namely, the high prevalence of pre-existing neutralizing antibodies against adenovirus in humans [45].

Using the high-throughput DARPin selection platform described here, adapters directed against fibroblast activation protein (FAP) were obtained [45], a cell-surface marker strongly expressed on cancer-associated fibroblasts (CAFs). FAP is a membrane-anchored serine protease that is mainly produced by activated fibroblasts during processes such as tissue remodeling, wound repair, fibrotic responses, and tumor development. Targeting this population enabled efficient delivery in vivo and local production of a therapeutic payload by CAFs within the tumor microenvironment (TME), which in turn led to a reduction in tumor growth. While the payload (in this case, a therapeutic antibody) acts on tumor cells, converting CAFs into a "biofactory" instead of the tumor cells themselves ensures that the therapeutic protein does not destroy the factory [45].

HIV. Broadly neutralizing antibodies for HIV have remained rare, difficult to generate, and are still quite elusive in vaccination attempts. The V3 loop of the HIV-1 envelope (Env) glycoprotein provokes a strong antibody response, although most of these antibodies target the V3 crown and show limited neutralizing activity. To investigate these mechanisms and to explore alternative strategies for viral neutralization, broadly neutralizing Designed Ankyrin Repeat Proteins (bnDs) were generated using the HT platform described here, achieving a breadth comparable to that of broadly neutralizing antibodies [55]. These molecules bind to the V3 crown and preferentially recognize the open Env conformation that is induced upon CD4 engagement. Their broad activity results from targeting highly conserved residues that become accessible in two different structural states of the V3 loop.

In addition, a separate class of V3-directed inhibitors based on the DARPin technology was identified [41]. These molecules reestablish the CD4-bound conformation as an important neutralization target and reach neutralization breadths exceeding 90%. Unlike other binders,

they interact with V3 only when the envelope adopts the open state, recognizing a four-turn amphipathic α-helix located in the C-terminal portion of the V3 loop. All these DARPins can thus help in the future development of novel therapeutics and prevention strategies.

In an orthogonal approach, the DARPin libraries were used to test the properties of the immunogen necessary for creating broadly neutralizing antibody responses (bnAb) for vaccine development. Using the DARPins as a completely orthogonal framework to antibodies, fundamental features of the immunogen could be elucidated [46].

Approaches to new Diagnostics

VCAM-1. Contrast-enhanced ultrasound molecular imaging (CEUMI) represents an emerging approach with potential for early diagnosis and risk assessment in diseases such as atherosclerosis and cancer. For successful clinical implementation, the technology requires binders that can be produced, modified, and coupled in a straightforward manner, while remaining suitable for in vivo applications. To this end, targeted microbubbles (MBs) were generated with DARPins directed against vascular cell adhesion molecule 1 (VCAM-1), an endothelial adhesion protein that plays a central role in inflammatory responses [56]. The microbubbles consist of a phospholipid shell, to which cysteine-tagged DARPins are attached through maleimide coupling. In a murine model of hind-limb inflammation, in vivo ultrasound molecular imaging revealed signal increases of up to fourfold for targeted microbubbles incorporating three of the five tested DARPins, compared with control particles [56]. While this research is still in an early stage, it shows yet another application of DARPins with diagnostic potential.

PSA. Advanced prostate cancer (PCa) continues to pose a major clinical challenge because tumors frequently develop resistance to standard chemotherapy and eventually progress to hormone-independent, therapy-refractory disease. For early detection, both prostate-specific membrane antigen (PSMA) and the circulating biomarker prostate-specific antigen (PSA) are commonly used; however, additional complementary approaches are needed to more precisely monitor disease progression. One such strategy is the non-invasive PET imaging of free PSA within PCa lesions. To enable this, DARPins with high specificity for PSA were identified and modified at a single C-terminal cysteine by attachment of the hexadentate chelator NODAGA, allowing radiolabeling with the positron-emitting isotope ^{68}Ga [47]. In vivo distribution studies in athymic nude mice carrying subcutaneous prostate cancer xenografts showed selective tumor accumulation, indicating their potential for tracking responses to androgen receptor (AR)-targeted treatments [47].

Biosensors

Biosensors for fibrin degradation products. DARPins can be used in biosensors, as they can be fused to almost any protein, and since they can be expressed in many formats. Using expression on the surface of mammalian cells, synthetic receptors were constructed that trigger the signal transducer and activator of transcription 3 (STAT3) transcription factor pathway and can thus act as an in vivo sensor [54]. It is of particular interest to create heterodimeric constructs, where either different binders are fused to the erythropoietin receptor (EpoR) extracellular domain, creating a heterodimeric assembly, or two binders are fused in tandem [54]. For proof of concept, binders directed against human fibrin degradation products (FDPs) were employed as components of cellular sensors designed to detect coagulation-related events. In this setting, several DARPins functioned effectively in combination with scFv fragments targeting a distinct epitope, which increased overall specificity. Engineered cell lines were created that sense pathological levels of FDPs and respond by producing both a reporter molecule and a therapeutic anti-thrombotic protein [54].

Biosensors for liver damage. To develop in vitro biosensors, a system was developed that goes in a reversible manner from an off-state to an on-state as a consequence of binding an analyte, in these examples mitochondrial aspartate aminotransferase, cytosolic aspartate aminotransferase, and alanine aminotransferase 1, which serve as markers for liver toxicity. Briefly, by creating a chimera of beta-lactamase with calmodulin and a DARPin binder to the target and a separate binder, fused to a calmodulin-binding peptide, the two binders will be brought into proximity by the target, and the ensuing calmodulin-peptide interaction converts the beta-lactamase into an active conformation [39]. The observed enzymatic activity is then proportional to the amount of analyte. The advantage of robust binding units such as DARPins is that they can be generated to many targets of interest, allowing their detection with a suitable dynamic range.

Cellular imaging

Actin. Actin is an evolutionarily conserved protein that is present in nearly all eukaryotic cells. It can shift from its monomeric, globular form (G-actin) to a polymerized, filamentous form (F-actin) through an ATP-dependent process. Numerous actin-binding proteins regulate this transition by promoting nucleation, capping filament ends, or modulating monomer activity. Given actin's wide range of cellular roles, monitoring its dynamic behavior is of considerable interest. To this end, several actin-binding DARPins were generated and expressed in living cells [40]. After fluorescent labeling, these binders localized along actin filaments, but with distinct patterns. Some preferentially marked highly dynamic structures, including filopodia,

lamellipodia, and blebs, whereas others were mainly found in stress fibers. In addition, pharmacological treatments that rapidly halted actin turnover caused a corresponding redistribution of certain DARPins. These findings suggest that such DARPins represent useful tools for visualizing or modulating actin structures in live cells [40].

Myosin VI. Although the actin cytoskeleton is widely regarded as essential for cellular architecture and plasticity, the presence and function of filamentous actin within the nucleus have long been debated. Recent findings, however, have linked nuclear F-actin to pathways involved in genome maintenance. These observations raise the question of whether, and in what manner, myosins — acting as actin-dependent molecular motors — contribute to these processes. Notably, myosin VI is the only myosin known to move toward the minus end of actin filaments and has been associated with multiple steps of transcription. DARPins were engineered to modulate myosin VI levels in specific cellular compartments, which made it possible to demonstrate its direct function within the nucleus [43]. When the DARPin was fused to the ubiquitin ligase RNF4, selective depletion of the cytoplasmic fraction of myosin VI produced little effect on the stabilization of stalled or reversed replication forks. In contrast, reducing the nuclear pool had a pronounced impact on the cellular response to replication stress [43]. These findings underscore the potential of DARPins as tools to control protein abundance in a compartment-specific manner.

Tubulin. We should mention for completeness that tubulin-binding DARPins have also been obtained and used in the studies of tubulin [63-68], still using technologies preceding the developments of the HT methods described here. Therefore, this is not described here in detail.

Fluorescent proteins. Binders to fluorescent proteins are of great interest for imaging, as well as for manipulation of fusions to fluorescent proteins in cells and in vitro. In a first set of experiments using libraries of DARPins with their high stability and diversification (see Methods), binders to GFP were obtained, albeit not yet using the high-throughput system described below [60]. They could be used in vitro, e.g., for large-scale purification of membrane proteins [69], to immobilize proteins for SPR analysis [70], to create scaffolds for host:guest crystallization [71] (see below), or be incorporated in a scaffold to facilitate cryo-EM structures [72]. Having determined the binding mode of different GFP binders, a "clamp" was designed that wraps around GFP [70] and permits binding in the low picomolar range which is nevertheless reversible.

These GFP binders can also be used to create exactly spaced nanodot arrays, that display these GFP clamps. Thereby, receptors can be spaced in an exact pattern and its effect on signaling be studied, as was done for Wnt signaling [73]. Because of the known structure of the DARPin-GFP complex, these DARPins have also been used to develop a technology of fluorogenic probes which massively increase their fluorescence upon target binding [74].

Briefly, a cysteine is site-specifically incorporated into the DARPin, which reacts reversibly with silicon-pyronine, quenching its fluorescence. Upon target binding, the target displaces the reversibly bound and tethered silicon-pyronine, leading to a very strong and fast fluorescence increase.

Binders directed against GFP have likewise facilitated the evaluation and optimization of targeted protein degradation through the ubiquitin–proteasome pathway (bioPROTACs) [75, 76]. Using a combination of microinjection and live-cell microscopy, degradation kinetics can be directly monitored at the single-cell level, providing a readout that is independent of degrader uptake or biosynthesis and comparable across different chemical classes. These studies identified the spatial configuration of the complex — specifically, the correct positioning of the substrate for ubiquitination and proteasomal recognition — as the critical determinant of efficient bioPROTAC activity in trans. By contrast, binding affinity and thermodynamic stability had only minor effects [76].

Since DARPins show very high specificity, binders against the related fluorescent proteins monomeric teal fluorescent protein 1 (mTFP1) [58] and mCherry [60] were made as well. All of these have been used not only to label proteins in cells, but also to localize them to different cell compartments, and/or bring cellular proteins to degradation [58, 60].

Functional studies

Respiratory syncytial virus (RSV) phosphoprotein. Respiratory syncytial virus (RSV) is an RNA virus and one of the most common infectious agents in humans. During infection, it forms specialized biomolecular condensates known as viral factories (VFs). Although condensate formation usually requires high local protein concentrations, it has been unclear how sufficient levels are achieved early in infection, given that VFs themselves are needed for efficient viral transcription and replication. To enable this analysis, phosphoprotein (P)-specific DARPins were generated and applied to monitor RSV infection with sensitivity at the level of individual vRNPs, making it possible to determine the spatial and temporal onset of VF formation and its connection to transcription and replication [62]. The results showed that VFs originate from incoming vRNPs rather than forming independently in the cytoplasm. Their nucleation depends on protein–protein interaction networks that are preassembled on vRNPs within the virion, creating so-called pre-replication centers (PRCs). These findings indicate that PRCs formed inside the virion initiate condensate formation immediately after entry into the host cell, helping to explain the observed cell-to-cell variability in RSV infection [62].

p53 family. The p53 protein family—comprising p53, p63, and p73—represents a group of transcription factors that share a conserved domain organization and overlapping DNA-binding

specificities. p53 was originally identified for its pivotal role as a tumor suppressor, but its wider functions include the regulation of cellular responses to stress by regulating genes involved in apoptosis, cell cycle arrest, and DNA repair. p63 as well as p73, discovered subsequently through sequence homology, play essential roles in development, differentiation, and tissue integrity. It is therefore of great interest to develop specific DARPins to each of the family members, and this was achieved [36, 37, 44]. The p53 family proteins are primarily nuclear transcription factors that function by binding to DNA and regulating gene expression. However, their subcellular localization is dynamic and tightly regulated, often involving shuttling between the nucleus and the cytoplasm, and this can vary depending on the specific protein isoform, cell type, and cellular stress conditions.

p53. The tumor suppressor p53 also plays a role in the cellular defense against infections with human papillomavirus (HPV). High-risk HPV strains can drive cancer development in several epithelial tissues. This transformation relies on two viral oncoproteins that disable key cellular control pathways. One of them, E6, forms a complex with an E3 ubiquitin ligase, which then binds p53 and targets it for degradation through the ubiquitin–proteasome system. DARPins have been developed that block this interaction [36], restoring p53-dependent transcriptional activity and thereby counteracting the oncogenic process. These results point to a possible route toward future clinical applications.

p63. DARPins with high specificity for p63 were engineered and applied as intracellular inhibitors to influence its transcriptional activity. By selectively blocking the DNA binding of the ΔNp63α isoform — which competes with p53 for the same promoter regions — p53 activity could be restored. Interestingly, interference with DNA binding also led to increased stability of p63, pointing to a negative feedback mechanism that is controlled at the transcriptional level. In addition, these DARPins proved useful for the selective detection of p63 in cultured cells as well as in primary tissues, making them versatile tools for investigating p63 function [50].

p73. DARPins were also developed to recognize the oligomerization domain and the Sterile Alpha Motif (SAM) domain of the transcription factor p73. In pull-down assays, these binders displayed high specificity for their targets [37]. When fused to the adaptor protein SPOP, which recruits substrates to cullin-3 E3 ubiquitin ligase complexes, they formed a bioPROTAC capable of promoting selective degradation of p73.

Both p63 and p73 control transcriptional programs in epithelial tissues, and many cells in these tissues express the two proteins simultaneously. Members of the p53 protein family function as tetramers in their active state. Although the oligomerization domains of p63 and p73 are highly similar, the corresponding region in p53 is more distinct, preventing it from forming mixed oligomers with the other two proteins. In contrast, p63 and p73 readily assemble into hetero-oligomers with different subunit compositions. Using specific DARPins, it was possible to

demonstrate for the first time the presence of the predicted $p63_2/p73_2$ hetero-tetramer in cells [44]. Notably, this complex was found at elevated levels in squamous cell carcinoma [44].

Histone deacetylase 6 (HDAC6). Ubiquitination is widely known as a signal that marks proteins for degradation (see above), but it also plays roles in innate immunity, regulation of RNA-sensing pathways, and cellular stress responses. When misfolded proteins are not efficiently degraded, they can accumulate together with ubiquitin chains in a perinuclear compartment known as the aggresome. Formation of this structure relies on intracellular transport processes and the activity of histone deacetylase 6 (HDAC6). The zinc finger (ZnF) domain of HDAC6 binds ubiquitin and contributes to influenza A virus infection, as well as to stress-related processes such as the assembly of aggresomes and stress granules. DARPins targeting this ZnF domain were generated and shown to block its interaction with ubiquitin both in vitro and in cells [53]. As a result, infection by influenza A and Zika viruses was reversibly reduced, and the formation of stress granules and aggresomes was diminished. These observations suggest potential applications in future drug discovery efforts [53].

Gephyrin. Gephyrin is a key organizer of inhibitory synapses, and it also plays different roles in neuronal metabolism. It acts as a conserved scaffold protein that assembles into multimers and associates with specific inhibitory synaptic partners. At postsynaptic sites, gephyrin anchors $GABA_A$ receptors opposite presynaptic release zones, thereby ensuring efficient inhibitory signaling. DARPins directed against gephyrin were developed to visualize gephyrin clusters in cultured rat neurons and in mouse brain tissue [49]. Using these binders, clusters could be identified that had previously gone unnoticed. Because the different DARPins recognized gephyrin in distinct ways, they enabled a more comprehensive mapping of its interaction network and revealed new groups of potential binding partners [49]. This work provides a basis for exploring gephyrin functions beyond the synapse.

SUMO from budding yeast (Smt3). SUMOylation is a post-translational modification in eukaryotic cells in which SUMO proteins are covalently linked to target proteins, influencing processes such as gene expression, nuclear transport, and cell division. DARPins were developed against the budding yeast SUMO protein Smt3, and structural analyses showed that they recognize SUMO in a manner distinct from that of natural SUMO-binding partners. Some of these DARPins increased cellular sensitivity to different stress conditions, and a subset was validated as reporters for SUMOylation inside cells [35]. For instance, they revealed a DNA damage–induced SUMOylation response in the nucleus that involved proteins not previously associated with this pathway, likely corresponding to later stages of homologous recombination [35]. These tools therefore make it possible to study SUMOylation dynamics within specific subcellular compartments.

CagI from *Helicobacter pylori*. *Helicobacter pylori* is a widespread bacterial pathogen that colonizes the human stomach, affecting roughly half of the global population. It employs a type IV secretion system to deliver the effector protein CagA into gastric epithelial cells. After entry, CagA associates with the inner surface of the plasma membrane, where it becomes phosphorylated by host kinases and engages numerous signaling proteins, ultimately promoting tumorigenic processes. Although the detailed composition of the secretion pilus is not fully understood, the protein CagI is known to be exposed on the bacterial surface and is essential for pilus assembly. DARPins were developed to target CagI [48]. These binders enabled the determination of crystal structures of CagI complexes and were found to reduce CagA translocation by as much as 65%. As such, CagI-directed DARPins act as effective inhibitors of the secretion machinery, which is an important contributor to gastric cancer risk [48].

Decapentaplegic (Dpp) from *Drosophila*. Morphogen gradients provide positional cues during development by exposing cells to different concentrations of signaling molecules, which in turn influence their fate. Despite their central role, the precise ways in which these gradients regulate tissue patterning and growth are still not fully understood, partly because of the limited tools available to manipulate them directly. In the developing *Drosophila* wing, the morphogen Decapentaplegic (Dpp) is essential for proper patterning and growth. To investigate its function, DARPins were engineered to bind and trap Dpp, thereby preventing both its spread and its signaling activity [57]. Using these tools, it was shown that posterior patterning and growth depend on Dpp dispersal, whereas anterior regions can develop largely without it. These findings challenge the long-standing view that Dpp dispersal is absolutely required to coordinate wing patterning and growth across the entire tissue.

DARPins in structural biology

Botulinum neurotoxin A1. Botulinum neurotoxins (BoNTs) rank among the most potent bacterial protein toxins. They are responsible for botulism, a potentially fatal condition, and have also been considered as biological threat agents. At the same time, BoNTs are widely used as therapeutic proteins for a range of neurological and non-neurological disorders, as well as in cosmetic treatments. DARPins were generated as research tools to investigate the structure and function of botulinum neurotoxin A1 (BoNT/A1) [42]. Structural studies using x-ray crystallography showed that the DARPin F5 inhibits toxin activity by binding near the substrate-recognition site. Interestingly, and in contrast to the in vitro findings, another DARPin accelerated substrate cleavage by BoNT/A1 in primary neurons and muscle tissue, apparently by enhancing toxin translocation. These observations may be relevant for therapeutic

applications in which a rapid onset of toxin activity, together with prolonged effects, is desirable [42].

LRRK2 in Parkinson's disease. Mutations in leucine-rich repeat kinase 2 (LRRK2) represent the most common genetic cause of familial Parkinson's disease. In addition to its kinase domain, LRRK2 contains several other structural elements, including multiple repeat motifs such as armadillo, ankyrin, and leucine-rich repeat domains. Many disease-associated variants display elevated kinase activity, making this enzyme an attractive target for inhibitor development. DARPins selected to bind LRRK2 were used to obtain improved cryo-EM structures at higher resolution [38]. The identified binder provides a useful tool for studying LRRK2 function and malfunction, and it may support the development of new inhibitors, including strategies that target domains such as the fused WD40 region rather than the kinase active site itself [38].

Adenyl cyclase 9. A large number of G protein–coupled receptor (GPCR) signaling pathways involve adenylate cyclases (ACs) to generate second messengers. In mammals, nine membrane-bound AC isoforms have been identified, each with distinct cellular locations, tissue distributions, and physiological roles. AC9 is of particular interest because certain polymorphisms have been linked to conditions such as asthma and heart disease, while the enzyme itself also appears to have cardioprotective functions. However, the structural changes that accompany AC9 activation had remained largely unclear. To address this, DARPins were raised against AC9, and one of these binders was found to act as an activator of the enzyme [52]. Cryo-EM analysis revealed that this DARPin associates with a region that overlaps with the Gα interaction site. The structures further indicated that rearrangements of secondary structure elements near the forskolin-binding pocket are crucial for AC9 activation [52].

Host:guest crystals: Leucinostatin as an example for a peptide structure. DARPins have also been employed in a host–guest strategy as tools to determine the structures of other biomolecules. For this purpose, a fusion construct was designed in which a DARPin is linked to a protein that forms crystals under well-defined conditions. The bacterial protein EngBF assembles into a porous yet well-diffracting crystal lattice. This lattice tolerates rigid fusions to a specific DARPin, creating an EngBF–DARPin host framework that can recruit a guest molecule at a defined position [71, 77].

This approach, known as host-lattice display, has been used to solve the structures of short peptides, and the EngBF–DARPin lattice can accommodate targets of up to about 40 kDa [71, 77]. However, the larger guests still tend to exhibit elevated B-factors and weaker electron density, which has prompted further efforts to redesign the system for more rigid positioning of the bound molecule.

As an example, DARPins were raised against a leucinostatin derivative, a highly hydrophobic peptide [51]. The peptide was immobilized in the host lattice via the DARPin, and the structure of the complex was determined by X-ray crystallography. In this arrangement, the peptide adopts a distorted α-helical conformation. When compared with related compounds analyzed in organic solvents, the termini appear more flexible, a feature that may be relevant to its biological activity [51].

DARPin D12 as a crystallization chaperone. DARPin D12 (originally named 5m3_D12) was obtained as one of the DARPins binding to the V3-crown of the of the HIV-1 envelope (see above) [55], but it was found to crystallize (in the absence of the V3 peptide target) unusually well, and in a wide variety of crystal forms [78]. The rigidity of the scaffold and the compatibility of different surfaces and orientations for crystal packing, while being monomeric in solution, probably explain these favorable properties. It was thus used to create rigidly connected DARPin-DARPin fusions [78], as well as a crystallization chaperone rigidly connected to a target-binding DARPin [79], and also in fusions to G protein coupled receptors, where it helped crystallization both in the vapor phase and the lipidic cubic phase [80, 81]. These applications have been previously reviewed [77].

General comments on structures of DARPin/target complexes

The structures of a number of DARPin/target complexes obtained from the HT selections with the methods described here were determined by x-ray crystallography or cryo-electron microscopy (cryo-EM) as described above and shown in **Figures 2 to 4**. It can be seen that, as expected and consistent with previous results [1], the randomized surface is the interface making contact to the target, engaging both the surface of the adjacent helices and the short loops connecting them in the DARPin. Thereby a contiguous concave binding interface is generated.

The complexes are mostly engaging folded proteins as targets, which can substantially differ in size (**Figure 3**), since only a suitable surface epitope needs to be bound. The notable exception is the complex of the hydrophobic leucinostatin derivative, an almost insoluble peptide, whose structure could be determined with host lattice display [51]. In this approach, the DARPin is rigidly linked to the large bacterial protein EngBF, which readily forms a highly stable crystal lattice. The target molecule is then incorporated into this host lattice by binding to the DARPin, ensuring that it is positioned in a consistent crystal environment. Under these conditions, the structure of the target can be obtained quickly from difference Fourier maps, with the resulting map quality depending on the size of the target and the orientation of the DARPin within the lattice [71].

Discussion

Since DARPins had shown many favorable properties in many applications [1], and their selection with Ribosome Display had been well established [31, 32], we received ever more requests for collaborations. For this purpose, and also to handle many internal projects, a high-throughput (HT) workflow was developed. The products of this work are summarized in exemplary publications reviewed in the Results section above. However, the HT methods themselves had not been published and their description in the cited publications as "essentially similar" to the manual method is only a rough approximation. To finally publish methods actually used in the manuscripts cited above, we wrote the extended method section below.

The fundamental virtues of Ribosome Display have been summarized elsewhere [29], and the present Methods section serves to extend this to carrying out multiple selections in parallel — up to 92. Briefly, a large library can be used, which is not constrained by the need to transform cells, and the interfacing with error-prone PCR is convenient, since PCR is part of the procedure anyway. While the high-throughput work summarized here and detailed in the methods is based on *E. coli* ribosomes from S30 extracts, it should be mentioned that eukaryotic ribosomes have also been used [82-84] as well as a system reconstituted from purified components [85, 86] in Ribosome Display, which could also be implemented in our high-throughput platform.

Ribosome Display is a method that involves in vitro translation. Therefore, its use with proteins containing disulfide bonds such as antibody fragments must include a disulfide-forming machinery [33, 87, 88]. Moreover, proteins such as scFv antibody fragments are aggregation-prone and are thus challenging and profit from the inclusion of chaperone systems [33, 87-90]. Antibody fragments are probably the most widely used type of protein library, and selection by phage display and yeast display allows exploitation of the secretion and disulfide-forming systems of either bacteria or yeast, leading to widespread use of these selection systems. Moreover, while peptide libraries can be used with Ribosome Display [91-94], peptides of very short length would not lead to sufficient mutations in error-prone PCR steps, and thus fail to exploit one of the advantages of Ribosome Display. Therefore, Ribosome Display plays to its strengths best with well-folding scaffolds — such as DARPins.

Carrying out so many selections in parallel is actually not overly cumbersome, provided suitable equipment for automation is available, most notably a KingFisher Flex instrument. The limiting factor is rather the subsequent screening, since in a well-executed Ribosome Display campaign, several 96-well plates of individual clones can be obtained — per target. Since there is no "focusing" of the library (typically, every clone has a different sequence), in principle,

every clone can be a potentially valid candidate that deserves to be tested in detail. When carrying out selections against many targets in parallel, limitations in the number of clones to be investigated may have to be introduced at this point.

Before any testing of biological effects, a screening for binding and specificity needs to be carried out. Depending on the subsequent use, the first test can either be on defined soluble protein (with ELISA or homogeneous time-resolved fluorescence (HTRF), which is actually time-resolved FRET (Förster resonance energy transfer)), or it can be by flow cytometry on cells if the target is a cell-surface receptor. We describe in the Methods section the pros and cons of these approaches and also recommendations about their sequential use. Specificity is application-dependent, which means that for every application it must be defined what should ***not*** be recognized, and what the conditions for binding are. Also, acceptable affinities are application-dependent and reachable affinities may depend on whether there are many additional constraints on an epitope, which might restrict the possible orientations and/or paratopes.

Since binding is (almost) never the end use, typically the candidate DARPins are then recloned into the format of their ultimate use, as an intracellular fusion protein, as a label on the outside of a cell, a growth inhibitor of a cell, a virus or a bacterium or as a chaperone or fiducial marker in structural biology, to name some examples. As this characterization is very project-dependent, this is not described here, but in the references mentioned in the Results section.

The DARPin scaffold has also been incorporated into larger structures, achieved by protein design [72, 95], where selection and design are blending. Nonetheless, for reasons summarized in the introduction, high affinity and specificity will require experimental affinity maturation in the foreseeable future to capture all aspects that contribute to the free energy of binding. Ribosome Display can also be used for affinity improvement of a single binder, but the effort is rather comparable to that of direct selection from a diverse library.

Together, these high-throughput methods provide a reliable and scalable framework for the efficient discovery and characterization of DARPins across diverse targets. While the methods have been worked out for DARPins, the various high-throughput methods can undoubtedly be adapted to other scaffolds with similar properties. Nonetheless, the detailed method description combines the usage of high-throughput Ribosome Display, high-throughput screening methods, and the DARPin scaffold, which have been developed together. The approach facilitates systematic selections and broadens the applicability of the DARPin technology in both research and therapeutic contexts.

Materials and methods

The work-flow presented here is the one used for identifying DARPins binding to the targets discussed in the Results section. It is subdivided in three main sections: (A) General preparations that can be done far in advance for all selections, such as the creation of one or more libraries, the preparation of the in vitro translation system as well as the individual quality control of the target, (B) the actual parallel selection against up to 92 targets (termed High-throughput Ribosome Display (HT RD) workflow) and (C) the screening and characterization of individual binders, also using an HT workflow. For orientation, the main steps of the overall workflow are shown as a simplified overview in **Figure 5**. The major steps are numbered as in the following sections. The actual HT RD cycle is illustrated in more detail below in **Figure 9**.

A plausible illustration of the ternary complex consisting of ribosome, mRNA and tethered protein has be shown previously [29], based on the cryo-EM reconstruction of the *E. coli* ribosome 70S complex with the TnaC stalling sequence from Seidelt et al. [96]. The unstructured connector within the tunnel (nascent chain) and emerging from it would correspond to the “spacer” or “tether” region in **Figures 5 and 9.**

A. General preparations

1. Description of the DARPin library

The HT RD workflow has been successfully used with different DARPin libraries, which are briefly summarized here. They mainly differ in the number of repeats, the randomized regions and the presence or absence of loops.

All of the libraries are based on internal consensus ankyrin repeats with randomized (potentially) interacting residues, flanked by N- and C-terminal capping repeats (N- and C-cap) that create a hydrophilic surface. Depending on the number of internal repeats present (typically 2 or 3), the libraries are then denoted as N2C or N3C. The use of a consensus framework essentially optimizes all intramolecular interactions by tracing back evolutionary diversification, and this gives the protein a great stability [97-103]. The library members, therefore, tolerate the inevitable stability losses very well when introducing residues designed for binding, and so the contribution of target-interacting residues to the framework stability can be ignored, as this stability is always very high.

The libraries have originally been assembled with oligonucleotides employing the trinucleotide technology [104], in which trinucleotides are used as building blocks of synthetic oligonucleotides for the randomized regions. This approach has the advantage that, in contrast to randomized mononucleotides as building blocks, stop codons can be completely avoided, and also undesired amino acids can be excluded. One design feature of DARPins is the absence of cysteines to avoid spurious disulfide formation, and so Cys codons are avoided. Also, since some of the randomized positions are in helices, Gly and Pro codons are avoided. In the present libraries used in the HT RD selections, an equimolar mixture of 17 codons was used [97, 105]. In one internal position, since the consensus was not very pronounced, a mixture of the codons was used (His, Asn and Tyr) [97], but this is probably not very critical, as no clear enrichment is typically observed.

It should be pointed out that an individual, biased distribution at different positions can also be achieved, e.g. to increase or decrease the hydrophobic content, and/or enrich or deplete positive or negative charges. Such custom libraries have been described elsewhere [106, 107]. Besides trinucleotide building blocks, other codon-centric randomization strategies have become available in recent years [108], and efficient DNA synthesis methods have become commercially available [109-111] that in principle allow library assembly from individual mixed oligonucleotides encoding individual sequences — the efficiency of these approaches, however, greatly depends on the length of the randomized regions, the desired diversity, and these methods come at a price.

The randomized positions of the internal residues cover the surface of the adjacent helices as well as the short loops connecting them (**Figures 2 and 6**), giving a contiguous concave interaction surface matching well the convex surface of a typical folded protein. Later versions of the libraries contain additional randomized regions outside the central ones (see below). Importantly, the diversity is not limited to the deliberately randomized residues, but two factors can introduce additional diversification. First, the multiple PCR steps in Ribosome Display can introduce random errors, which when advantageous for affinity will be selected, as with the somatic mutations of antibodies. These do not necessarily have to be directly in the interaction surface, but can also help to slightly adjust the geometry of the framework [112-114]. Second, very rare imperfections in the synthetic oligonucleotides, such as deletions of one or two codons, have occasionally been selected as apparently fitting better than the consensus loop structure, e.g. the anti-EpCAM DARPins of the "Ec series" [115]. To deliberately extend this diversity further, a loop has also been inserted into the library [105], but this library is currently not routinely used.

In the course of the HT RD work, different libraries have been used, which differ predominantly in the capping repeats. The original capping repeats were derived from natural ankyrin repeat

proteins [97]. However, it was found that the original C-cap in particular was less stable than the internal repeats, and a new stabilized cap was generated after testing different designs [103]. In subsequent steps, randomized residues in these stabilized caps were also introduced [105]. The different capping repeats are aligned in **Figure 6**.

Over the years, the original library in N2C and N3C format [97], the two N3C loop libraries having stabilized caps with and without randomization [105] and the two N3C libraries without loop, having stabilized caps with and without randomization, have been used (**Figure 7**). More recently, the latter two N3C libraries are mixed in a 1:1 ratio, such that half of the molecules are randomized in the caps, while the others have the consensus sequence. It should be pointed out that the assembly process may not go to 100% completion, so that there are N2C molecules in the N3C library. Furthermore, during the many cycles of PCR amplification containing ORFs with similar sequence repeats, a repeat can get deleted from the N3C library, with the consequence, that the final binder collection will typically also contain N2C DARPins, and very occasionally even N1C (see below), which in some epitopes can be sterically preferred.

The DARPin libraries have all been assembled using type IIS restriction enzymes such as *Bsa*I and *Bpi*I, whose recognition site is remote from the cutting site. By using identical, non-palindromic overhangs, segments can be ligated which become resistant to cutting with either enzyme. Thereby, segments such as repeats can be assembled in a stepwise and directional manner [105, 116, 117]. While the actual protocol of library assembly is not described here, the original publications give a rather detailed methodological description.

2. Preparation of the in vitro translation system

2.1. Overview

The preparation of the in vitro translation system has to be done only once for very many selections and is thus much less onerous than it might seem at first. Different in vitro translation systems have been used for Ribosome Display, including commercial ones and those based on purified components, as previously described [32, 33, 82-86, 88, 90]. In our HT RD protocol, however, we use *E. coli* ribosomes derived from S30 extracts. Here, we provide a detailed procedure for preparing a suitable S30 extract (see also [32]). Notably, certain commercial translation mixes contain reducing agents, which are not suitable for disulfide-bonded libraries, such as those of antibody fragments, but pose no issue for a DARPin library. Precautions regarding disulfides or free cysteines in the target are discussed further below.

In the course of in vitro translation using the procedure described further below [32], DARPins are synthesized by ribosomes isolated from *E. coli* MRE600 (ATCC 29417), which lacks functional RNase I [118, 119]. The ribosome enrichment process in an S30 extract is adapted from earlier work described elsewhere [120-123]. All other components required are prepared separately with an optimized composition, referred to as PremixZ [30-33].

A key feature of the translation reaction is the special mRNA template, which lacks a stop codon, but extends beyond the open reading frame (ORF) of interest. This design retains the mRNA and the nascent protein on the ribosome, while the C-terminal TolA tether ensures full emergence of the protein from the ribosomal tunnel [29]. Probably, different tether sequences can be used, but in the experiments described here, a tether from the *E. coli* TolA protein has been used because of its long unstructured region [29]. This feature enables genotype-to-phenotype linkage throughout the selection process. HT in vitro translation is performed in 96-well PCR plates, allowing up to 96 simultaneous translation reactions. Binder-ribosome-mRNA complexes are subsequently isolated, using magnetic beads coated with the immobilized target, on a KingFisher 96-well platform.

2.2. Preparation of S30 extract

A 100 mL culture of *E. coli* MRE600 (ATCC 29417) is grown in incomplete rich medium overnight at 37°C with shaking (see **Materials Section** below). Subsequently, 10 mL of the overnight culture is transferred to 1 L of fresh media in a 5 L baffled shake flask and grown at 37°C with shaking until an OD_{600nm} of 1.0–1.2 is reached. Typically, 8–10 mL of S30 extract are obtained per liter of culture. Since the S30 extract remains stable for years when stored at −80°C, the procedure can be scaled up as needed. After reaching the desired OD_{600nm}, shake flasks are chilled for 10 min in an ice-water bath with gentle shaking. Following this step, cultures are centrifuged at 4°C and 3,500 × *g* for 15 min, and the supernatant is discarded. The pellet is washed three times with 100 mL of ice-cold S30 buffer per 1 L culture by centrifugation at 4°C and 5,000 × *g* for 20 min. Finally, the cell pellet is rapidly frozen in liquid nitrogen and stored overnight at −80°C. The cell pellet is resuspended to a total volume of 40 mL and centrifuged at 4°C and 5,000 × *g* for 20 min. The supernatant is discarded, and the pellet is resuspended in 4 mL S30 buffer per gram of wet cells.

Cell lysis is achieved by one single passage through a French press applying 1,000 psi. The lysed cells are then centrifuged at 4°C and 47,750 × *g* for 30 min. The supernatant is transferred to fresh centrifugation bottles and the centrifugation step repeated. The resulting supernatant is transferred into a sterile Erlenmeyer flask and 1 mL of pre-incubation mix is added for every 6.5 mL of supernatant. The solution is gently shaken at 25°C for 1 h to facilitate the translation of all endogenous mRNAs and degradation of mRNA and DNA by cellular nucleases [124]. Subsequently, the S30 cell extract is dialyzed using a molecular weight cut-

off of 6000–8000 Da against a 50-fold volume of S30 buffer at 4°C, repeating the process three times for 4 h each. The dialyzed S30 extract is centrifuged at 4°C and 4,000 × *g* for 10 min. When both the library members and target lack disulfide bonds, 1 mM DTT can be added to the extract. The S30 extract is then aliquoted at 4°C into appropriate volumes as it should not be subjected to repeated freeze-thaw cycles to preserve optimal activity. Finally, the aliquots are flash-frozen in liquid nitrogen and stored at −80°C.

2.3. Preparation of PremixZ

PremixA is prepared on ice (full composition listed in **Materials Section**). Note that PremixA contains an anti-ssrA oligonucleotide to prevent the recycling of stalled ribosomes via the transfer-mRNA encoded by the gene *ssrA* [88, 125, 126]. An in vitro translation reaction should be set up using PremixA, but the optimal concentrations of the following three components need to be determined empirically for the final PremixZ. The optimum for magnesium acetate ($MgAc_2$) typically falls within the range of 7–15 mM, for potassium glutamate (KGlu) within the range of 180–220 mM and for PEG-8000 within the range of 2–15% (w/v). All concentrations provided refer to the composition of the ultimate translation mix. PremixA should be adjusted using the optimal concentrations of $MgAc_2$, KGlu and PEG to obtain the final PremixZ (we are usually using concentrations of 21.4 mM $MgAc_2$, 481 mM KGlu and 7% PEG-8000 in the PremixZ). Once optimized, PremixZ should be aliquoted and flash-frozen in liquid nitrogen. Long-term storage should be at −80°C, however PremixZ is stable for several months at −20°C and can withstand multiple freeze-thaw cycles.

2.4. Testing the components: β-lactamase assay

This assay serves to evaluate the activity of the S30 extract and to optimize the concentration of components of PremixZ. The concept is to use the mRNA of a monomeric enzyme without cofactors, which folds in the in vitro translation and whose activity can be conveniently measured by a spectrophotometric assay in the extract, in order to rapidly compare the optimal PremixZ composition. Such an enzyme is β-lactamase, whose two cysteines have both been mutated to alanines [127] to work without requiring disulfide formation.

As a first step, β-lactamase mRNA derived from the pRDV_β-lactamase template DNA (**Figure 8**), encoding the double Cys to Ala mutant of β-lactamase [127] is prepared via PCR, using the primers T7B and tolAk (as described in **Section 4.2**). Subsequently, an in vitro transcription is performed, and the mRNA is purified (see **Section 4.2**). For the in vitro translation the following mix is prepared on ice:

0.4 µL	200 mM methionine
8.2 µL	PremixZ
x µL	in vitro transcribed RNA (total 2 µg)

10.0 µL S30 extract
Nuclease-free water is added to 22 µL

To optimize the activity of the S30 extract, PremixA is used, and the concentrations of magnesium acetate, potassium acetate and PEG-8000 are titrated. After preparation, the translation mix is incubated at 37°C for 10 min, followed by the addition of 88 µL of Stop buffer. Subsequently, 5 µL of the stopped in vitro translation is used for the activity assay with the chromogenic substrate nitrocefin [128]. The nitrocefin substrate is prepared by diluting at a ratio of 1:100 in β-lactamase buffer from a stock solution (see Materials below). In each reaction, 195 µL diluted nitrocefin solution is combined with 5 µL stopped translation reaction. Then the OD_{486nm} is measured immediately and continuously monitored for approximately 12 min, measuring at least once every minute. For optimization of the activity of the S30 extract, the data is evaluated and the condition yielding the highest activity is determined.

Materials

In vitro translation

PCR thermocycler (Bio-Rad, cat. no. 1851196)

96-well PCR plate (Corning, cat. no. PCR-96-FS-C)

96-deep well plate (Corning, cat. no. P-2ML-SQ-C)

200 mM methionine (Sigma-Aldrich, cat. no. M9625): Dissolve in nuclease-free water; store at −20°C

S30 extract

PremixZ

S30 extract

E. coli strain MRE600, lacking ribonuclease I activity [118, 119]. (ATCC, cat. no. 29417)

Incomplete rich medium: 5.6 g KH_2PO_4, 28.9 g K_2HPO_4, 10 g yeast extract, 15 mg thiamine for 1 L medium. Autoclave and then add 50 mL 40% glucose (w/v) and 10 mL 0.1 M magnesium-acetate, both sterile-filtered.

S30 buffer: 10 mM Tris-acetate (pH 7.5 at 4°C), 14 mM magnesium-acetate, 60 mM potassium-acetate. Cool to 4°C before use.

Pre-incubation mix (Prepare directly before use): 3.75 mL 2 mM Tris-acetate (pH 7.5 at 4°C), 71 µL 3 M magnesium-acetate, 150 µL amino acid mix (5 mM of each of the 20 amino acids; Sigma-Aldrich, cat. no. LAA21-1KT), 120 µL 0.5 M ATP (Sigma-Aldrich, cat. no. A2383), 50 units pyruvate kinase (Sigma-Aldrich, cat. no. P9136), 0.13 g phosphor(enol)pyruvic acid trisodium salt (Sigma-Aldrich, cat. no. P7002); add to 10 mL with nuclease-free water.

Dialysis tubing with a MW cutoff of 6000–8000 Da (Spectrum Laboratories, cat. no. 132665).

PremixZ

PremixA (the final concentration is fivefold lower in the final volume of the in vitro translation reaction):

250 mM Tris-acetate from a 2 M stock solution (pH 7.5 at 4°C),

18 µM anti-ssrA oligonucleotide (5'-TTAAGCTGCTAAAGCGTAGTTTTCGTCGTTTGCGACTA-3') from a 200 µM stock solution,

1.75 mM of each amino acid except for methionine,

10 mM ATP from a 1 M stock solution (Sigma-Aldrich; cat. no. A2383),

2.5 mM GTP from a 0.2 M stock solution (Sigma-Aldrich; cat no. G8877),

5 mM cAMP from a 0.4 M stock solution (Sigma-Aldrich; cat. no. A6885),

150 mM acetyl phosphate from a 2 M stock solution (Sigma-Aldrich; cat. no. A0262),

2.5 mg/mL *E. coli* tRNA from strain MRE600 from a 25 mg/mL stock solution (Roche Diagnostics, cat. no. 10109541001),

0.1 mg/mL folinic acid from a 10 mg/mL stock solution (Sigma-Aldrich; cat. no. 47612).

PremixZ (the final concentration is approximately 2.68-fold lower in the final volume of the in vitro translation reaction):

134.15 mM Tris-acetate from a 2 M stock solution (pH 7.5 at 4°C),

9.66 µM anti-ssrA oligonucleotide (5'-TTAAGCTGCTAAAGCGTAGTTTTCGTCGTTTGCGACTA-3') from a 200 µM stock solution,

0.94 mM of each amino acid except for methionine,

5.37 mM ATP from a 1 M stock solution,

1.34 mM GTP from a 0.2 M stock solution,

2.68 mM cAMP from a 0.4 M stock solution,

80.49 mM acetyl phosphate from a 2 M stock solution,

1.34 mg/mL *E. coli* tRNA from strain MRE600 from a 25 mg/mL stock solution,

0.05 mg/mL folinic acid from a 10 mg/mL stock solution,

481 mM potassium-glutamate from a 4 M stock solution,

24.3 mM magnesium-acetate from a 1 M stock solution,

7% PEG-8000 from a 40% stock solution.

Concentrations of KGlu, $MgAc_2$ and PEG-8000 are typical values but need to be optimized for each preparation of S30 extract as explained above.

β-lactamase assay

pRDV plasmid encoding the double Cys to Ala mutant of β-lactamase

β-lactamase buffer: 100 mM sodium phosphate (pH 7.0)
Stop buffer: 50 mM Tris-acetate (pH 7.5 at 4°C), 50 mM magnesium-acetate, 150 mM NaCl, 0.05% Tween20 (v/v), 0.5% bovine serum albumin (w/v)
Nitrocefin (Glaxo Research, obtained from Oxoid Ltd., cat. no. SR0112C), 1 mg nitrocefin dissolved in 500 µL DMSO and stored at −20°C
Transparent 96-well plate (Greiner, cat. no. 655101)
Microplate reader (Agilent, BioTek Synergy HT)

3. Preparation of targets and target protein QC

The target for any selection must be of excellent purity and homogeneity, including structural uniformity. Variations of the target surface between rounds, such as those arising from partial denaturation, can prevent effective selection due to the presentation of inconsistent interaction surfaces to the library. A clear correlation between target homogeneity and DARPin binders obtained has been observed in many selections. Depending on available resources, the target can either be expressed and purified by methods of choice or, if available, acquired directly from a commercial supplier. Obviously, the same criteria always apply.

Thorough quality control of the purified, biotinylated target is crucial to ensure homogenous immobilization. The purity and homogeneity of the target can be rapidly assessed using SDS-PAGE and analytical size-exclusion chromatography, respectively. Structural homogeneity can be estimated by obtaining unfolding curves (e.g., followed by CD spectroscopy or by differential scanning fluorimetry [76, 129].

In principle, multiple strategies can be used for immobilization of the target to capture the ternary complexes, including His-tagging, GFP- or Fc-fusion, or fusion with a streptavidin-binding peptide or biotinylation. However, it is worth noting that the affinity of the His-tag to nickel-chelators (such as Ni-NTA) and cobalt-chelators is only micromolar [130-133], and that chromatography columns mostly work because of the very high density and high number of chelators present. Therefore, His-tags do not provide a suitable immobilization technology. An early version of a streptavidin-binding peptide showed the same limitation [58], but later high-affinity versions overcame this problem [39, 48]. The large surface of GFP in a GFP fusion, or the antibody Fc part in a corresponding fusion has been successfully used [70, 115], but it requires extensive counter-selection to eliminate binders targeting these fusion partners, introducing additional steps.

Therefore, biotinylation is strongly recommended, as it is the most robust immobilization method for very stringent washing procedures, including those involving detergents. The

primary advantage of immobilizing biotinylated targets lies in its general applicability, functioning equally well for proteins, peptides, oligonucleotides, and small molecules. By circumventing any direct binding to the surface, biotinylation preserves the structural integrity of the target, resulting in more homogenous target immobilization. In addition, non-biotinylated targets serve as convenient competitors in off-rate selections. Biotinylation can be achieved in two ways:

- Fusion of the target to an AviTag (GLNDIFEAQKIEWHE) and mono-biotinylation of the K residue in vivo or in vitro using the *E. coli* biotinylation enzyme BirA [134], following the guidelines posted on the Avidity Web page (https://www.avidity.com).
- Chemical biotinylation of surface lysine amino acid residues using NHS-biotin reagents, e.g. from Pierce, following the manufacturer's instructions.

The AviTag method is preferred, whenever feasible as it yields uniformly labeled mono-biotinylated targets distal from potential epitopes. After biotinylation, free biotin must be effectively removed by extensive dialysis, or by desalting columns such as Zeba Spin or PD-10 desalting columns, following the manufacturer's protocols. Detailed Materials lists are found at the end of each section. Residual non-biotinylated targets can be removed using a monomeric avidin column, as instructed.

Biotinylation of the target is quantified using a streptavidin shift assay (adapted from Petris et al. [135]): the strong complex formation between biotin and streptavidin allows the quantification of the biotinylated species by SDS-PAGE, since the complex does not dissociate on the gel and thus shifts to higher molecular weights. In contrast, the non-biotinylated species is detected as non-shifted protein.

To perform the streptavidin shift assay, two aliquots of 2 µg of target are boiled in SDS loading buffer for 10 min. Once the samples have cooled to room temperature, a sixfold molar excess of streptavidin is added to one of the samples and incubated for 30 min at room temperature. Subsequently, the samples are run by SDS-PAGE, and the gel is imaged. The degree of biotinylation is quantified by comparing the shifted and non-shifted bands using Fiji software [136].

Finally, a quality control ELISA is performed to investigate the potential interaction between the target and detection antibodies to be used (either anti-tag or anti-DARPin). This step is crucial to ensure accurate single clone analysis of bound DARPins to the target (see **Section 6**), as spurious cross-reactivity of detection antibodies with the target could result in ambiguous screening results.

Materials:

Streptavidin (Pierce, cat. no. 21125): 1.2 mg/mL in water; store at −20°C

Zeba Spin desalting columns (Thermo Fisher, cat. no. 89882) or

PD-10 desalting columns (Cytiva, cat. no. 17085101)

Monomeric avidin column (Pierce, cat. no. 53146)

B. High-Throughput Ribosome Display

4. Ribosome Display selection using the KingFisher 96-well platform

4.1. Overview

The actual HT RD workflow, adapted for the processing of up to 92 parallel selections, consists of the following steps, which are schematically shown in **Figure 9**. The DARPin library is a PCR fragment containing all elements for in vitro transcription (**Section 4.2**), which is transcribed in vitro, purified and the transcription is quantitated (**Section 4.3**). The so obtained mRNA is translated in vitro (**Section 4.4**). The mRNA has been designed such that it does not contain a stop codon and extends beyond the ORF of the actual binder to include an in-frame C-terminal tether (see above). Thereby, each mRNA molecule is engaged by a ribosome, produces a different protein molecule, and both mRNA and protein remain bound to the ribosome (in the reactions we use, approximately 10^{12} complexes can form, limited by the number of ribosomes present in the reaction volume). The binders (including the attached ribosomes and the attached mRNA) are engaged by the immobilized target, and they can be separated by a multiplexed magnetic bead procedure (**Section 4.5**). The mRNA of the selected binder-ribosome-mRNA complexes is isolated ("rescued") (**Section 4.6**), cDNA is produced by reverse transcription (**Section 4.7**) and dsDNA amplified by PCR (**Section 4.8**). The resulting PCR product is purified (**Section 4.9**). It is then ligated into a vector, but not used for transformation of *E. coli*, but the ligated vector provides ribosome binding site (rbs) and C-terminal tether (**Section 4.10**). This *in-vitro*-ligated vector provides then the template for the PCR starting the next round of HT RD, with in vitro transcription and translation (**Section 4.11**).

The protocol detailed here starts from a library of about $>10^{12}$ DNA molecules in the form of a PCR fragment (**Section 4.2**). In a newly constructed library, the diversity cannot be higher than the number of DNA molecules used in this step. Whether this number corresponds to the actual functional library size, i.e., whether all these $>10^{12}$ molecules are all different and at least potentially functional, depends both on the design and DNA synthesis quality of input library template as well as the amount of the DNA input template used from which this PCR fragment

is generated. Using the procedures described here, the number of ribosomes should not be limiting. What limits the functional library in Ribosome Display is also discussed elsewhere [29].

The first round should, in general, not be highly selective; it is more important to capture the full diversity of binders, as a binder lost at this stage can never be recovered. Since mutations can be generated through the numerous PCR steps in the procedure (**Section 4.2**), an affinity maturation can be achieved, offering various strategies for selecting the tightest binders (or those with other desired properties) (see below). The diversity of the library members can thus be deliberately increased by error-prone PCR [137] (**Section 4.12**, optional route), and this additional randomization step can readily be integrated in the protocol. The theoretical considerations for designing efficient off-rate selection experiments have been summarized [138] (see also **Section 4.5**).

While it is possible to select for properties other than high thermodynamic affinity, e.g. high stability or stability against aggregation, this is not the focus of the present Methods, and the interested reader is instead directed to a review article [29].

A plasmid map of the Ribosome Display vector pRDVLDnew is shown in **Figure 10**. It has been adapted from the original pRDV plasmid (GenBank accession code AY327136).

4.2. Description of the library starting material

4.2.1. Overview

How the actual DARPin insert library is created depends on whether it is synthesized from oligonucleotides from scratch [97, 105], or adapted from a previous library construct. The libraries used here are based on and derived from the initial N3C library described [97, 116]. The randomized internal repeats were amplified by PCR using the primers EWT3 and WTC3no [32], followed by digestion with either *Bst*API/*Apo*I or *Bst*API/*Bpu*10I. The digested PCR fragments were then ligated into the ligation-ready pRDVLDnew plasmid (**Figure 10**) to introduce the non-randomized caps or into the pRDVJSCNCran plasmid to introduce the randomized caps [105], respectively, at a vector-to-insert molar ratio of 1:5. This generated the DARPin libraries *N3C nonrand* and *N3C rand* (see **Figure 6** and **7**).To synthetize sufficient quantities of these libraries, after ligation, additional consecutive PCR reactions using the outer primers T7B/tolAk and agarose gel purifications are carried out (**Figure 9**), always ensuring that the initial diversity is kept, generated the starting material for HT RD.

4.2.2. Template preparation by PCR

The library used in our binder selection platform consists of a mixture of the DARPin-encoding N3C format with non-randomized caps [100] and randomized caps [105] (**Figure 6** and **7**) in a

molar ratio 1:1 at the state of the working stock (cf. **Figure 9**), as detailed in **Section 1**. The library is a length-defined DNA template suitable for in vitro transcription. To increase the material for the many selections the library is amplified by PCR using the outer primers T7B and tolAk (**Figure 9**). The resulting product includes a T7 promoter, a ribosome binding site (rbs), a *tolA* spacer (tether) sequence, and mRNA with stabilizing 5′ and 3′ stem-loop structures to protect against exonucleases.

4.2.3. PCR amplification

The initial library is amplified using the following 50 µL PCR reaction mixture:

10.0 µL	5× Herculase II buffer
2.0 µL	dNTP mix (5 mM each)
2.5 µL	DMSO
0.3 µL	T7B primer (100 µM)
0.3 µL	tolAk primer (100 µM)
1.0 µL	Library DNA
0.5 µL	Herculase II fusion DNA polymerase
Nuclease-free water is added to 50 µL	

Thermal cycling is performed with a hot-start protocol to improve specificity:

Initial denaturation: 95°C for 5 min
30 cycles:
  95°C for 30 s
  68°C for 45 s
  72°C for 1 min
Final extension: 72°C for 5 min

The size and integrity of the PCR products are confirmed by agarose gel electrophoresis prior to transcription.

Materials

Herculase II Fusion DNA polymerase (Agilent, cat. no. 600677) and 5× Herculase II buffer
dNTP mix: 5 mM each (Eurogentec, cat. no. NU-0010-10)
Dimethyl sulfoxide (DMSO; Sigma-Aldrich, cat. no. 41640)
Primers dissolved to 100 µM in nuclease-free water; aliquot and store at −20°C
T7B: 5’-ATACGAAATTAATACGACTCACTATAGGGAGACCACAACGG-3’
tolAk: 5’-CCGCACACCAGTAAGGTGTGCGGTTTCAGTTGCCGCTTTCTTTCT-3’
PCR thermocycler (Bio-Rad, cat. no. 1851196)

4.3. In vitro transcription of PCR Products for Ribosome Display

4.3.1. Overview

In vitro transcription is carried out using T7 RNA polymerase to synthetize mRNA from the DARPin-encoding DNA template pool. These templates are designed to include all necessary sequence elements for efficient transcription and downstream in vitro translation during Ribosome Display (**Figure 9**). Notably, 5′ and 3′ stem-loop structures are incorporated to enhance mRNA stability and protect it from ribonuclease degradation [88, 139]. Following transcription, the mRNA is purified and used as the input for in vitro translation and subsequent selection processes (see next sections).

To prevent RNA degradation, all work should be carried out using nuclease-free water, chemicals, and consumables. Commercially available water is typically nuclease-free (e.g. PanReac AppliChem, cat. no. A7398); alternatively, 0.1% diethylpyrocarbonate (DEPC) can be used to inactivate RNases by reacting with nucleophilic groups, such as histidine residues. Note that DEPC is incompatible with Tris-based buffers. All chemicals should be handled using gloves and flamed spatulas. Purchase only RNase-free plastic consumables. If glassware is required, it should be baked at 180°C for a minimum of 6 h. Pipettes and work surfaces should be treated with an RNase decontamination solution (e.g. RNaseZap; Invitrogen).

4.3.2. In vitro transcription (initial library)

At this initial stage, all diversity should be retained, and thus purification steps are avoided. When using the PCR products directly as templates without purification, commercially available RNA polymerase buffers often yield suboptimal results. Therefore, a homemade RNA polymerase buffer is strongly recommended to improve transcription efficiency. (For the in vitro transcription of later rounds, see **Section 4.11**).

Transcription reactions are prepared on ice in a total volume of 100 µL as follows:

20.0 µL	5× T7 RNA polymerase buffer
14.0 µL	NTP mix (50 mM each)
4.0 µL	T7 RNA polymerase (20 U/µL)
2.0 µL	Ribolock RNase inhibitor (40 U/µL)
25.0 µL	DARPin-encoding library (used directly, without purification)
Nuclease-free water is added to 100 µL	

The reactions are incubated at 37°C for 2 h 45 min in a heat block. Upon completion, RNA is immediately purified without prior DNase I treatment and is subsequently used for in vitro translation and selection steps.

Materials

T7 RNA polymerase (Thermo Scientific, cat. no. EP0111)

T7 RNA polymerase buffer (5×): 1 M HEPES, 150 mM magnesium acetate, 10 mM spermidine, 200 mM DTT; adjust to pH 7.6 with KOH; aliquot and store at −20°C

NTP mix: 50 mM adenosine 5'-triphosphate (ATP; Sigma-Aldrich, cat. no. A2383), 50 mM cytidine 5'-triphosphate (CTP; Sigma-Aldrich, cat. no. C1506), 50 mM guanosine 5'-triphosphate (GTP; Sigma-Aldrich, cat. no. G8877), 50 mM uridine 5'-triphosphate (UTP; Sigma-Aldrich, cat. no. U6625); dissolve in nuclease-free water; aliquot and store at −20°C

RiboLock RNase inhibitor (Thermo Scientific, cat. no. EO0381)

4.3.3. mRNA purification (from initial library)

Following in vitro transcription, mRNA is purified using the SV Total RNA Isolation System. To each 100 µL transcription reaction, the following solutions are added:

175 µL	RNA lysis buffer (from SV Total RNA Isolation System)
350 µL	RNA dilution buffer (SV Total RNA Isolation System)
200 µL	95% ethanol

RNA purification is then performed following the manufacturer's protocol, using centrifugation.

Materials

SV Total RNA Isolation System (Promega, cat. no. Z3100)

KingFisher Flex device (Thermo Scientific, cat. no. 5400630)

96-well deep-well plates (Axygen, cat no. P-2ML-SQ-C)

96-well KingFisher plate (Thermo Scientific, cat. no. 97002540)

Liquidator96 (Mettler Toledo, cat. no. 17010335)

Filter tips for Liquidator96 (Mettler Toledo, cat. no. 17010646)

4.3.4. mRNA quantification (all rounds of Ribosome Display)

After purification, RNA concentration is quantified using a UV-transparent half-area 96-well plate. Each well is pre-filled with 45 µL nuclease-free water, and absorbance is measured at 230, 260, and 280 nm using a plate reader. Then, 5 µL of purified RNA is added to each well, and absorbance is re-measured.

The RNA concentration (ng/µL) is calculated using the formula:

$$RNA\ concentration\ in\ ng/\mu L = \frac{Abs_{Sample} - Abs_{Blank}}{E \times l} \times df$$

where E is the extinction coefficient of RNA ($E = 0.027(ng/\mu l)^{-1}(cm)^{-1}$), l is the optical path length ($l = 0.3155\ cm^{-1}$ used here) and df is the dilution factor.

For high-quality RNA, absorbance ratios at 260/230 nm and 260/280 nm typically fall between 1.8 and 2.2. RNA concentrations are typically within the range of 1–3 µg/µL.

Materials

UV-Star half-area 96-well plate (Greiner, cat. no. 675801)
Microplate reader (Agilent, BioTek Synergy HT)

4.4. In vitro translation, detailed procedure

For one in vitro translation the following mix is set up in a 96-well PCR plate on ice:

1.0 µL	200 mM methionine
20.5 µL	PremixZ with optimized composition (for preparation of PremixZ, see **Section 3.3**)
x µL	in vitro transcribed RNA (total 5 µg)
25.0 µL	S30 extract (for preparation of S30 extract, see **Section 3.2**)
	and add to 55 µL with nuclease-free water
0.625 µL	Protein disulfide isomerase; add only if the library scaffold requires the formation of disulfide bonds [33, 87, 140]

All components are mixed carefully, and the PCR plate is incubated at 37°C for 10 min in a PCR thermocycler. We have provided incubation times and temperatures for the DARPin libraries used, when using different libraries and/or scaffolds, the optimal parameters must be empirically determined. Following the incubation, the translation reactions are transferred into a 96-deep well plate, prefilled with 450 µL/well ice-cold Stop buffer (see Materials), using a manual 96-channel pipetting device. Mix by pipetting up and down and proceed immediately with the HT RD selection.

Materials

96-well PCR plate (Corning, cat. no. PCR-96-FS-C)
PCR thermocycler (Bio-Rad, cat. no. 1851196)

96-deep well plate (Corning, cat. no. P-2ML-SQ-C)
Methionine (Sigma-Aldrich, cat. no. M9625)
PDI (Sigma-Aldrich, cat.no. P3818)
Stop buffer: 50 mM Tris-acetate pH 7.5, 50 mM Mg-acetate, 150 mM NaCl, 2.5 mg/mL heparin, 0.5% BSA, 0.05% Tween20
Liquidator96 device (Mettler Toledo, cat. no. 17010335)
Filter tips for Liquidator96 (Mettler Toledo, cat. no. 17010646)

4.5. HT Ribosome display (HT RD) selection of DARPin binders

4.5.1. Overview

To allow the selection of DARPin binders, the biotinylated target is immobilized on magnetic beads. Streptavidin- or neutravidin-coated magnetic beads are alternated to immobilize the biotinylated target. The likelihood of enriching proteins binding to streptavidin or neutravidin (a chemically modified derivative of avidin) is reduced by this alternation. Following immobilization, the magnetic beads are incubated with the protein-ribosome-mRNA complexes, a process usually termed as panning. The stringency of subsequent wash steps is adjusted and generally increased in successive rounds of HT RD to eliminate non-binding or weakly binding complexes (**Table 1**).

Additionally, counterselection of binders targeting an undesired domain or isoform (**Section 4.5.3**) can be depleted prior to panning through a pre-panning step (**Figure 11**), and/or by adding the non-biotinylated competitor during the panning step (**Figure 12**). Further enhancement of the affinity of selected binders can be achieved by incorporating an off-rate selection (**Figure 13**), wherein an excess of non-biotinylated target is added following the incubation with immobilized target.

The composition of buffers used during the HT RD selection may be adjusted to specific requirements of the library and target, but it is important that the wash buffer always contains 50 mM Mg^{2+} to stabilize the ribosome. It is recommended to test buffer conditions with a known binder — we use the DARPin off7 binding to MBP [116] — beforehand to ensure stability of the nascent chain complex throughout the whole selection.

4.5.2. Target plate preparation

The target plate may be prepared in advance and stored at −80°C, or prepared on the day of selection. A selection campaign is conducted for a maximum of 92 targets and four controls using a 96 well format. The four controls are pipetted as follows. Position A1 contains the negative control for non-specific binding, comprising of no coated target and the input RNA for

DARPin off7, which binds to the maltose binding protein (MBP) [116]. Position A4 contains the corresponding positive control for binding, namely the target maltose binding protein (MBP) and the same input RNA for the MBP-binding DARPin off7. Position A2 and A3 are used as controls for individual steps during the HT RD. Position A2 is a control for cross-contamination and contains no mRNA; it serves as a general negative control for the in vitro translation (ivT), RT and PCRs. In position A3, the positive control for the RT reaction (containing mRNA for off7) is pipetted after the panning to verify successful mRNA purification, reverse transcription and PCR.

The target amounts used for the different rounds are indicated in **Table 1**. Targets are typically diluted in 150 µL of WBT buffer (see **Materials Section** below) in the target plate. If a particular target requires an alternative buffer, it can be adjusted in the respective target well.

4.5.3. Counterselection: pre-panning and/or competition in solution

To enhance the specificity of binder selection, a pre-panning step may be implemented, using a pre-panning target whose recognition should be avoided [35, 41, 43, 46, 49, 57, 141-147]. This step is particularly crucial if the target is fused to an additional domain or contains a region for which no binders are desired. During pre-panning, the undesired domain or region is immobilized on magnetic beads in the same manner as the targets in the actual panning rounds, thereby depleting binders that interact with the undesired part prior to selection against the desired target. Additionally, this step may serve to eliminate misfolded or non-specific binders, as they are expected to already interact with the pre-panning target at this step. The amount of target used for the pre-panning can be varied between 125 pmol to 250 pmol, and it is typically applied in rounds 2 to 4. In round 1, the main goal is not to lose binders with affinity to the target, and thus pre-panning is usually avoided.

Another approach to enhance the specificity of binder selection is to add the unwanted competitors in solution during the panning steps, typically in rounds 2 to 4, for the same reasons as described above (**Figure 12**) [141, 144, 148, 149]. This can also be carried out in conjunction with pre-panning (see above). A large excess of the non-biotinylated competitor is needed to be effective, ideally 30 to 100-fold, which can preclude the application of this method and give preference to pre-panning.

4.5.4. Off-rate selection

To further enhance the chance for finding library members with high affinities, binders exhibiting the lowest dissociation rate constant (k_{off}) from the target are preferentially selected, since k_{off} correlates with K_D [45, 112, 150-153]. An "off-rate selection" (**Figure 13**) may be applied during the selection with the original library, or to previously identified individual binders (following randomization to essentially generate a novel library, see **Section 4.12**). In the

context of selection from the original library, an off-rate selection is typically incorporated in the third round of HT RD. Given the stringency of this condition, it is advisable to follow it with a less stringent “rescue" round to amplify selected binders. During off-rate selection, a large excess of non-biotinylated target [138] is added after an initial incubation with the immobilized target in the panning step. Binders possessing a high k_{off} will be rapidly occupied by non-biotinylated target (**Figure 13**), thereby preventing their capture by streptavidin-immobilized target on the magnetic beads. In contrast, high-affinity binders with a slow off-rate will remain bound to their biotinylated target and can thus be captured. The optimal duration of competitor incubation and excess concentrations can vary significantly depending on the expected off-rates [138]. For the initial off-rate selection, an incubation period of 1 to 2 h with a 10 to 100-fold molar excess of competitor is recommended. For affinity maturation of a known binder, this may be extended to 14 h of incubation and a 1,000 to 10,000-fold molar excess of competitor. The theoretical considerations have been modeled and discussed elsewhere [138]. Following off-rate selection, the washing steps and the elution are performed according to **Table 1**.

4.5.5. HT RD selection in solution

The parallel selection process for up to 92 targets consists of two days. The first day is dedicated to preparation and the second day to selection, the so-called panning day. On day one, the wells of the pp-p-pd plate (pre-panning, panning, pull-down plate; **Table 1)** and the target plate are blocked with 750 µL or 250 µL TBS-B buffer, respectively, and incubated at 4°C overnight. Streptavidin- or neutravidin-coated magnetic beads (depending on the round) are washed in TBS-T, followed by TBS-TB buffer and then equilibrated in WBT buffer for panning on the next day.

During round one, only panning beads are prepared. A total of 750 µL/well of TBS-T are filled into a 96 deep-well plate and 20 µL/well of fully resuspended magnetic beads are added. Two additional plates are prepared, each with 750 µL/well, one containing TBS-TB and the other WBT buffer. For rounds 2 and 4, selective pre-panning and panning beads (for immobilization of pre-panning or panning targets, respectively) are washed with TBS-T and TBS-TB and equilibrated in WBT. For round 3, due to the small amount of target protein used, only 10 µL/well of panning beads are processed as described above. The process is conducted overnight in a cold room using an automatic magnetic particle processor, the KingFisher Flex system (see below).

On the next morning, the blocking solution of the pp-p-pd plate is discarded and the plate is filled with 450 µL/well of Stop buffer and kept on ice. Washing plates for the panning are prepared as follows: for round 1, plates Wash 2-Wash 5, are each filled with 750 µL/well of WBT. For rounds 2 to 4, five wash plates are prepared.

All plates (the wash plates, selective pre-panning beads plate, panning beads plate, the target plate and the pp-p-pd plate) are placed onto the dedicated positions of the KingFisher Flex (**Figure 14**). The elution plate is filled with 150 µL of elution buffer and placed onto the dedicated position of the KingFisher system 30 min before the end of the selection protocol.

The Kingfisher Flex instrument is equipped with 96 magnetic rods (the magnetic head), and 96 sleeves for the rods (the tip comb). The magnet head can be slid into or retracted from the tip comb. During the mixing and release processes of the beads, the magnet head is retracted. During the binding and the transfer processes of the beads, the magnet head is slid into the plastic tip comb (see **Figure 15**) Only two movements are performed on this instrument: the up and down motion of the head and comb, and the rotation of the sample carousel to the next plate position (**Figure 14**).

The protocol is initiated, and the beads (prewashed overnight) are bound in the panning beads plate (position 3) before being transferred to the target plate (position 1) (**Figure 14**). The beads are then released and mixed, during which the target proteins are bound to the beads via streptavidin or neutravidin. The beads are bound and transferred to the pp-p-pd plate (position 2). The beads are released and mixed with the reaction from the in vitro translation (ivT), which contains the ternary complexes (still position 2). The beads are bound and sequentially transferred to the washing plates (positions 4 to 7). The stringency of the washing steps varies depending on the round (see **Table 2**). In the final washing plate (position 7), the beads are bound and transferred to the elution plate (position 8), where they are mixed. Due to the presence of EDTA in the buffer, the mRNA-ribosome-DARPin complex disassembles, and the mRNA is released. In the elution plate, the beads are bound and transferred into an earlier used plate that serves as waste.

Since the number of plates processed during round two to four exceeds the eight positions available on the KingFisher Flex, the protocol is interrupted after wash step 3 to allow for plates exchange. The plates in **Table 2,** named after the slash in positions 3 to 5, are then introduced. In round 3, if competition or off-rate selection with unbiotinylated target is performed, the process is additionally interrupted after the panning with the targets, and the competitors are added manually to the pp-p-pd plate.

Following completion of the KingFisher protocol, the elution plate is recovered from the instrument and mRNA rescue is performed thereafter.

Materials

Target plate, pre-panning target plate, elution plate: Kingfisher plate 200 µL (Thermo Scientific, cat. no. 97002540)

pp-p-pd plate, prepanning beads plate, panning beads plate, wash plates: 96 deep-well plate (Axygen, cat. no. P-2ML-SQ-C)

Streptavidin magnetic beads (Invitrogen, cat. no. 65602)

Neutravidin magnetic beads (Cytiva, cat. no. 11528692)

TBS-B: 50 mM Tris (pH 7.4 at 4°C), 150 mM NaCl, 0.5% (w/v) BSA

TBS-T: 50 mM Tris (pH 7.4 at 4°C), 150 mM NaCl, 0.05% (v/v) Tween20

TBS-TB: 50 mM Tris (pH 7.4 at 4°C), 150 mM NaCl, 0.05% (v/v) Tween20, 0.5% (w/v) BSA

WBT (Wash Buffer Tween): 50 mM Tris-acetate (pH 7.5 at 4°C), 150 mM NaCl, 50 mM Mg-acetate, 0.05% (v/v) Tween20

Stop buffer: WBT, 0.5% (w/v) BSA

Elution buffer: 50 mM Tris-acetate (pH 7.5 at 4°C), 150 mM NaCl, 25 mM EDTA, 0.05 µg/µl *S. cerevisiae* RNA

KingFisher Flex system (Thermo Scientific, cat. no. A39966)

4.6. mRNA rescue (after every round)

4.6.1. Overview

After every round, the mRNA from the selected complexes has to be purified to be prepared for RT-PCR, which is described in this section.

4.6.2. Output mRNA isolation after panning

RNA purification should be conducted immediately after panning to preserve sample integrity. For quality control, 2 µL of mRNA encoding for the DARPin off7 [116] are diluted with 150 µL of elution buffer when using the Zymo-Research 96 RNA Clean & Concentrator or 200 µL when using the High Pure RNA isolation kit and processed in parallel with the experimental samples.

The mRNA isolation procedure is adjusted according to the number of selections performed, with distinct protocols applied for either 1-24 or 25-92 parallel selections. Two different RNA isolation kits are recommended depending on the scale of selection.

4.6.3. mRNA purification (1 to 24 selections)

For up to 24 selections, the output mRNA is purified using the High Pure RNA Isolation Kit. Each 200 µL eluate is added to 400 µL of lysis buffer. RNA purification is then performed according to the manufacturer's instructions, including an on-column DNase I treatment to remove any residual DNA contamination.

4.6.4. mRNA purification (25 to 92 selections)

For experiments involving more than 25 selections, the Zymo-Research 96 RNA Clean & Concentrator Kit is used in a 96-well plate format. To each 150 µL eluate, a mixture of 300 µL

RNA binding buffer and 300 µL of 100% ethanol is added. RNA purification is subsequently carried out according to the manufacturer's protocol, including an on-column DNase I treatment to remove any residual DNA contamination.

Materials

Zymo-Research 96 RNA Clean & Concentrator kit (Zymo Research, cat. no. R1080)
High Pure RNA Isolation Kit (Roche, cat. no. 11828665001)
DNase I & reaction buffer (Roche, cat. no. 04 716 728 001)
U-bottom PP Microplate (Greiner, cat. no. 650201)
PCR plates (Corning, cat. no. PCR-96-FS-C)
Flat bottom blocks (QIAGEN, cat. no. 19579)
Liquidator96 (Mettler Toledo, cat. no. 17010335)
Filter tips for Liquidator96 (Mettler Toledo, cat. no. 17010646)

4.7. Reverse Transcription - Polymerase Chain Reaction (RT-PCR)

4.7.1. Overview

Although RNA can be stable for years when flash-frozen and stored at −80°C, we recommend proceeding immediately with cDNA synthesis followed by PCR amplification to ensure optimal recovery of putative binder sequences.

Two controls should be run in parallel to the RT reactions:

- "No RT" control: Reverse transcriptase is omitted in this reaction.
- "No template" control: This reaction contains all components except mRNA.

4.7.2. Procedure

Following purification, the mRNA is first denatured at 70°C for 10 min and then chilled on ice to eliminate secondary structures.

cDNA synthesis is performed in a 96-well PCR plate using the following 20 µL RT reaction mixture:

2.0 µL	10× Affinity Script buffer
0.5 µL	dNTP mix (5 mM each)
1.25 µL	DTT at 160 mM (prepared freshly from 1 M stock, 10 mM final concentration)
0.3 µL	JSCRDir2 reverse primer (100 µM)
0.5 µL	Ribolock RNase inhibitor (40 U/µL)
15.0 µL	RNA (or nuclease-free water for controls)

0.5 µL Affinity Script Reverse Transcriptase (50 U/µL)

The 96-well PCR plate is then incubated at 50°C for 1 h.

As cDNA (as a DNA-RNA hybrid) is relatively unstable, PCR amplification should follow immediately after the RT step.

Materials

10× Affinity Script buffer (Agilent, cat. no. 600100-52)

Affinity Script Reverse Transcriptase (50 U/µL, Agilent, cat. no. 600107)

Ribolock (40 U/µL, Thermo Scientific, cat. no. EO0381)

JSCRDir2 reverse primer,

(5'-ATCTGCTTCGGCCTTCGCTTTAGCATCTGCCGCCGCTTTCG-3')

PCR plates (Corning, cat. no. PCR-96-FS-C)

PCR thermocycler (Bio-Rad, cat. no. 1851196)

4.8. PCR on Reverse Transcription

4.8.1. Overview

Following reverse transcription (RT) in HT RD (**Section 4.7**), the resulting cDNA is used as templates for PCR amplification with the inner primers JSCRDif4 and JSCRDir2 (**Figure 9**). A control reaction, containing all components except the template, is included to detect potential contaminations.

The number of PCR cycles is adjusted based on the selection round. In the first round, 32–40 cycles (typically 40) are recommended to ensure sufficient product, as only a limited number of clones are expected to possess the desired properties. In subsequent rounds, as specific binders are enriched and the yield of eluted RNA molecules increases, cycle numbers are reduced to 28–35 (typically 35) in round 3 and to 26 in later rounds to minimize nonspecific amplification. However, when the selection pressure is increased, such as during off-rate selection in round 3, the yield of PCR product may decrease, requiring an increase in cycle numbers.

If the PCR product's quality or quantity (<10 ng/µL) is inadequate, the PCR is repeated. Re-amplification of the PCR product is avoided to prevent nonspecific amplification of unwanted by-products.

4.8.2. PCR amplification of the RT template

A 50 µL reaction mixture is prepared with the following components:

10.0 µL	5× Herculase II buffer
2.0 µL	dNTP mix (5 mM each)
2.5 µL	DMSO
0.25 µL	JSCRDif4 forward primer (100 µM)
0.25 µL	JSCRDir2 reverse primer (100 µM)
5 µL	RT template (or nuclease-free water for the no template control)
0.25 µL	Herculase II Fusion DNA polymerase
Nuclease-free water is added to 50 µL	

Thermal cycling is performed with a hot-start protocol to improve specificity:

Initial denaturation: 95°C for 5 min
Cycling (adjusted by round):
  40 cycles in rounds 1 and 3
  35 cycles in round 2
  26 cycles in round 4
  Each cycle:
    95°C for 30 s
    68°C for 45 s
    72°C for 1 min
Final extension: 72°C for 5 min

Specific considerations for round 4

In the final round of HT RD, before single-clone analysis is performed, two PCR reactions on RT templates are conducted (across two plates) to ensure one serves as a backup.

Materials

Herculase II Fusion DNA polymerase (Agilent, cat. no. 600677) and 5× Herculase II buffer
dNTP mix: 5 mM each (Eurogentec, cat. no. NU-0010-10)
Dimethyl sulfoxide (DMSO; Sigma-Aldrich, cat. no. 41640)
Primers dissolved to 100 µM in nuclease-free water; aliquoted and stored at −20°C
JSCRDif4:
5'-AGAGGATCGCATCACCATCACCATCACGGATCCGACCTGGG-3'
JSCRDir2:
5'-ATCTGCTTCGGCCTTCGCTTTAGCATCTGCCGCCGCTTTCG-3'
PCR plates (Corning, cat. no. PCR-96-FS-C)
PCR thermocycler (Bio-Rad, cat. no. 1851196)

4.9. Gel purification of RD products

4.9.1. Overview

Gel purification of PCR products of selected binders is an important quality control step. This process enables the separation of DNA fragments encoding DARPins of varying sizes, including those that may have lost one repeat during PCR amplification, or might have been an N2C "contamination" which got preferentially amplified as a shorter DNA. This step ensures the selective recovery of fragments corresponding to the desired constructs. Additionally, the relative abundance of fragments of different sizes provides insights into selection biases toward DARPins with distinct numbers of internal repeats.

4.9.2. Procedure gel purification of RD products

PCR reactions are combined with Orange G DNA loading buffer and loaded onto a freshly prepared 1.5% (w/v) agarose gel. Desired N3C fragments are excised from the gel using extraction tools, but N2C fragments can also be retained. In the final round of HT RD, all fragments are purified to maximize the number and diversity of potential binders, depending on the number of parallel HT RD selections. For up to 24 parallel selections, the DNA is extracted from the gel using the GenElute Gel Extraction Kit (spin column-based), while for a greater number, a 96-well plate-based purification (ZR-96 Zymoclean Gel DNA Recovery Kit) is used, following the manufacturers' protocols.

Materials

Agarose (Eurogentec, cat. no. EP-0010-05)

Ethidium bromide solution (Carl Roth, cat. no. HP47.1)

Gel system Midi S PerfectBlue (VWR, cat. no. 700-0814)

Power supply peqPOWER (Peqlab, cat. no 55-E250-230V)

10× Orange G DNA loading buffer: 40% (w/v) glycerol, 2 mg/mL Orange G dye (AppliChem, cat. no. A1404) in water

1 kb Plus DNA Ladder (New England Biolabs, cat. no. N3200L)

1× TAE buffer: 40 mM Tris, 20 mM acetic acid, 1 mM EDTA; pH 8

x-tracta gel extraction tools (Sigma-Aldrich, cat. no. Z722390)

ZR-96 Zymoclean Gel DNA Recovery Kit (Zymo Research, cat. no. D4022)

GenElute Gel Extraction Kit (Sigma-Aldrich, cat. no. NA1111)

4.10. Ligation into pRDVLnew

4.10.1. Overview

To incorporate promoter elements, a ribosome binding site, the *tolA* Spacer, and mRNA-stabilizing stem-loops, purified DNA fragments are cloned into the pRDVLDnew vector using the restriction enzymes *Bam*HI and *Hin*dIII (**Figure 9**).

4.10.2. Restriction digest of DNA fragments

Purified PCR products are digested with 1 µL each of FastDigest restriction enzymes *Bam*HI and *Hin*dIII in a final volume of 60 µL. The digestion is performed at 37°C for 40 min, followed by heat-inactivation of the enzymes at 80°C for 10 min. Depending on the number HT RD selections performed in parallel, different kits for PCR purification are recommended. For up to 24 parallel selections, the DNA is purified using a spin column-based kit (QIAquick PCR Purification kit), while for a greater number, a 96-well plate-based purification (ZR-96 DNA Clean & Concentrator-5 kit) is used. Both purifications are performed following the manufacturers' protocols, except for the elution step of the ZR-96 DNA Clean & Concentrator-5 kit, which is performed using homemade elution buffer (5 mM Tris-HCl, pH 8.5). DNA concentration is quantified using a UV-Vis spectrophotometer.

Materials

FastDigest *Bam*HI (Thermo Scientific, cat. no. FD0055)
FastDigest *Hind*III (Thermo Scientific, cat. no. FD0505)
10× FastDigest buffer (Thermo Scientific, cat. no. B64)
ZR-96 DNA Clean & Concentrator-5 kit (Zymo Research, cat. no. D4067)
QIAquick PCR Purification kit (QIAGEN, cat. no. 28106)
NanoDrop UV-Vis spectrophotometer (Thermo Scientific, cat. no. ND-ONE-W)

4.10.3. Ligation into pRDVLDnew

Digested PCR fragments are ligated into the *Bam*HI – *Hind*III digested pRDVLDnew vector with a molar ratio of vector to insert of 1:5, using a maximum of 300 ng of digested pRDVLDnew in a final volume of 20 µL. The ligation reactions are incubated at 22°C for 45 min, followed by heat inactivation of the enzyme at 70°C for 10 min. The resulting ligated plasmid is not used for transformation, but directly used as a template for subsequent PCR amplification with the outer primers T7B and tolAk (**Section 4.11**). If further diversity is desired at this point, an error-prone PCR may be performed instead (**Section 4.12**).

Materials

*Bam*HI – *Hind*III digested pRDVLDnew

T4 DNA ligase (Thermo Scientific, cat. no. EL0011)
10× T4 DNA ligase buffer (Thermo Scientific, cat. no. B69)
NanoDrop UV-Vis spectrophotometer (Thermo Scientific, cat. no. ND-ONE-W)
PCR plates (Corning, cat. no. PCR-96-FS-C)
PCR thermocycler (Bio-Rad, cat. no. 1851196)

4.11. Preparation of starting material for the next round of Ribosome Display

4.11.1. Overview

At the end of rounds 1, 2 and 3 of HT RD, DNA pools are ligated into the vector pRDVLDnew, which is then used as a template for PCR amplification with the outer primers, T7B and tolAk to introduce the T7 promoter, RBS, and 5' and 3' stem loops. The amplified PCR products then serve as template for in vitro transcription, thereby initiating the next round of HT RD selection.

4.11.2. PCR amplification of the DNA pools in the pRDVLDnew vector

The reaction mixture (50 µL total) consists of:

10.0 µL	5× Herculase II buffer
2.0 µL	dNTP mix (5 mM each)
2.5 µL	DMSO
0.25 µL	T7B primer (100 µM)
0.25 µL	tolAk primer (100 µM)
x µL	ligated DNA (50 ng total)
0.25 µL	Herculase II Fusion DNA polymerase
Nuclease-free water is added to 50 µL	

Thermal cycling is performed with a hot-start protocol to improve specificity:

Initial denaturation: 95°C for 5 min
30 cycles (28 cycles in round 3):
  95°C for 30 s
  68°C for 45 s
  72°C for 1 min
Final extension: 72°C for 5 min

4.11.3. In vitro transcription (later rounds of HT RD)

Following amplification (optionally with error-prone PCR), in vitro transcription is essentially carried out as described in **Section 4.3**. The transcription reaction is incubated at 37°C for 2.5 h. However, unlike the transcription preceding the first round, to eliminate any residual DNA,

20 U DNase I solution (10 U/µL) and 6.6 mM $MgCl_2$ are added, followed by an additional incubation at 37°C for 20 min.

4.11.4. mRNA purification (later rounds of HT RD)

During later rounds of HT RD, mRNA is immediately purified using the NucleoMag RNA Kit in combination with a KingFisher Flex device. Four 96-well deep-well plates and one 96-well KingFisher plate are prepared as follows:

Lysis/Binding Plate with 250 µL Lysis buffer MR1, 350 µL Binding buffer MR2 and 27.5 µL magnetic beads per well
MR3 Wash Plate with 600 µL Washing buffer MR3 per well
MR4 Wash I and II Plates each with 900 µL Washing buffer MR4 per well
In addition, a 96-well KingFisher plate is pre-filled with 50 µL elution buffer MR5 buffer to collect the purified RNA

The entire transcription reaction is transferred to the Lysis/Binding plate using a manual 96-channel pipetting system. Plates are loaded onto the KingFisher Flex device at 4°C, and the following purification program is executed:

5 min incubation in the Lysis/Binding plate
10 min beads drying
5 min wash in MR3
5 min wash in MR4 I
5 min wash in MR4 II
15 min beads drying
10 min elution in MR5

After this step, the procedure is continued to begin the next round of HT RD selection at **Section 4.3 mRNA quantification**, followed by **Section 4.4. in vitro translation.**

Materials

PCR amplification

See **Section 4.3**

in vitro transcription

See **Section 4.3**

DNase I (Roche, cat. no. 04716728001)

100 mM $MgCl_2$: Dissolve in nuclease-free water; store at −20°C

RNA purification

See **Section 4.3**

NucleoMag RNA Kit (Macherey-Nagel, cat. no. 744350.1)

KingFisher Flex system (Thermo Scientific, cat. no. A39966)
Liquidator96 (Mettler Toledo, cat. no. 17010335)
Filter tips for Liquidator96 (Mettler Toledo, cat. no. 17010646)

4.12. Optional step: Affinity maturation

4.12.1. Overview

Instead of conventional PCR with the outer primers, error-prone PCR can be used. Error-prone PCR is a powerful technique for introducing controlled random mutations into enriched DNA libraries during Ribosome Display, significantly enhancing library diversity. Unlike other selection methods, Ribosome Display enables continuous evolution of the binding library by incorporating mutations across the entire DNA pool, which occur at a low rate during the many PCR amplification steps. However, to increase this rate, it is necessary to deliberately introduce additional random errors during amplification. This process further expands the library's diversity beyond its initial composition, facilitating the identification of novel binders with improved affinity, specificity, or stability. It can be applied to either the entire pool, to the enriched pool in a later selection round, or to an individual binder [89, 112, 142, 144, 147, 150, 151, 153-156]. While these examples were not carried out in the HT RD workflow but with "classical" RD, more recent HT RD examples with affinity maturation have not been published yet.

It has often been found that it is most efficient to carry out this step at round 3, by which point the pool has already been enriched. As already described for off-rate selection (**Section 4.5.4**), it is useful to carry out a "rescue round", and even more appropriate after error-prone PCR, since the rather harsh conditions can reduce the number of molecules. This means that a fourth round under rather non-selective pressure is performed to merely amplify all molecules obtained in the selective round(s).

The mutation rate is modulated by varying concentrations of nucleotide analogues (e.g., dPTP and 8-oxo-dGTP) [157], such as 0, 3, or 10 µM, which yield distinct levels of mutational loads. This strategy has the advantage that both transitions and transversions are generated. Since the mutation rate is typically unknown, mixing libraries generated under different conditions allows the selection itself to determine the optimal error rate. The tightest binders are best obtained with off-rate selection (see **Section 4.5**)

Concentrations of nucleotide analogues up to 20 µM may be used, although PCR product yield is significantly reduced at this level. Using Platinum Taq Polymerase (Invitrogen), a mutational load of approximately 1.5 mutations per kb is achieved with 1 µM nucleotide analogues, and 3.2 mutations per kb with 3 µM. These mutation rates assume fresh nucleotide analogue

batches, as hydrolysis of triphosphates can decrease incorporation efficiency. A low to medium mutational load, applied over two or three selection rounds, is recommended to balance library diversity and protein functionality. Excessive mutation rates may increase the risk of protein misfolding, potentially leading to non-specific interactions between library members and the surface of the selection vessel.

4.12.2. Method: Error-prone PCR for Enriched Library Diversification

PCR reactions of 50 µL are prepared with varying concentrations of nucleotide analogues (1–10 µM) to introduce controlled mutations. The reaction mixture is composed as follows:

5.0 µL	10× Taq Polymerase buffer
3.0 µL	$MgCl_2$ (50 mM)
4.0 µL	dNTP mix (5 mM each)
x µL	dPTP and 8-oxo-dGTP (adjusted to desired concentration, e.g., 1–10 µM)
0.5 µL	T7B primer (100 µM)
0.5 µL	tolAk primer (100 µM)
x µL	pRDVLDnew_DARPin template (50 ng)
0.2 µL	Platinum Taq polymerase
Nuclease-free water is added to 50 µL	

Thermal Cycling Conditions

A hot-start protocol is employed to enhance specificity. Cycling parameters are adjusted based on the primers and template used. A typical protocol is as follows:

Initial denaturation at 95°C for 3 min
25 cycles of:
  95°C for 30 s
  50°C for 30 s
  72°C for 1 min
Final extension at 72°C for 5 min

The size and integrity of PCR products are verified by agarose gel electrophoresis. PCR products are pooled in equimolar amounts to serve as a template for in vitro transcription.

Materials

Platinum® Taq DNA Polymerase (5 u/µL; Invitrogen, cat. no. 10966083) and 10× polymerase buffer.

50 mM $MgCl_2$ provided with the Platinum® Taq DNA Polymerase

DARPin encoding DNA in pRDVLDnew

dNTP mix: 5 mM each (Eurogentec, cat. no. NU-0010-10)

Nucleotide analogs dPTP and 8-oxo-dGTP (Jena Biosciences) at 100 µM in nuclease-free water, aliquot and store at −20°C.

Primers dissolved to 100 µM in nuclease-free water; aliquot and store at −20°C

T7B: 5'-ATACGAAATTAATACGACTCACTATAGGGAGACCACAACGG-3'

tolAk: 5'-CCGCACACCAGTAAGGTGTGCGGTTTCAGTTGCCGCTTTCTTTCT-3'

C. Screening and characterization of individual binders

5. Parallel subcloning into *E. coli* expression plasmids for small scale expression and screening

5.1. Overview

After the HT RD rounds, the final binder candidates are obtained as an enriched pool of mRNA variants in vitro. To isolate these binders as individual molecules for further evaluation, cloning is required. Specifically, *E. coli* cells are transformed such that, on average, only one copy of the genetic information is introduced per cell, given the unique sequence of each mRNA variant.

For this purpose, the final mRNA pool is reverse-transcribed, PCR-amplified and inserted into an *E. coli* expression plasmid, a pQIq derivative [158] containing a *lacIq* gene and T5/lac promoter. The selected vector is designed to incorporate N-terminal and C-terminal tags into the DARPins. Typically, an N-terminal His tag ($MRGSH_6$) is used for purification alongside a C-terminal FLAG tag, although alternative tags can be used [35-54, 56-61, 159]. The choice of tags is guided by the intended screening strategy (see next sections). It is important to assess whether the anti-tag antibody may cross-react with the target; if so, selecting an alternative tag is necessary. If tags have to be avoided altogether, such as due to steric constraints, binding can be detected using a polyclonal anti-DARPin serum, which recognizes DARPins regardless of their target specificity [160].

Before conducting specific assays, such as binding to cells or enzyme inhibition, semi-quantitative binding data are obtained, to narrow down the potentially large pool of candidates. In some projects, several hundred binders have been initially identified [35-54, 56-61, 159].

For this purpose, a small-scale expression (110 µL) in 96-well microtiter plates is carried out, enabling the evaluation of a very large number of candidate clones. The bacterial cells are lysed and the crude extracts are tested for binding (see following section). It should be noted

that, while DARPin expression yields are reasonably consistent, variability in lysis efficiency is observed under high-throughput conditions, as not all cell suspensions are lysed quantitatively. Consequently, the signal obtained in downstream screening, like ELISA (Enzyme-linked Immunosorbent Assay), HTRF (Homogeneous Time-Resolved Fluorescence) or flow cytometry, from crude extract reflects a combination of affinity, expression yield and lysis efficiency. Therefore, hit validation (see below) is critical, as it confirms the initial findings with purified candidate binders at normalized concentration following the testing of crude extracts.

5.2. Cloning into expression vector

PCR fragments digested with *Bam*HI – *Hin*dIII are ligated into a ligation-ready *E. coli* expression plasmid, specifically a pQIq derivative [158] (**Figure 16**), at a molar ratio of vector to insert of 1:5. Usually 100 – 150 ng of the *Bam*HI – *Hin*dIII - digested and dephosphorylated pQIq derivative is used in a final ligation volume of 20 µL. Using 1 U of T4 DNA ligase, the DNA is ligated at 22°C for 45 min followed by heat inactivation. Subsequently, 4 µL of the ligation reaction is used for transformation of *E. coli* XL1-Blue cells. For each sample pool, 2 dilutions (1:2 and 1:5) are prepared in a final volume of 200 µL of 2×YT medium. These dilutions are spread onto 12 × 12 cm petri dishes, each containing 60 mL of 2×YT agar supplemented with 100 µg/mL ampicillin and 3% sucrose and incubated at 37°C overnight.

Materials

FastDigest *Bam*HI (Thermo Scientific, cat. no. FD0055)

FastDigest *Hind*III (Thermo Scientific, cat. no. FD0505)

10× FastDigest buffer (Thermo Scientific, cat. no. B64)

T4 DNA ligase (Thermo Scientific, cat. no. EL0011)

10× T4 DNA ligase buffer (Thermo Scientific, cat. no. B69)

E. coli XL1 Blue cells (Agilent, cat. no. 200249); genotype: *recA1 endA1 gyrA96 thi-1 hsdR17 supE44 relA1 lac [F proAB lacIqZΔM15 Tn10 (Tet^r)]*

2×YT medium (Condalab 1507)

12 × 12 cm Petri Dish (Greiner, cat no. 688102)

2×YT agar (Carl Roth, cat. no. X967.1)

5.3. Small scale expression in microtiter plates

The following morning, the two agar plates containing different dilutions of the transformation, are checked for the suitability for the K6-2 automated colony picker, i.e. whether separate colonies of sufficient number are seen. If suitable, either 190 or 380 colonies per binder pool are transferred from the agar plate to either two or four microtiter plates, each well containing

100 µL of LB medium supplemented with 100 µg/mL ampicillin and 1% glucose. The well position H12 is reserved for manually added controls. These controls are *E. coli* XL1 Blue transformed with a plasmid encoding either the control DARPin E3_5 [97, 161] or off7 [116]. The microtiter plates are covered with a lid and incubated at 37°C, 300 rpm, and relative humidity of 85 % for 16 h in a Multitron shaker equipped with two microtiter boxes to minimize media evaporation.

The next morning, expression microtiter plates are prepared by filling each well with 90 µL of TB media followed by the transfer of 10 µL of overnight cultures to the corresponding well of the expression plates. These plates are incubated at 37°C, 300 rpm, and a relative humidity of 85 % for 60 min.

Meanwhile, 80 µL/well of LB/glycerol/ampicillin is added per well to the overnight cultures, which are designated as the master glycerol stock plates and stored at −80°C.

DARPin expression is induced by adding 10 µL per well of TB/IPTG, achieving a final IPTG concentration of 0.5 mM. Expression is carried out at 37°C, 300 rpm, and 85 % relative humidity for 3 h. Following expression, *E. coli* cells are lysed by adding 13 µL per well of B-Per Direct solution, prepared according to the manufacturer's instructions. Alternative lysis reagents, such as FastBreak Cell Lysis, can be used as well. The plates are shaken at 750 rpm for 1 minute on a Heidolph Titramax shaker at room temperature and left at room temperature until cultures become clear, which can take up to 1 h. These plates, referred to as crude extract plates, are stored at −20°C until further use.

Materials

K6-2 colony picker (KBiosystems)

96-well U-bottom microtiter plate (MTP) (Greiner, cat. no. 650201)

Lid (Greiner, cat. no. 656170)

Infors HT Multitron Pro shaker

LB/Glucose/Ampicillin: LB medium (Condalab, cat. no. 1551), 1% glucose, 100 µg/mL ampicillin

LB/Glycerol/Ampicillin: LB medium (Condalab, cat. no. 1551), 30% glycerol, 100 µg/mL ampicillin

TB/Amp/IPTG: TB medium, 100 µg/mL ampicillin, 50 mM IPTG

B-Per Direct (Thermo Scientific, cat. no. 90080)

FastBreak Cell Lysis Reagent (Promega Corp., cat. no. V8573)

6. Initial screening of crude extracts

6.1. Overview

The initial screening is done using *E. coli* crude extracts containing the expressed DARPin candidates to be tested. In the initial screening phase, a total of 190-380 crude extracts are screened per target. Typically, these crude extracts are tested through ELISA (**Section 6.2**) or HTRF [162] (**Section 6.3**) methodologies. Both methods have their pros and cons: ELISA is a very robust technology, which requires more pipetting steps, however. Since the target is available in biotinylated form anyway (from the HT RD rounds), a directed immobilization without the danger of denaturation on the ELISA plate is possible. In HTRF, a simple measurement in solution can be carried out. Förster energy transfer is measured between one bead and a labeled detection reagent (e.g. a labeled anti-tag antibody). HTRF thus also requires immobilization of the target. The strength of the signal is not only dependent on affinity, but also on the geometry of the interaction. Furthermore, when the analyte concentration (the binder) is high, it can saturate the antibodies, preventing the formation of the sandwich complex (often referred to as the hook effect) [163].

For specific projects, it was required to identify DARPins binding to a cell surface receptor at early stages using bacterial crude extracts. Therefore, a workflow based on flow cytometry as the initial screening has also been developed and implemented [45, 56] (**Section 6.4**). Ultimately, it must ***both*** be verified whether candidate binders bind on cells ***and*** whether the binding occurs through the desired target. For this reason, both ELISA and flow cytometry must be carried out. It appears more efficient to first carry out the flow cytometry, as unspecific binders to cells appear quite rare, while binders that only react in ELISA but not in flow cytometry (e.g. because the epitope is hidden on the cell surface) seem to occur more frequently. However, this is of course target-dependent.

6.2. ELISA protocol for the screening of *E. coli* crude extracts

NOTE: All solutions are prepared using ultra-pure water. Solutions are dispensed using a microplate dispenser, unless specified otherwise. Each wash step is performed using a microplate washer. During all incubation periods, ELISA plates are constantly covered with lids.

A 384-well microtiter plate is coated with 20 µL streptavidin or neutravidin at a concentration of 66 nM per well in PBS and incubated at 4°C overnight. Alternatively, the incubation can be performed at 37°C for 1 h. The coating solution is discarded, and the plate blotted dry on a stack of paper towels. All wells are then blocked with 45 µL PBS-TB (see Materials at the end of the section) at 4°C with orbital shaking at 900 rpm for 1 h. The blocking solution is discarded and the plate blotted dry on a stack of paper towels. The biotinylated target protein is

immobilized by the addition of 20 µL target solution at a concentration of 50 nM in PBS-TB. As a control for nonspecific binding, PBS-TB without the target is added. Typically, the diluted target solution is initially dispensed into a 96-well PCR plate using a multi-dispenser pipette and subsequently transferred to the ELISA plate using a manual 96-channel pipetting system. PBS-TB can be added in the same manner or by using the microplate dispenser. The plate is then incubated at 4°C with orbital shaking at 900 rpm for 1 h and subsequently washed three times with 110 µL PBS-T (PBS containing 0.1% (v/v) Tween20) per well.

To each well, 20 µL crude extract at a dilution of 1:1,000 in PBS-TB is added. The crude extract contains the DARPin of interest with an N-terminal RGS$(H)_6$ or RGS$(H)_8$ tag and a C-terminal FLAG tag. Following the incubation with the crude extract, the plate is washed three times with 110 µL PBS-T. Detection of target-bound DARPins is carried out utilizing the C-terminal FLAG tag. For detection, 20 µL of the mouse anti-FLAG-M2 antibody at a dilution of 1:5,000 in PBS-TB is added to each well. The plate is incubated at 4°C with orbital shaking at 900 rpm for 1 h and then washed three times with 110 µL PBS-T. To each well, 20 µL of the alkaline phosphatase-coupled goat anti-mouse IgG secondary antibody at a dilution of 1:10,000 in PBS-TB is added. The plate is then incubated at 4°C with orbital shaking at 900 rpm for 1 h and washed four times with 110 µL PBS-T. Finally, 20 µL pNPP (4-nitrophenyl phosphate disodium salt) substrate at a concentration of 3 mM in 50 mM $MgCl_2$ and 50 mM $NaHCO_3$ is added to each well. After incubating the plate at 37°C with orbital shaking at 900 rpm for 30 min, the OD_{405nm} is measured using an ELISA plate reader. By comparing the signal intensities between wells containing the target and their respective control wells, DARPins specifically binding to the target are identified.

In cases where the primary mouse anti-FLAG-M2 antibody interferes with detection, as it may bind directly to the target protein, the DARPin can be expressed with a C-terminal HA tag and the primary mouse anti-HA antibody may be used instead. Alternatively, a primary mouse anti-RGS$(His)_4$ antibody may be used as well to detect the N-terminal His-tag. When DTT is essential for maintaining the conformational integrity of the target (to avoid spurious disulfide formation), it is possible to add 1 mM DTT to all solutions up to the incubation with the crude extract [145]. In later washes and incubation steps, however, DTT has to be excluded entirely, to ensure proper binding of the detection antibodies.

Materials

384-well microtiter plates (Greiner, cat no. 781061)

96-well PCR plates (Axygen, cat. no. PCR-96-FS-C)

Lids with condensation rings (Greiner, cat no. 656170)

Microplate dispenser (Agilent, BioTek MicroFlo Select)

Microplate washer (Agilent, BioTek ELx405 Select CW)
Liquidator96 (Mettler Toledo, cat. no. 17010335)
Shaker for microplates (Heidolph Titramax 1000)
Shaker/Incubator combi (Heidolph Titramax 1000/Incubator 1000)
Multi dispenser pipette (Eppendorf Multipette E3, cat. no. 4987000010)
Microplate reader (Agilent, BioTek Synergy HT)
Streptavidin (Pierce, cat no. 21125) or Neutravidin (Pierce, cat. no. 31000): dissolve 1.2 mg/mL in water (300× stock), store at −20°C; the final working concentration is 66 nM
PBS: 137 mM NaCl, 3 mM KCl, 8 mM Na_2HPO_4, 1.5 mM KH_2PO_4; pH 7.4
PBS-T: PBS containing 0.1% (v/v) Tween20
PBS-TB: PBS containing 0.1% (v/v) Tween20 and 0.2% (w/v) BSA
Mouse anti-FLAG-M2 antibody (Sigma-Aldrich, cat. no. F3165), mouse anti-HA antibody (Sigma-Aldrich, cat. no. H9658) or mouse anti-RGS(His)$_4$ antibody (QIAGEN, cat. no. 34650)
Alkaline phosphatase-coupled goat anti-mouse IgG antibody (Sigma-Aldrich, cat. no. A3562)
4-nitrophenyl phosphate disodium salt (Sigma-Aldrich, cat no. 71768): 1 M stock in pNPP buffer, store at −20°C; the final working concentration is 3 mM
pNPP buffer: 50 mM $MgCl_2$, 50 mM $NaHCO_3$

6.3. HTRF protocol for the screening of *E. coli* crude extracts

NOTE: All HTRF reagents (Cisbio) are delivered in lyophilized form and must be resuspended as recommended by the manufacturer. Then the reagents are aliquoted and frozen at −20°C. The HTRF donor reagent, Lumi4®-Tb cryptate conjugated to streptavidin, is binding to the biotinylated target protein (usually the same as was used as target in HT RD). The HTRF acceptor reagent, an anti-FLAG antibody labeled with the chromophore d2, is binding to the FLAG-tagged DARPin.

A white flat bottom 384-well plate is filled with 20 µL/well of PBS/0.5 % BSA. The plate is incubated at 4°C and orbital shaking at 1000 rpm overnight. In the next morning, the plate is washed once with 20 µL/well of PBS/0.2% BSA. The plate is then emptied and dried. 5 µL of 1:1,000 diluted crude extract is added to each corresponding well. Always two 96-well crude extracts plates are pooled on one 384-well plate, this allows for measuring each binder plus and minus target protein. Usually, the dilution and the addition of the crude extracts is done using a CyBio FeliX robot. The HTRF reagents working stocks (Cisbio) are prepared as 2 × the final dilution in PBS/0.2% BSA. 10 µL/well of this HTRF reagent stock are added to the crude extracts in the 384-well plate. The target protein working stocks are prepared in a PCR plate, at 4 × the final dilution (32 nM) in PBS/0.2% BSA. In well H12, the control protein MBP is

prepared. 5 µL of the target protein stock are added to half of the wells of crude extracts and the HTRF reagents in the 384-well plate. To the other half of the wells 5 µL of PBS/0.2% BSA are added. Usually, this addition of the target stock is processed on a CyBio FeliX robot.

After 2 h of incubation, the 384-well plate is read on a Perkin Elmer EnVision instrument. The HTRF signals are recorded using the following settings: delay time 60 µs, integration time 400 µs, time between flashes 2,000 µs, number of flashes 150. HTRF ratios are obtained by dividing the acceptor signal (665 nm) by the donor signal (620 nm) and multiplying this value by 10,000 to derive the 665/620 ratio.

Materials:

White 384-well plate, flat bottom (Greiner, cat. no. 784075)

HTRF donor: Lumi4®-Tb Cryptate conjugated Streptavidin (Streptavidin-Tb) (Cisbio, cat. no. 610ATLB)

HTRF acceptor: Anti-FLAG® (M2) d2 (Cisbio, cat. no. 61FG2DLB)

PCR plate (Axygen, cat. no. PCR-96-FS-C)

CyBio FeliX robot (Analytik Jena, cat. no. OL5015-24-100)

EnVision 2104 Multilabel Reader (Perkin Elmer, cat. no. 2104-0020)

6.4. Flow cytometry protocol for the screening of *E. coli* crude extracts

6.4.1. Overview

Flow cytometry (FC)-based screening is utilized in HT RD projects to identify DARPins that bind specifically to epitopes on the extracellular domain (ECD) of membrane proteins within their native cellular context. In contrast to in vitro screening with isolated ECDs, which may result in DARPins binding to inaccessible epitopes due to membrane proximity or glycosylation, FC-based screening maintains biological relevance by targeting epitopes that are accessible in the cellular environment. Direct comparison of DARPin binding between a cell line engineered to overexpress the target membrane protein and its parental (non-transformed) cell line enables the selection of highly specific binders, recognizing the membrane target. A useful system to create defined overexpression of membrane proteins is the Flp-In system [137, 141, 164]. Biological relevance, specificity of the binders selected, and its high-throughput capability screening in a 96-well plate format are three advantages of FC-based screening.

6.4.2. Screening setup considerations

Each crude extract (CE) contains the DARPin of interest, tagged with a C-terminal FLAG tag, which is detected using an anti-FLAG antibody conjugated to allophycocyanin (APC).

Controls. Four controls are incorporated into each 96-well plate to ensure assay reliability. A homogeneous population of single cells is defined via forward and side scatter, using a cell-only control. Cell viability is evaluated with Zombi NIR (diluted 1:1000 in PBS only), as the live/dead staining control. Background fluorescence is quantified by incubating cells with anti-FLAG-APC antibody alone (diluted 1:1000), in the absence of DARPin, acting as the negative control. Target protein expression is confirmed prior to screening using a fluorophore-conjugated, target-specific antibody.

Screening Layout. For each screening experiment, a total of four 96-well plates are used, with two plates allocated to the parental cell line and two to the overexpressing cell line. Approximately 5×10^5 cells per well are seeded, resulting in a total of 10^8 cells required per cell line across the two plates. To ensure stable expression of the target protein, cell passages are kept to a minimum, as extended passaging may lead to the overgrowth of non-transformed cells, potentially reducing target protein expression.

Washing Precautions. Washing steps are performed with care and consistently to avoid significant variation in cell numbers across wells or plates, as centrifugation will concentrate cells at the bottom of the plate, regardless of binding status. Each plate is processed individually, inverted after centrifugation, and gently tapped on an absorbent paper towel to remove residual liquid. A manual 96-channel pipetting system is recommended for accurate and uniform addition of FC buffer and for the transfer of DARPin crude cell extracts.

6.4.3. Experimental procedure

The cells are detached using Accutase, preferred over trypsin to better preserve surface-expressed proteins. After harvesting, cells are washed once with medium and twice with cold FC-buffer. During cell counting, cells are kept on ice and then centrifuged at 300 × *g* for 3 min. The cell pellets are resuspended to a final concentration of 5-10 × 10^6 cells/mL in FC buffer. A single-cell suspension is ensured using cell strainers with snap caps.

The crude extracts (CEs) are diluted in the following way: 96-well plates containing the DARPin-CEs are thawed at 4°C overnight or on the day of use at room temperature. Immediately prior to the assay, 147 µL of cold FC buffer is added to each well of a dilution 96-well plate, followed by the transfer of 3 µL of the DARPin-CEs from the source plate into the corresponding well of the dilution plate. The plates are gently shaken to ensure homogeneity. From these diluted solutions, 50 µL is transferred into FC-96-well plates labeled according to the parental or overexpressing cell line.

The cell-based binding assay consists of three key steps. First, DARPins-CE are incubated with cells. Cell suspensions of the parental and overexpressing cell lines are transferred to a StarTub Reagent Reservoir, and 50 µL of each cell suspension is added to the appropriate

wells of the FC-96-well plates. The plates are covered with lids and incubated at 4°C for 1 h. Following incubation, the plates are washed three times with 200 µL of FC buffer per well. Second, DARPins-CE bound to cells are incubated with the antibodies. All assay and control antibodies are diluted according to manufacturer's recommendations. After the final wash, 100 µL of the diluted antibody solution is added to each well and the plates are incubated at 4°C for 1 h in the dark. The plates are then washed twice with 200 µL of FC buffer per well. Finally, cells are prepared for flow cytometry. The cells are resuspended in 75 – 100 µL of FC buffer per well, and the plates are stored at 4°C in the dark, with measurements performed using a FACS Canto 2L equipped with High Throughput Sampler (HTS) within 5 h to ensure data quality.

Materials

FC-Buffer: 1 × PBS; 0.1% BSA; 0.1 % NaN_3
Accutase (Innovative Cell Technologies, cat. no. AT-104)
Anti-Flag-APC antibody (Biolegend, cat. no. 637308)
Zombi NIR (Biolegend, cat. no. 423106)
FC-96-well plate (Greiner, cat. no. 651201)
Dilution 96-well plate (Greiner, cat. no. 650201)
Cell Strainer Snap Cap, 5 mL (Falcon, cat. no. 352235)
StarTub Reagent Reservoir (Starlab, cat. no. E2310-1010)
Liquidator96 (Mettler Toledo, cat. no. 17010335)

7. Cherry-picking and sequencing

7.1. Overview

For subsequent characterizations, typically involving laborious experiments on or in cells and/or structure determinations of complexes, the number of candidate clones has to be reduced. In successful HT RD selections with well-behaved targets, the number of remaining candidates after screening can still be very large, when starting with 380 wells, and even with 190 wells. Often, we have restricted the further characterization to the 32 top clones that display unique sequences and specific binding to the target during screening to achieve a balance between exhaustive screening and the necessity to handle many targets in parallel.

In the absence of other criteria, often the clones with the highest ELISA signal are chosen or, alternatively, those with the highest signal in flow cytometry. Alternatively, to initially cover a wide variety of potentially different epitopes, in HTFR binders with rather different signals have been chosen, since a subsequent affinity maturation is always possible. For some demanding

projects, however, where it was expected that unusual properties, such as a particular epitope, were needed, a larger number or even all validated hits were further examined.

As the first step, the sequence of 32 clones (or more, if needed) is determined. In general, the sequence of all clones is different at this point, as there is no "sequence focusing", unlike in other selection technologies that go through a cell transformation step that restricts the library size. The sequence determination will normally show that at this step almost all molecules have correct reading frames.

The repeat-domain nature of the libraries used in this work can lead to the deletion of one repeat during the PCR cycles or the preferred amplification of shorter constructs, such that binders of N2C format can be obtained from an N3C library. It should be mentioned, however, that most of these still have excellent affinities, specificities and biophysical properties, and the epitope often engages only 2 repeats even in an N3C molecule. Occasionally, the repeats found in the N2C molecules resemble one of the repeats in some N3C molecules. More rarely, also N1C molecules have been obtained [46, 112], often with a more hydrophobic surface, and in some cases with still high affinities and specificities were observed (unpublished results). We suspect that these are selected to bind to an epitope offering little space.

The interesting and unique property of Ribosome Display is that it allows for somatic mutations through the PCR cycles, and of course also through deliberate error-prone PCR. This can lead to massively increased affinities, even involving residues not in direct contact with the target [112]. Alternatively, a very strongly selected binder can undergo some diversification resulting in sequences that are functionally equivalent. Furthermore, rare mutations in the original library can be amplified (e.g. a shortened loop), if they lead to a better fit to the target.

Therefore, after the sequencing, typically an alignment is done to determine the number of repeats, composition of the randomized regions and the appearance of additional framework mutations. It is useful to plot the sequences in a repeat-wise manner, in a similar fashion as shown in Suppl. Fig. 3C of [115].

While there has been enormous progress in next-generation sequencing [165-168], which can illuminate pathways of evolutionary changes and enrichment, we have not used it in this workflow, since there is in general no simple correlation between the level of enrichment and the desired properties of the binder.

At this stage, it would be convenient if the epitope, and more precisely the structure of the DARPin-target complex, could be determined computationally. However, while this is possible in some cases [169], it is clearly still far from general, even though the prediction of the target structure by itself is usually very good, and that of the DARPin by itself can be considered equivalent to an experimental structure. However, at the time of writing, extensive testing with

AlphaFold 2 or AlphaFold multimer [170, 171], as well as with AlphaFold 3 [170] and Alpha-Red [172] with crystallized but not published DARPin-target complexes has shown correct epitope identification and DARPin orientation only in a fraction of the cases. AI-based docking is trained on the co-evolution of natural protein complexes and compensatory mutations, but since neither antibodies and antigens co-evolve, nor DARPins with their target, this evolutionary signature is missing.

7.2. Experimental procedure for cherry-picking and sequencing

Glycerol master plates, as described in **Section 5.3**, are fully thawed on shakers at room temperature or 37°C. A 96-well plate is prepared by dispensing 100 µL of LB medium supplemented with 100 µg/µL ampicillin and 1% glucose into each well. A BioRobot 8000 or comparable pipetting system is employed to inoculate each well with 10 µL of glycerol stock from the selected clones. Clones from up to twelve 96-well plates can be pooled into a single destination 96-well plate. This destination plate is incubated at 37°C with shaking at 300 rpm and 85% relative humidity for 16 h.

On the subsequent day, 45 µL of LB medium containing 100 µg/mL ampicillin and 1% glucose is dispensed into each well of a barcoded PCR plate to be sent for sequencing using the primer Qe30-for. Each well is inoculated with 5 µL of the overnight culture, and the plate is incubated at 37°C with gentle shaking at 50 rpm for 4 h prior to shipment to a sequencing company.

To the remaining overnight culture, 80 µL of LB medium supplemented with 100 µg/µL ampicillin and 30% glycerol is added per well, creating a glycerol stock for subsequent small-scale expressions.

Materials

BioRobot 8000 (QIAGEN)

96-well U-bottom microtiter plate (MTP) (Greiner, cat. no. 650201)

Microplate shaker (Heidolph Titramax 1000)

Primer Qe30-for: 5’-CTTTCGTCTTCACCTCGAG-3’

LB/Glucose/Ampicillin: LB medium (Condalab, cat. no. 1551), 1% glucose, 100 µg/mL ampicillin

LB/Glycerol/Ampicillin: LB medium (Condalab, cat. no. 1551), 30% glycerol, 100 µg/mL ampicillin

Microtiter plate lid (Greiner, cat. no. 656170)

Infors HT Multitron Pro shaker

7.3. Methods for sequence analysis

Raw sequencing data generated externally are first analyzed to distinguish clones with clear, unambiguous sequences from those exhibiting any ambiguity. Ambiguous sequences are subsequently categorized into double clones and clones with other sequence deviations.

Double clones, characterized by double peaks predominantly in the randomized regions, are typically resulting from the transformation of two plasmids with distinct DARPin sequences into a single *E. coli* cell (**Section 5.1, 5.2**). If the number of monoclonal binders with perfect sequence and properties meeting the project goals is insufficient, these double clones can be rescued by a process we term "monoclonalization". Plasmids in *E. coli* can coexist as monomers and covalent dimers or even multimers [173, 174], which means that different binder genes would be covalently linked in a circular plasmid. Therefore, a new digestion, ligation, transformation, and sequencing is needed. Whether these steps are necessary obviously depends on whether enough DARPins of the right specifications (e.g. binding the right epitope) have already been obtained or not.

Other sequence deviations can encompass sequences with unclear sequence positions from the sequencing process itself, such as those identified by software tools at the sequencing company, secondary peaks within the open reading frame, or truncated or non-canonical DARPin sequencing outcomes. While these issues may be partially sequence-inherent, they can also arise from issues during plasmid preparation and the sequencing process itself. To address this, re-sequencing of such clones is routinely performed following fresh inoculation.

8. Parallel small-scale expression and purification of DARPins

8.1. Overview

After the sequences of 32 (or more) clones have been verified to match the expected composition, they are expressed at a 2 mL scale in deep-well plates. The cells are chemically lysed using a detergent solution supplemented with 0.4 mg/mL lysozyme and 80 U/mL nuclease. The expressed DARPins are then purified using IMAC plates. This process permits a subsequent hit validation at normalized concentrations, and free of potential interfering components in the *E. coli* extract.

The yield from 2 mL deep-well culture is typically around 400 µg using the procedures described, which is sufficient for downstream hit validation (see next section). Variability in yield is often observed at this step, and this is the reason why it is important to normalize the concentrations before hit validation. This variability arises from several factors, such as non-uniform bacterial growth in the deep-well plates, incomplete cell lysis, and losses during the 96-well purification. While yields could be made more uniform through additional steps, such

measures would increase the complexity of the protocol, rendering it less suitable for the simultaneous expression and characterization of DARPins in batches of 96.

8.2. Expression in deep well plates

A standard 96-well U-bottom microtiter plate (MTP) is filled with 230 µL medium supplemented with glucose and ampicillin (LB/glucose/ampicillin) per well. Each well is inoculated with 10 µl from a previously thawed, corresponding *E. coli* glycerol stock plate (refer to **Section 7.2**). The MTP is shaken at 450 rpm on a microplate shaker for 2 min to ensure thorough mixing. From each well, 120 µL of the *E. coli* culture is transferred to a second standard MTP, and both MTPs are covered with corresponding MTP lids. The MTPs are incubated at 37°C, 300 rpm, and 85% relative humidity for 16 h (± 1 h). Two deep-well plates are then prepared, with each well filled with 900 µL of Terrific Broth (TB) medium. Each well is inoculated with 80 µL of the overnight culture. The deep-well plates are sealed with gas-permeable covers and incubated at 37°C, 250 rpm, and 85% relative humidity for 1 h 45 min. Protein expression is induced by adding 10 µL of TB medium supplemented with ampicillin and isopropyl β-D-1-thiogalactopyranoside (TB/Amp/IPTG). The two deep-well plates are incubated for an additional 5 h under the same conditions. The expression is stopped by centrifuging the deep-well plates at 3,200 × *g* for 10 min, after which the supernatant is discarded. The cell pellets are then stored at −80°C overnight.

8.3. Purification in deep well plates

To each bacterial pellet from a 1 mL *E. coli* expression culture, 400 µL of lysis buffer is added. The pellets are resuspended by shaking the plate at maximum rpm on a microplate shaker at room temperature for 10 min. Afterwards, the plate is incubated at room temperature for 20 to 30 min, during which the solution becomes clear, indicating complete lysis. The plate is centrifuged at 3,200 × *g* for 10 min and the supernatants (2 × 400 µL) from each well are combined in a new 96-deep-well plate.

A 96-well HisPur Cobalt Spin Plate is centrifuged at 500 × *g* for 3 min to remove the storage buffer. Each well is equilibrated with 400 µL of ultra-pure water and centrifuged at 500 × *g* for 3 min. Two additional equilibrations are then performed with 400 µL of equilibration buffer and centrifuged at 500 × *g* for 3 min. About 300 µL of each sample is applied to the purification matrix of the HisPur Cobalt plate and incubated with moderate agitation on a microtiter plate shaker for 3 min. The plate is centrifuged at 500 × *g* for 3 min, and the process is repeated until the entire sample volume has been processed. The resin with bound DARPin is washed with 350 µL of wash buffer per well and centrifuged at 500 × *g* for 3 min. This washing step is repeated additional four times. For elution, 200 µL of elution buffer is added to each well and incubated for with moderate agitation on the microtiter plate shaker for 1 min. The eluate is

collected by centrifugation at 500 × *g* for 3 min. The eluate is filtered, using a Pall AcroPrep filter plate, by centrifugation at 1,500 × *g* for 2 min.

DARPin concentrations are measured using the Pierce 660 nm assay kit. For this purpose, a 96-well flat bottom plate is prepared with 5 µL of 0.05% sodium azide buffer per well and 5 µL of the purified DARPins are added. In a second 96-well flat bottom plate, triplicates of 10 µL of pre-diluted BSA standards are added. These are used to create a standard curve which serves to calculate the concentrations of the purified DARPins. Subsequently, 150 µL of assay reagent is added to each well of both plates and the plates shaken on a microtiter plate shaker at 300 rpm for 1 min. The reaction is incubated for 5 min and absorbance at 660 nm is measured using a plate reader. DARPin concentrations are calculated based on the BSA standard curve.

A new 96-well U-bottom MTP is prepared for subsequent hit validation, containing DARPins normalized to a final concentrations of 10 µM in PBS. These dilutions are performed using an automated pipetting system.

Materials

E. coli glycerol stock plate (preparation described in **Section 7.2**)

96-well U-bottom microtiter plate (MTP) (Greiner, cat. no. 650201)

Microplate shaker (Heidolph Titramax 1000)

LB/Gluocse/Ampicillin: LB medium (Condalab, cat. no. 1551), 1% glucose, 100 µg/mL ampicillin

Microtiter plate lid (Greiner, cat. no. 656170)

Infors HT Multitron Pro shaker

96-deep well plates (Thermo, cat. no. AB0661)

TB medium: 12 g/L tryptone (Condalab, cat. no. 1612), 24 g/L yeast extract (Condalab, cat. no. 1702), 0.4% (v/v) glycerol, 17 mM KH_2PO_4, 72 mM K_2HPO_4

Gas-permeable seal (Sigma-Aldrich, cat. no. A9224)

TB/Amp/IPTG medium: TB medium, 100 µg/mL ampicillin, 50 mM IPTG

CelLytic™ B 10× (Sigma-Aldrich, cat. no. C8740)

Pierce™ Universal Nuclease for Cell Lysis (ThermoFisher Scientific, cat. no. 88700)

HisPur Cobalt Spin Plate (ThermoFisher Scientific, cat. no. 90095)

Lysis buffer: 50 mM NaH_2PO_4/Na_2HPO_4 (pH 7.4), 300 mM NaCl, 1× CellLytic B, 0.4 mg/mL lysozyme and 80 U/mL Pierce nuclease

Equilibration buffer: 50 mM NaH_2PO_4/Na_2HPO_4 (pH 7.4), 300 mM NaCl

Wash buffer: 50 mM NaH_2PO_4/Na_2HPO_4 (pH 7.4), 300 mM NaCl, 15 mM imidazole (pH 8)

Elution buffer: 50 mM NaH_2PO_4/Na_2HPO_4 (pH 7.4), 300 mM NaCl, 250 mM imidazole (pH 8)

Pall AcroPrep 96 well filter plate (Avantor, cat. no. 518-0022)

Pierce™ 660nm Protein Assay Kit (ThermoFisher Scientific, cat. no. 22662)

Pierce™ Bovine Serum Albumin Standard Pre-Diluted Set (ThermoFisher Scientific, cat. no. 23208)

0.05% sodium azide buffer: PBS, 0.05% NaN_3

Microplate reader (Agilent, BioTek Synergy HT)

PBS: 137 mM NaCl, 3 mM KCl, 8 mM Na_2HPO_4, 1.5 mM KH_2PO_4; pH 7.4

Andrew+ Pipetting Robot (Waters, cat. no. 176004568)

9. Hit validation

9.1. Overview

To validate the binding capability of unique DARPins exhibiting positive binding signals in the preliminary screening of crude extracts, a hit validation assay is performed with purified DARPins, i.e., in the absence of any potential interfering components of the *E. coli* extract. The hit validation assay also allows for a first semi-quantitative assessment of affinity, since the concentrations of the purified binders can be normalized. Furthermore, an assessment of cross-reactivity of DARPins towards structurally similar targets or isoforms can be carried out.

Depending on the nature of the target protein, this validation process can be done by ELISA or flow cytometry. For DARPins targeting extracellular domains of proteins, it is essential to use flow cytometry analysis due to the potential influence of the cell membrane on the accessibility of binding epitopes. Even if flow cytometry has been used in the crude extract screening, it is necessary to validate the findings with the purified proteins. It is still important to carry out the orthogonal testing by ELISA to exclude non-specific cell binding, or binding to another cell surface component. In this case, the integrity of the extracellular domain of the target protein must be carefully controlled.

After being validated, the potential hits should also be analyzed at this stage by size-exclusion chromatography (**Section 9.4**), in order to eliminate binding proteins that might show non-monodisperse behavior and/or some aggregation tendencies.

9.2. ELISA protocol for the hit validation of purified DARPins

Hit validation by ELISA using purified DARPins is essentially performed as the screening procedure described in **Section 6.2**. The key difference is the use of 20 µL purified DARPins at a concentration of 100 nM in PBS-TB during the hit validation. Additionally, during this step, cross-reactivity of DARPin candidates against homologous proteins or isoforms is commonly assessed. Biotinylated off-targets are immobilized as described in **Section 6.2**.

The same considerations regarding the use of alternative tags and antibodies, as outlined in **Section 6.2**, also apply to the hit validation by ELISA.

Materials and Methods

See **Section 6.2**

9.3. Flow cytometry protocol for the hit validation of purified DARPins

Flow cytometry is essentially carried out as described in **Section 6.4**. For hit validation, purified DARPins of known concentration are used, and this is essential to ensure an accurate comparison of signals. Using purified DARPins also eliminates interference from bacterial contaminants present in crude extracts, such as host cell proteins or proteases, which could skew measurements or introduce non-specific interactions. DARPin purification is described in **Section 8.3.**

Hit validation with purified DARPins is carried out as follows:

Immediately before the assay, the 10 µM DARPin stock is diluted to a final concentration of 1 µM (1:10 dilution) using a manual 96-channel pipetting system.

- 99 µL of cold FC buffer is added to each well of a dilution 96-well plate.
- 11 µL of the DARPin from the source plate is transferred into the corresponding well of the dilution plate.

Materials and Methods

See **Section 6.4**

9.4. Size exclusion chromatography (SEC)

A 96-well clear V-bottom polypropylene plate, referred to as SEC plate from here on, is loaded with 50 µL of purified DARPins (at normalized concentration of 10 µM). To prevent evaporation during analysis on the cooling unit of the Agilent HPLC instrument, the plate is sealed with Scotch tape. The HPLC system is equipped with an autosampler capable of accommodating up to two 96-well SEC plates. Samples are processed sequentially using a standardized method, with a Superdex 75 Increase column. The column is equilibrated with water at a flow rate of 0.15 mL/min for 2 h, followed by equilibration with the mobile phase, in this case, PBS for 3 h. Prior to each analytical campaign, a protein standard mix is analyzed to assess column performance and to estimate the molecular weight of the binders, ensuring accuracy without reliance on previous standard runs.

The following method is used in the SEC procedure. The mobile phase, PBS, is run at a flow rate of 0.15 mL/min through the SEC column. A 10 µL sample is injected, and absorbance at

230 nm, 260 nm, and 280 nm is monitored for 30 min. Following the run, the column is equilibrated with PBS for an additional 10 min. The chromatographic profile and molecular weight of the binder are determined, based on the absorbance data at 280 nm collected during the 30 min run.

Materials

96-well clear V-bottom polypropylene: Costar storage plate (Corning Inc., cat. no. 3363)
Magic tape 810 (Scotch, cat. no. 810-1933)
Agilent HPLC 1260 Infinity (Agilent Technologies)
Superdex 75 Increase 5/150 GL column (Cytiva, cat. no. 29148722)
PBS: 137 mM NaCl, 3 mM KCl, 8 mM Na_2HPO_4, 1.5 mM KH_2PO_4; pH 7.4
Protein standard mix (Sigma-Aldrich, cat. no. MWGF70)

10. Medium scale expression and purification and reformatting for applications

10.1. Overview

After hit validation, DARPins that bind the target will have been identified. At this stage, specificity as well as cross-reactivity against homologous targets or those from a different species can usually be assessed with the amount of protein obtained in this small-scale purification. Since the next steps will be an application- and target-dependent characterization, resulting in a further reduction of the number of candidates, the more quantitative evaluation of binding (regarding e.g. equilibrium affinities (K_D) or dissociation rate constants (k_{off})) or epitope mapping is typically conducted only on this smaller number of clones.

Therefore, in many cases re-cloning into eukaryotic expression vectors is carried out at this stage, e.g. for DARPins to be tested intracellularly, and/or sometimes as fusion proteins [35-61]. The literature examples give some guidance, but the strategy will obviously depend on the intended application. DARPins have been successfully expressed in many cell types and cellular compartments and therefore, this expression and characterization technology can be broadly applied.

It is usually advantageous to convert the DARPins emerging from the hit validation into the configuration required for their intended application, allowing to directly evaluate their properties in this format. Examples include trimeric adapters for adenovirus retargeting [45], biosensors fusions [39, 54], fusions to engage the ubiquitin proteasome system [37, 76, 175], or large assemblies to facilitate structure determination by electron microscopy [72] or in a host-guest system for x-ray crystallography [51].

Often, for the final binders obtained from the HT RD selection, the structure of the complex was determined, either by x-ray crystallography [41, 42, 44, 48, 51, 55, 58, 76] or cryo-electron microscopy [52, 53, 72]. For this reason, we provide an expression and purification scheme suitable for structure determination by x-ray crystallography.

10.2. Medium-scale purification for structure determination or labeling

For structural studies or detailed characterization (e.g., labeling), DARPins must be produced at a larger scale. The following protocol details the expression and purification of DARPins in *E. coli,* typically in a scale of 200 mL (described here) or 1 L.

10.2.1 DARPin expression

The *E. coli* strain BL21 (DE3) (genotype see Materials) is most suitable for expression, as it is devoid of protease activity of Lon and OmpT. The DE3 prophage carrying an inducible T7 polymerase is not used here, and BL21 can be used just as well. Since DARPins are very robust, other *E. coli* strains can be used as well, provided expression is induced only when needed [176].

A 200 mL volume of Terrific Broth (TB) supplemented with 100 µg/mL ampicillin is inoculated with 4 mL of an overnight culture (1:50 dilution) of *E. coli* BL21 (DE3) containing the construct of interest in a pQIq vector [158]. The culture is incubated at 37°C with shaking at 240 rpm (25 mm amplitude shaker) for approximately 2 h until an OD_{600nm} of 0.8 to 1.0 is reached. DARPin expression is induced by the addition of 500 µM isopropyl β-D-1-thiogalactopyranoside (IPTG). Incubation is continued at 37°C for 4 h with shaking. Cells are harvested by centrifugation at 4°C and 4,000 × *g* for 15 min. The cell pellet is washed with 20 mL of ice-cold PBS, directly purified or flash-frozen in liquid nitrogen and stored at −80°C until purification.

10.2.2 DARPin purification

DARPins are purified through a two-step process involving immobilized metal affinity chromatography (IMAC) followed by buffer exchange, performed on an ÄKTA Pure system equipped with a HisTrap FF crude (1 mL) column and a HiPrep 26/10 desalting column. An autosampler is integrated into the system, enabling sequential purification of up to eight DARPins.

Cell lysis. The bacterial pellet is thawed at 4°C overnight in an ice-filled bucket. Cells are resuspended in 3.6 mL of lysis buffer, and 100 units of Pierce Universal Nuclease are added. Lysis is achieved through two cycles of sonication (5 min per cycle) using an automated sonifier. The lysate is clarified by ultracentrifugation at 4°C and 20,000 × *g* for 30 min. The supernatant is supplemented with 1.2 mL (1/4 volume) of 5× Ni-adjusting buffer. The

supernatant is filtered through a 0.2 µm filter, transferred into a 6 mL headspace crime top vial, and loaded into the ALIAS autosampler.

IMAC purification. IMAC is performed using a 1 mL Ni-NTA HisTrap FF crude column equilibrated with running buffer. The clarified supernatant is loaded onto the column. Bound proteins are washed sequentially with low-salt wash buffer, high-salt wash buffer, and running buffer. Proteins are eluted with elution buffer.

Buffer exchange and analysis. Eluted proteins are buffer-exchanged into storage buffer using a HiPrep 26/10 desalting column. Protein concentration is determined using the Pierce 660 nm assay kit, as described in **Section 8.3**. Purity is assessed by SDS-PAGE. The pure fractions are pooled, aliquoted, flash-frozen in liquid nitrogen, and stored at −80°C.

Column regeneration. For sequential purification of up to eight DARPins, the HisTrap FF crude column is regenerated between runs. The column is washed with the following sequence: running buffer (2 column volumes (CV)), water (5 CV), stripping buffer (5 CV), running buffer (5 CV), water (5 CV), recharging buffer (5 CV), water (5 CV), elution buffer (5 CV). The HiPrep 26/10 desalting column is washed with storage buffer (1.6 CV) before the next sample is loaded.

Materials

E. coli BL21 (DE3) (Novagen, cat. no. 69450); genotype: *B F– ompT gal dcm lon hsdSB(rB–mB–) λ(DE3 [lacI lacUV5-T7p07 ind1 sam7 nin5]) [malB+]K-12(λS)*

ÄKTA Pure chromatography system (Cytiva, cat. no. 29018224)

ALIAS Autosampler (Cytiva, cat. no. 29347721)

HisTrap FF crude (GE Healthcare, cat. no. 11-0004-58)

HiTrap 26/10 Desalting (GE Healthcare, cat. no. 17-5087-01)

Pierce™ Universal Nuclease for Cell lysis (Thermo Scientific, cat. no. 88702)

0.22 µm Millipore filter, type GSWP (Millipore, cat. no.GSWP04700)

Pierce™ 660nm Protein Assay Kit (ThermoFisher, cat. no. 22662)

6 mL Headspace Crime Top vials (Thermo Scientific, cat. no. 6-CV)

Ethanol without any additive

All buffers are filtered through 0.2 µm filter and degassed for 30 min (500 mL) or 1 h (1 L)

Lysis buffer: 20 mM Na_2HPO_4/NaH_2PO_4, 500 mM NaCl; pH 7.4 at 4°C

5× Ni-adjusting buffer, adapted to the His-tag type used: for 6-His-tag DARPins, the buffer contains 20 mM Na_2HPO_4/NaH_2PO_4, 500 mM NaCl, 100 mM imidazole, 50% glycerol; pH 7.4 at 4°C; for 8-His-tag DARPins, 250 mM imidazole is used instead.

Running buffer: 20 mM Na_2HPO_4/NaH_2PO_4, 500 mM NaCl, 20 mM imidazole for 6-His-tag or 50 mM imidazole for 8-His-tag, 10% glycerol; pH 7.4 at 4°C

Low-salt wash buffer: 20 mM Na_2HPO_4/NaH_2PO_4, 137 mM NaCl, 20 mM or 50 mM imidazole, 10% glycerol; pH 7.4 at 4°C

High-salt wash buffer: 20 mM Na_2HPO_4/NaH_2PO_4, 1 M NaCl, 20 mM or 50 mM imidazole, 10% glycerol; pH 7.4 at 4°C

Stripping buffer: 20 mM Na_2HPO_4/NaH_2PO_4, 500 mM NaCl, 50 mM EDTA; pH 7.4 at 4°C

Recharging buffer: 100 mM $Ni(SO_4)_2$

Elution buffer: 20 mM Na_2HPO_4/NaH_2PO_4, 500 mM NaCl, 250 mM imidazole, 10% glycerol; pH 7.4 at 4°C

Storage buffer: 8 mM NaH_2PO_4, 1.5 mM KH_2PO_4, 400 mM NaCl, 2.7 mM KCl, 10% glycerol; pH 7.4 at 4°C

10.2.3 Variations and additional chromatography steps

DARPins can alternatively be expressed by autoinduction in 1 L autoinduction medium [177] at 25°C for 24 h.

An alternative lysis method is to use a French Press: Lysis buffer is added and cells are lysed with a French press.

For biological assays, it is essential to also remove nucleic acids and other components. Protein samples are diluted 1:1 with double-distilled water for subsequent anion exchange chromatography (AEX) using a MonoQ 5/50 GL column on an ÄKTA Pure system. The protein is loaded using AEX running buffer and eluted by gradient from 0-100% elution buffer over 40 CV. Samples are pooled and flash-frozen in liquid nitrogen for storage at −80°C.

For structure determination of complexes, AEX of the DARPin is advantageous but not absolutely necessary, since the complex with target must be purified by preparative SEC. The purification of the target is of course completely dependent on its nature. Protein complexes are usually mixed with an excess of the DARPin, since the target needs to be saturated. The complexes are isolated by preparative SEC using a HiLoad 16/600 SD 75 pg or a HiLoad 16/600 SD 200 pg column in SEC buffer. The protein is concentrated to approximately 10 mg/mL [76].

It is often advantageous to use a cleavable His tag, e.g. by TEV protease, to avoid interference with crystal formation [76]. After IMAC, proteins are then buffer-exchanged by overnight dialysis at 4°C against dialysis buffer. If a cleavable His tag is used, TEV cleavage can be done simultaneously at a molar ratio of 1:10 (enzyme to substrate).

If single-cysteine DARPin constructs are used, e.g. for subsequent labeling with maleimides, they should be expressed at 25°C and expression continued for 16 h [76]. Single-cysteine

containing DARPins are additionally reduced before dialysis with 10 mM DTT for 30 min, and 1 mM DTT is added to the dialysis buffer. Uncleaved protein and His-tagged TEV are removed by bench-top reverse IMAC with dialysis buffer, where the proteins of interest are in the flow-through. Before coupling, the DTT must be carefully and quantitatively removed, e.g. by SEC.

Materials

Lysis buffer: 50 mM Tris, 500 mM NaCl, 10% w/v glycerol, 0.5 mM EDTA, 0.2 mM 4-(2-aminoethyl) benzene sulfonyl fluoride hydrochloride (AEBSF), 1.4 µM pepstatin-A, 1 µM leupeptin and 1 mg/mL lysozyme, pH 8 at 4°C
AEX running buffer: 10 mM Tris, 50 mM NaCl; pH 8 at 4°C
AEX elution buffer: 10 mM Tris, 500 mM NaCl; pH 8 at 4°C
SEC buffer: 8 mM HEPES, 10 mM NaCl; pH 7.5 at 4°C
ÄKTA Pure chromatography system (Cytiva, cat. no. 29018224)
MonoQ 5/50 GL (Cytiva, cat. no. 17-5166-01)
HiLoad 16/600 SD 75 pg (Cytiva, cat. no. 28989333)
HiLoad 16/600 SD 200 pg (Cytiva, cat. no. 28989335)
Dialysis buffer: 20 mM Tris, 100 mM NaCl; pH 8 at 4°C

10.3. Affinity determination

Affinities of DARPins with their target have been determined with a variety of methods, most frequently Surface Plasmon Resonance (SPR) [42, 43, 45, 47, 48, 54, 60, 76], but also other methods such as fluorescence anisotropy [50, 58, 60, 76]. Since the target will usually be available in biotinylated form from the HT RD selection, it is most convenient to immobilize the target and detect binding of the DARPin. Since there are many alternative methods for affinity determination, all with their pros and cons, a comprehensive review would be out of the scope for this article. Since the keys to obtain correct binding constants by SPR have been well reviewed [178], this will not be further described here.

Acknowledgements

The authors want to sincerely thank Dr. Jonas Schaefer who has decisively shaped the procedures described here and had led the high-throughput efforts over many years. The authors also want to acknowledge former coworkers who have contributed to the developments of the methods and to the results presented, including Christa Booy, Andreas Bosshart, Willy Decurtins, Ralph Degen, Aleksandra Djekic, Julia Godau, Mareike Göranson, Simon Hansen, Thamar Looser, Joana Marinho, Thomas Reinberg, Karola Schlinkmann,

Oliver Scholz, Nikolas Stefan, Julia Thielicke and Cristian Thom. And finally, we thank all our colleagues who contributed and shaped the original manual Ribosome Display. Work in the authors' lab was funded by the Schweizerische Nationalfonds grants 310030_192689, 310030B_166676 and 31003A_146278.

References

[1] A. Plückthun, Designed Ankyrin Repeat Proteins (DARPins): binding proteins for research, diagnostics, and therapy, Annu. Rev. Pharmacol. Toxicol. 55 (2015) 489-511. https://doi.org/10.1146/annurev-pharmtox-010611-134654.

[2] C. Jost and A. Plückthun, Engineered proteins with desired specificity: DARPins, other alternative scaffolds and bispecific IgGs, Curr. Opin. Struct. Biol. 27C (2014) 102-112. https://doi.org/10.1016/j.sbi.2014.05.011.

[3] Y.L. Boersma and A. Plückthun, DARPins and other repeat protein scaffolds: advances in engineering and applications, Curr. Opin. Biotechnol. 22 (2011) 849-857. https://doi.org/10.1016/j.copbio.2011.06.004.

[4] R. Tamaskovic, M. Simon, N. Stefan, M. Schwill and A. Plückthun, Designed ankyrin repeat proteins (DARPins) from research to therapy, Meth. Enzymol. 503 (2012) 101-134. https://doi.org/10.1016/B978-0-12-396962-0.00005-7.

[5] M.T. Stumpp, V. Kirkin, M.P. Sanderson, K.M. Dawson and P. Legenne, A decade of clinical experience with DARPins in oncology and virology: a systematic review, medRxiv (2025) 2025.2005.2021.25328103. https://doi.org/10.1101/2025.05.21.25328103.

[6] M. Gebauer and A. Skerra, Engineered protein scaffolds as next-generation therapeutics, Annu. Rev. Pharmacol. Toxicol. 60 (2020) 391-415. https://doi.org/10.1146/annurev-pharmtox-010818-021118.

[7] R.N. Gilbreth and S. Koide, Structural insights for engineering binding proteins based on non-antibody scaffolds, Curr. Opin. Struct. Biol. 22 (2012) 413-420. https://doi.org/10.1016/j.sbi.2012.06.001.

[8] R. Vazquez-Lombardi, T.G. Phan, C. Zimmermann, D. Lowe, L. Jermutus and D. Christ, Challenges and opportunities for non-antibody scaffold drugs, Drug Discov. Today 20 (2015) 1271-1283. https://doi.org/10.1016/j.drudis.2015.09.004.

[9] R. Simeon and Z. Chen, In vitro-engineered non-antibody protein therapeutics, Protein Cell 9 (2018) 3-14. https://doi.org/10.1007/s13238-017-0386-6.

[10] N.R. Bennett, J.L. Watson, R.J. Ragotte, A.J. Borst, D.L. See, C. Weidle, R. Biswas, Y. Yu, E.L. Shrock, R. Ault, P.J.Y. Leung, B. Huang, I. Goreshnik, J. Tam, K.D. Carr, B. Singer, C. Criswell, B.I.M. Wicky, D. Vafeados, M.G. Sanchez, H.M. Kim, S.V. Torres, S. Chan, S.M. Sun, T. Spear, Y. Sun, K. O'Reilly, J.M. Maris, N.G. Sgourakis, R.A. Melnyk, C.C. Liu and D. Baker, Atomically accurate de novo design of antibodies with RFdiffusion, Nature 649 (2026) 183-193. https://doi.org/10.1038/s41586-025-09721-5.

[11] B. Liu, N.F. Greenwood, J.E. Bonzanini, A. Motmaen, J. Sharp, C. Wang, G.M. Visani, D.K. Vafeados, N. Roullier, A. Nourmohammad, K.C. Garcia and D. Baker, Design of high specificity binders for peptide-MHC-I complexes, Science 389 (2025) 388-391. https://doi.org/10.1126/science.adv0185.

[12] V.R. Shanker, T.U.J. Bruun, B.L. Hie and P.S. Kim, Inverse folding of protein complexes with a structure-informed language model enables unsupervised antibody

evolution, bioRxiv (2023) 2023.2012.2019.572475. https://doi.org/10.1101/2023.12.19.572475.
[13] J. Ramirez-Villarreal and R. Alvarez-Martinez, Application of I TASSER, trRosetta, UCSF Chimera, HADDOCK server, and HEX loria for de novo and in silico design of proteins, J. Vis. Exp. (2025) doi:10.3791/68003. https://doi.org/10.3791/68003.
[14] H. Jiang, K.M. Jude, K. Wu, J. Fallas, G. Ueda, T.J. Brunette, D.R. Hicks, H. Pyles, A. Yang, L. Carter, M. Lamb, X. Li, P.M. Levine, L. Stewart, K.C. Garcia and D. Baker, De novo design of buttressed loops for sculpting protein functions, Nat. Chem. Biol. 20 (2024) 974-980. https://doi.org/10.1038/s41589-024-01632-2.
[15] F. Soleymani, E. Paquet, H. Viktor, W. Michalowski and D. Spinello, Protein-protein interaction prediction with deep learning: A comprehensive review, Comput. Struct. Biotechnol. J. 20 (2022) 5316-5341. https://doi.org/10.1016/j.csbj.2022.08.070.
[16] N.R. Bennett, B. Coventry, I. Goreshnik, B. Huang, A. Allen, D. Vafeados, Y.P. Peng, J. Dauparas, M. Baek, L. Stewart, F. DiMaio, S. De Munck, S.N. Savvides and D. Baker, Improving de novo protein binder design with deep learning, Nat. Commun. 14 (2023) 2625. https://doi.org/10.1038/s41467-023-38328-5.
[17] L. Cao, B. Coventry, I. Goreshnik, B. Huang, W. Sheffler, J.S. Park, K.M. Jude, I. Markovic, R.U. Kadam, K.H.G. Verschueren, K. Verstraete, S.T.R. Walsh, N. Bennett, A. Phal, A. Yang, L. Kozodoy, M. DeWitt, L. Picton, L. Miller, E.M. Strauch, N.D. DeBouver, A. Pires, A.K. Bera, S. Halabiya, B. Hammerson, W. Yang, S. Bernard, L. Stewart, I.A. Wilson, H. Ruohola-Baker, J. Schlessinger, S. Lee, S.N. Savvides, K.C. Garcia and D. Baker, Design of protein-binding proteins from the target structure alone, Nature 605 (2022) 551-560. https://doi.org/10.1038/s41586-022-04654-9.
[18] X. Liu, K. Pang, H. Wu, B. Chong, Z. Yin, Z. Sun and X. Wang, AlphaFold3 prediction of protein-protein complex: Is it ready for thermodynamic analysis?, Comput. Struct. Biotechnol. J. 27 (2025) 4373-4383. https://doi.org/10.1016/j.csbj.2025.10.015.
[19] M.L. Verteramo, O. Stenstrom, M.M. Ignjatovic, O. Caldararu, M.A. Olsson, F. Manzoni, H. Leffler, E. Oksanen, D.T. Logan, U.J. Nilsson, U. Ryde and M. Akke, Interplay between conformational entropy and solvation entropy in protein-ligand binding, J. Am. Chem. Soc. 141 (2019) 2012-2026. https://doi.org/10.1021/jacs.8b11099.
[20] A.H. Mahmoud, M.R. Masters, Y. Yang and M.A. Lill, Elucidating the multiple roles of hydration for accurate protein-ligand binding prediction via deep learning, Commun. Chem. 3 (2020) 19. https://doi.org/10.1038/s42004-020-0261-x.
[21] B. Breiten, M.R. Lockett, W. Sherman, S. Fujita, M. Al-Sayah, H. Lange, C.M. Bowers, A. Heroux, G. Krilov and G.M. Whitesides, Water networks contribute to enthalpy/entropy compensation in protein-ligand binding, J. Am. Chem. Soc. 135 (2013) 15579-15584. https://doi.org/10.1021/ja4075776.
[22] K.K. Frederick, M.S. Marlow, K.G. Valentine and A.J. Wand, Conformational entropy in molecular recognition by proteins, Nature 448 (2007) 325-329. https://doi.org/10.1038/nature05959.
[23] J.A. Caro, K.W. Harpole, V. Kasinath, J. Lim, J. Granja, K.G. Valentine, K.A. Sharp and A.J. Wand, Entropy in molecular recognition by proteins, Proc. Nat. Acad. Sci. U. S. A. 114 (2017) 6563-6568. https://doi.org/10.1073/pnas.1621154114.
[24] E. King, E. Aitchison, H. Li and R. Luo, Recent developments in free energy calculations for drug discovery, Front. Mol. Biosci. 8 (2021) 712085. https://doi.org/10.3389/fmolb.2021.712085.
[25] S. Wagle, C.I. Bayly and D.L. Mobley, Advancing binding affinity calculations: A non-equilibrium simulations approach for calculation of relative binding free energies in systems with trapped waters, J. Chem. Theory Comput. 21 (2025) 7593-7604. https://doi.org/10.1021/acs.jctc.5c00758.
[26] J. Ministro, A.M. Manuel and J. Goncalves, Therapeutic antibody engineering and selection strategies, Adv. Biochem. Eng. Biotechnol. 171 (2020) 55-86. https://doi.org/10.1007/10_2019_116.
[27] S.Z.B. Mahdavi, F. Oroojalian, S. Eyvazi, M. Hejazi, B. Baradaran, N. Pouladi, M.R. Tohidkia, A. Mokhtarzadeh and S. Muyldermans, An overview on display systems

(phage, bacterial, and yeast display) for production of anticancer antibodies; advantages and disadvantages, Int. J. Biol. Macromol. 208 (2022) 421-442. https://doi.org/10.1016/j.ijbiomac.2022.03.113.

[28] D.J. King, P.M. Bowers, M.R. Kehry and R.A. Horlick, Mammalian cell display and somatic hypermutation in vitro for human antibody discovery, Curr. Drug Discov. Technol. 11 (2014) 56-64. https://doi.org/10.2174/15701638113109990037.

[29] A. Plückthun, Ribosome display: a perspective, Methods Mol. Biol. 805 (2012) 3-28. https://doi.org/10.1007/978-1-61779-379-0_1.

[30] P. Amstutz, H.K. Binz, C. Zahnd and A. Plückthun, Ribosome Display: in vitro selection of protein-protein interactions in: J. Celis (Ed.) *Cell Biology - A Laboratory Handbook*, 3rd edit., Vol. 1, 4 vols, Elsevier Academic Press, 2006, pp. 497-509.

[31] C. Zahnd, P. Amstutz and A. Plückthun, Ribosome display: selecting and evolving proteins in vitro that specifically bind to a target, Nat. Meth. 4 (2007) 269-279. https://doi.org/10.1038/nmeth1003.

[32] B. Dreier and A. Plückthun, Rapid selection of high-affinity binders using ribosome display, Methods Mol. Biol. 805 (2012) 261-286. https://doi.org/10.1007/978-1-61779-379-0_15.

[33] B. Dreier and A. Plückthun, Rapid selection of high-affinity antibody scFv fragments using ribosome display, Methods Mol. Biol. 1827 (2018) 235-268. https://doi.org/10.1007/978-1-4939-8648-4_13.

[34] C. Schaffitzel, C. Zahnd, P. Amstutz, B. Luginbühl and A. Plückthun, In vitro selection and evolution of protein-ligand interactions by ribosome display in: E. Golemis and P. Adams (Eds.), *Protein-protein interactions: A molecular cloning manual*, 2nd edit., Cold Spring Harbor Laboratory Press, Cold Spring Harbor, NY, 2005, pp. 517-548.

[35] V. Tröster, R.P. Wong, A. Borgel, B. Cakilkaya, C. Renz, M.M. Möckel, K. Eifler-Olivi, J. Marinho, T. Reinberg, S. Furler, J.V. Schaefer, A. Plückthun, E. Wolf and H.D. Ulrich, Custom affinity probes reveal DNA-damage-induced, ssDNA-independent chromatin SUMOylation in budding yeast, Cell Rep. 44 (2025) 115353. https://doi.org/10.1016/j.celrep.2025.115353.

[36] P. Münick, A. Strubel, D.I. Balourdas, J.S. Funk, M. Mernberger, C. Osterburg, B. Dreier, J.V. Schaefer, M. Tuppi, B. Yüksel, B. Schäfer, S. Knapp, A. Plückthun, T. Stiewe, A.C. Joerger and V. Dötsch, DARPin-induced reactivation of p53 in HPV-positive cells, Nat. Struct. Mol. Biol. 32 (2025) 790-801. https://doi.org/10.1038/s41594-024-01456-7.

[37] P. Münick, J. Zielinski, A. Strubel, N. Gutfreund, B. Dreier, J.V. Schaefer, B. Schäfer, J. Gebel, C. Osterburg, A. Chaikuad, S. Knapp, A. Plückthun and V. Dötsch, DARPins as a novel tool to detect and degrade p73, Cell Death Dis. 15 (2024) 909. https://doi.org/10.1038/s41419-024-07304-2.

[38] V. Dederer, M. Sanz Murillo, E.P. Karasmanis, K.S. Hatch, D. Chatterjee, F. Preuss, K.R. Abdul Azeez, L. Vu Nguyen, C. Galicia, B. Dreier, A. Plückthun, W. Versees, S. Mathea, A.E. Leschziner, S.L. Reck-Peterson and S. Knapp, A designed ankyrin-repeat protein that targets Parkinson's disease-associated LRRK2, J. Biol. Chem. 300 (2024) 107469. https://doi.org/10.1016/j.jbc.2024.107469.

[39] Z. Cui, C.E. Ayva, Y.J. Liew, Z. Guo, R. Mutschler, B. Dreier, M.M. Fiorito, P. Walden, C.B. Howard, F. Ely, A. Plückthun, C. Pretorius, J.P. Ungerer, A.M. Buckle and K. Alexandrov, mRNA display pipeline for protein biosensor construction, ACS Sens. 9 (2024) 2846-2857. https://doi.org/10.1021/acssensors.3c02471.

[40] J.R. Ivanova, A.S. Benk, J.V. Schaefer, B. Dreier, L.O. Hermann, A. Plückthun, D. Missirlis and J.P. Spatz, Designed ankyrin repeat proteins as actin labels of distinct cytoskeletal structures in living cells, ACS Nano 18 (2024) 8919-8933. https://doi.org/10.1021/acsnano.3c12265.

[41] M. Glögl, N. Friedrich, G. Cerutti, T. Lemmin, Y.D. Kwon, J. Gorman, L. Maliqi, P.R.E. Mittl, M.C. Hesselman, D. Schmidt, J. Weber, C. Foulkes, A.S. Dingens, T. Bylund, A.S. Olia, R. Verardi, T. Reinberg, N.S. Baumann, P. Rusert, B. Dreier, L. Shapiro, P.D. Kwong, A. Plückthun and A. Trkola, Trapping the HIV-1 V3 loop in a helical

conformation enables broad neutralization, Nat. Struct. Mol. Biol. 30 (2023) 1323-1336. https://doi.org/10.1038/s41594-023-01062-z.

[42] O. Leka, Y. Wu, G. Zanetti, S. Furler, T. Reinberg, J. Marinho, J.V. Schaefer, A. Plückthun, X. Li, M. Pirazzini and R.A. Kammerer, A DARPin promotes faster onset of botulinum neurotoxin A1 action, Nat. Commun. 14 (2023) 8317. https://doi.org/10.1038/s41467-023-44102-4.

[43] J. Shi, K. Hauschulte, I. Mikicic, S. Maharjan, V. Arz, T. Strauch, J.B. Heidelberger, J.V. Schaefer, B. Dreier, A. Plückthun, P. Beli, H.D. Ulrich and H.P. Wollscheid, Nuclear myosin VI maintains replication fork stability, Nat. Commun. 14 (2023) 3787. https://doi.org/10.1038/s41467-023-39517-y.

[44] A. Strubel, P. Münick, O. Hartmann, A. Chaikuad, B. Dreier, J.V. Schaefer, J. Gebel, C. Osterburg, M. Tuppi, B. Schäfer, V. Buck, M. Rosenfeldt, S. Knapp, A. Plückthun, M.E. Diefenbacher and V. Dötsch, DARPins detect the formation of hetero-tetramers of p63 and p73 in epithelial tissues and in squamous cell carcinoma, Cell Death Dis. 14 (2023) 674. https://doi.org/10.1038/s41419-023-06213-0.

[45] K.P. Hartmann, M. van Gogh, P.C. Freitag, F. Kast, G. Nagy-Davidescu, L. Borsig and A. Plückthun, FAP-retargeted Ad5 enables in vivo gene delivery to stromal cells in the tumor microenvironment, Mol. Ther. 31 (2023) 2914-2928. https://doi.org/10.1016/j.ymthe.2023.08.018.

[46] L. Maliqi, N. Friedrich, M. Glögl, S. Schmutz, D. Schmidt, P. Rusert, M. Schanz, M. Zaheri, C. Pasin, C. Niklaus, C. Foulkes, T. Reinberg, B. Dreier, I. Abela, D. Peterhoff, A. Hauser, R.D. Kouyos, H.F. Günthard, M.J. van Gils, R.W. Sanders, R. Wagner, A. Plückthun and A. Trkola, Assessing immunogenicity barriers of the HIV-1 envelope trimer, NPJ Vaccines 8 (2023) 148. https://doi.org/10.1038/s41541-023-00746-3.

[47] M. Gut, B. Dreier, S. Furler, J. Sobek, A. Plückthun and J.P. Holland, Designed ankyrin repeat proteins for detecting prostate-specific antigen expression in vivo, RSC Chem. Biol. 4 (2023) 494-505. https://doi.org/10.1039/d3cb00010a.

[48] M. Blanc, C. Lettl, J. Guerin, A. Vieille, S. Furler, S. Briand-Schumacher, B. Dreier, C. Berge, A. Plückthun, S. Vadon-Le Goff, R. Fronzes, P. Rousselle, W. Fischer and L. Terradot, Designed Ankyrin Repeat Proteins provide insights into the structure and function of CagI and are potent inhibitors of CagA translocation by the Helicobacter pylori type IV secretion system, PLoS Pathog. 19 (2023) e1011368. https://doi.org/10.1371/journal.ppat.1011368.

[49] B.F.N. Campbell, A. Dittmann, B. Dreier, A. Plückthun and S.K. Tyagarajan, A DARPin-based molecular toolset to probe gephyrin and inhibitory synapse biology, eLife 11 (2022). https://doi.org/10.7554/eLife.80895.

[50] A. Strubel, P. Münick, A. Chaikuad, B. Dreier, J. Schaefer, J. Gebel, C. Osterburg, M. Tuppi, B. Schäfer, S. Knapp, A. Plückthun and V. Dötsch, Designed Ankyrin Repeat Proteins as a tool box for analyzing p63, Cell Death Differ. 29 (2022) 2445-2458. https://doi.org/10.1038/s41418-022-01030-y.

[51] C. Kiss, F.M. Gall, B. Dreier, M. Adams, R. Riedl, A. Plückthun and P.R.E. Mittl, Structure of a hydrophobic leucinostatin derivative determined by host lattice display, Acta Crystallogr. D Struct. Biol. 78 (2022) 1439-1450. https://doi.org/10.1107/S2059798322010762.

[52] C. Qi, P. Lavriha, V. Mehta, B. Khanppnavar, I. Mohammed, Y. Li, M. Lazaratos, J.V. Schaefer, B. Dreier, A. Plückthun, A.N. Bondar, C.W. Dessauer and V.M. Korkhov, Structural basis of adenylyl cyclase 9 activation, Nat. Commun. 13 (2022) 1045. https://doi.org/10.1038/s41467-022-28685-y.

[53] L. Wang, E.A. Moreira, G. Kempf, Y. Miyake, B.I. Oliveira Esteves, A. Fahmi, J.V. Schaefer, B. Dreier, Y. Yamauchi, M.P. Alves, A. Plückthun and P. Matthias, Disrupting the HDAC6-ubiquitin interaction impairs infection by influenza and Zika virus and cellular stress pathways, Cell Rep. 39 (2022) 110736. https://doi.org/10.1016/j.celrep.2022.110736.

[54] T. Strittmatter, Y. Wang, A. Bertschi, L. Scheller, P.C. Freitag, P.G. Ray, P. Stuecheli, J.V. Schaefer, T. Reinberg, D. Tsakiris, A. Plückthun, H. Ye and M. Fussenegger,

Programmable DARPin-based receptors for the detection of thrombotic markers, Nat. Chem. Biol. 18 (2022) 1125-1134. https://doi.org/10.1038/s41589-022-01095-3.

[55] N. Friedrich, E. Stiegeler, M. Glogl, T. Lemmin, S. Hansen, C. Kadelka, Y. Wu, P. Ernst, L. Maliqi, C. Foulkes, M. Morin, M. Eroglu, T. Liechti, B. Ivan, T. Reinberg, J.V. Schaefer, U. Karakus, S. Ursprung, A. Mann, P. Rusert, R.D. Kouyos, J.A. Robinson, H.F. Günthard, A. Plückthun and A. Trkola, Distinct conformations of the HIV-1 V3 loop crown are targetable for broad neutralization, Nat. Commun. 12 (2021) 6705. https://doi.org/10.1038/s41467-021-27075-0.

[56] A. Kosareva, M. Punjabi, A. Ochoa-Espinosa, L. Xu, J.V. Schaefer, B. Dreier, A. Plückthun and B.A. Kaufmann, Designed Ankyrin Repeat Proteins as novel binders for ultrasound molecular imaging, Ultrasound Med. Biol. 47 (2021) 2664-2675. https://doi.org/10.1016/j.ultrasmedbio.2021.04.027.

[57] S. Matsuda, J.V. Schaefer, Y. Mii, Y. Hori, D. Bieli, M. Taira, A. Plückthun and M. Affolter, Asymmetric requirement of Dpp/BMP morphogen dispersal in the Drosophila wing disc, Nat. Commun. 12 (2021) 6435. https://doi.org/10.1038/s41467-021-26726-6.

[58] M.A. Vigano, D. Bieli, J.V. Schaefer, R.P. Jakob, S. Matsuda, T. Maier, A. Plückthun and M. Affolter, DARPins recognizing mTFP1 as novel reagents for in vitro and in vivo protein manipulations, Biol. Open 7 (2018) bio036749. https://doi.org/10.1242/bio.036749.

[59] U. Anders, J.V. Schaefer, F.E. Hibti, C. Frydman, D. Suckau, A. Plückthun and R. Zenobi, SPRi-MALDI MS: characterization and identification of a kinase from cell lysate by specific interaction with different designed ankyrin repeat proteins, Anal. Bioanal. Chem. 409 (2017) 1827-1836. https://doi.org/10.1007/s00216-016-0127-3.

[60] M. Brauchle, S. Hansen, E. Caussinus, A. Lenard, A. Ochoa-Espinosa, O. Scholz, S.G. Sprecher, A. Plückthun and M. Affolter, Protein interference applications in cellular and developmental biology using DARPins that recognize GFP and mCherry, Biol. Open 3 (2014) 1252-1261. https://doi.org/10.1242/bio.201410041.

[61] C.S. Umbaugh, M. Groth, C. Erkut, K.-S. Lee, J. Marinho, S. Linder, F. Iser, J.N.S. Kapp, P, S. Dolaner, A. Kayserili, D. Helm, M. Schneider, J. Hartmann, P. Walch, T.F.E. Barth, K. Mellert, B. Dreier, J.V. Schaefer, A. Plückthun, S. Fröhling and C. Scholl, Selective targeting of TBXT with DARPins identifies regulatory networks and therapeutic vulnerabilities in chordoma, Sci. Adv. 11 (2025) eadu2796. https://doi.org/10.1126/sciadv.adu2796.

[62] D. Ratnayake, M. Galloux, S. Boersma, M. Noerenberg, C. Sizun, C. Sacristan, J. Sourimant, A.J. Lakerveld, A.T. Gelderloos, L. Apperloo, Y. Demyanenko, M.J.D. Baars, R. Banerjee, B. Dreier, S. Furler, N.I. Mazur, L.J. Bont, S. Mohammed, A. Plückthun, J.-F. Éléouët, G.J.P.L. Kops, A. Castello, P.B. van Kasteren, M.-A. Rameix-Welti and M.E. Tanenbaum, Pre-assembly of biomolecular condensate seeds drives RSV replication, Nature (2026) in press. https://doi.org/10.1038/s41586-025-10071-5.

[63] G. Henkin, C. Brito, A. Plückthun and T. Surrey, Preparation of polarity-marked microtubules using a plus-end capping DARPin, Bio-Protoc. 14 (2024) e5109. https://doi.org/10.21769/BioProtoc.5109.

[64] V. Campanacci, A. Urvoas, S. Cantos-Fernandes, M. Aumont-Nicaise, A.A. Arteni, C. Velours, M. Valerio-Lepiniec, B. Dreier, A. Plückthun, A. Pilon, C. Pous, P. Minard and B. Gigant, Insight into microtubule nucleation from tubulin-capping proteins, Proc. Natl. Acad. Sci. U. S. A. 116 (2019) 9859-9864. https://doi.org/10.1073/pnas.1813559116.

[65] S. Ahmad, L. Pecqueur, B. Dreier, D. Hamdane, M. Aumont-Nicaise, A. Plückthun, M. Knossow and B. Gigant, Destabilizing an interacting motif strengthens the association of a designed ankyrin repeat protein with tubulin, Sci. Rep. 6 (2016) 28922. https://doi.org/10.1038/srep28922.

[66] B. Gigant, W. Wang, B. Dreier, Q. Jiang, L. Pecqueur, A. Plückthun, C. Wang and M. Knossow, Structure of a kinesin-tubulin complex and implications for kinesin motility, Nat. Struct. Mol. Biol. 20 (2013) 1001-1007. https://doi.org/10.1038/nsmb.2624.

[67] I. Mignot, L. Pecqueur, A. Dorleans, M. Karuppasamy, R.B. Ravelli, B. Dreier, A. Plückthun, M. Knossow and B. Gigant, Design and characterization of modular scaffolds for tubulin assembly, J. Biol. Chem. 287 (2012) 31085-31094. https://doi.org/10.1074/jbc.M112.383869.
[68] L. Pecqueur, C. Duellberg, B. Dreier, Q. Jiang, C. Wang, A. Plückthun, T. Surrey, B. Gigant and M. Knossow, A designed ankyrin repeat protein selected to bind to tubulin caps the microtubule plus end, Proc. Natl. Acad. Sci. U. S. A. 109 (2012) 12011-12016. https://doi.org/10.1073/pnas.1204129109.
[69] A. Kumar and A. Plückthun, In vivo assembly and large-scale purification of a GPCR - Galpha fusion with Gbetagamma, and characterization of the active complex, PLoS One 14 (2019) e0210131. https://doi.org/10.1371/journal.pone.0210131.
[70] S. Hansen, J.C. Stüber, P. Ernst, A. Koch, D. Bojar, A. Batyuk and A. Plückthun, Design and applications of a clamp for Green Fluorescent Protein with picomolar affinity, Sci. Rep. 7 (2017) 16292. https://doi.org/10.1038/s41598-017-15711-z.
[71] P. Ernst, A. Plückthun and P.R.E. Mittl, Structural analysis of biological targets by host:guest crystal lattice engineering, Sci. Rep. 9 (2019) 15199. https://doi.org/10.1038/s41598-019-51017-y.
[72] I. Vulovic, Q. Yao, Y.J. Park, A. Courbet, A. Norris, F. Busch, A. Sahasrabuddhe, H. Merten, D.D. Sahtoe, G. Ueda, J.A. Fallas, S.J. Weaver, Y. Hsia, R.A. Langan, A. Plückthun, V.H. Wysocki, D. Veesler, G.J. Jensen and D. Baker, Generation of ordered protein assemblies using rigid three-body fusion, Proc. Natl. Acad. Sci. U. S. A. 118 (2021) e2015037118. https://doi.org/10.1073/pnas.2015037118.
[73] M. Philippi, C.P. Richter, M. Kappen, I. Watrinet, Y. Miao, M. Runge, L. Jorde, S. Korneev, M. Holtmannspotter, R. Kurre, J.C.M. Holthuis, K.C. Garcia, A. Plückthun, M. Steinhart, J. Piehler and C. You, Biofunctional nanodot arrays in living cells uncover synergistic co-condensation of Wnt signalodroplets, Small 18 (2022) e2203723. https://doi.org/10.1002/smll.202203723.
[74] M. Nakadate, R. Kojima, N. Seike, R. Tachibana, K. Fujita, R. Tsuchiya, M. Kamiya, A. Plückthun and Y. Urano, Design of antigen-targeting fluorogenic probes utilizing intramolecular addition reaction of protein-dye hybrids, J. Am. Chem. Soc. (2025). https://doi.org/10.1021/jacs.5c04193.
[75] D. Vukovic, D. Winkelvoss, J.N. Kapp, A.C. Hänny, H. Bürgisser, L. Riermeier, A. Udovcic, P. Tiefenboeck and A. Plückthun, Protein degradation kinetics measured by microinjection and live-cell fluorescence microscopy, Sci. Rep. 14 (2024) 27153. https://doi.org/10.1038/s41598-024-76224-0.
[76] D. Winkelvoss, D. Vukovic, A.C. Hanny, L. Riermeier, A. Udovcic, J. Kolibius, A. Honegger, P.R.E. Mittl, E. Michel, S. Hansen and A. Plückthun, Molecular features defining the efficiency of bioPROTACs, Commun. Biol. 8 (2025) 946. https://doi.org/10.1038/s42003-025-08352-w.
[77] P.R. Mittl, P. Ernst and A. Plückthun, Chaperone-assisted structure elucidation with DARPins, Curr. Opin. Struct. Biol. 60 (2020) 93-100. https://doi.org/10.1016/j.sbi.2019.12.009.
[78] Y. Wu, A. Batyuk, A. Honegger, F. Brandl, P.R.E. Mittl and A. Plückthun, Rigidly connected multispecific artificial binders with adjustable geometries, Sci. Rep. 7 (2017) 11217. https://doi.org/10.1038/s41598-017-11472-x.
[79] Y. Wu, A. Honegger, A. Batyuk, P.R.E. Mittl and A. Plückthun, Structural basis for the selective inhibition of c-Jun N-terminal kinase 1 determined by rigid DARPin-DARPin fusions, J. Mol. Biol. 430 (2018) 2128-2138. https://doi.org/10.1016/j.jmb.2017.10.032.
[80] M. Deluigi, A. Klipp, C. Klenk, L. Merklinger, S.A. Eberle, L. Morstein, P. Heine, P.R.E. Mittl, P. Ernst, T.M. Kamenecka, Y. He, S. Vacca, P. Egloff, A. Honegger and A. Plückthun, Complexes of the neurotensin receptor 1 with small-molecule ligands reveal structural determinants of full, partial, and inverse agonism, Sci. Adv. 7 (2021) eabe5504. https://doi.org/10.1126/sciadv.abe5504.
[81] M. Deluigi, L. Morstein, M. Schuster, C. Klenk, L. Merklinger, R.R. Cridge, L.A. de Zhang, A. Klipp, S. Vacca, T.M. Vaid, P.R.E. Mittl, P. Egloff, S.A. Eberle, O. Zerbe,

D.K. Chalmers, D.J. Scott and A. Plückthun, Crystal structure of the alpha1B-adrenergic receptor reveals molecular determinants of selective ligand recognition, Nat. Commun. 13 (2022) 382. https://doi.org/10.1038/s41467-021-27911-3.

[82] J. Hanes, L. Jermutus, C. Schaffitzel and A. Plückthun, Comparison of *Escherichia coli* and rabbit reticulocyte ribosome display systems, FEBS Lett. 450 (1999) 105-110. https://doi.org/10.1016/s0014-5793(99)00475-5.

[83] R. Chance and A.S. Kang, Eukaryotic ribosome display for antibody discovery: A review, Hum. Antibodies 32 (2024) 107-120. https://doi.org/10.3233/HAB-240001.

[84] M. He and M.J. Taussig, Eukaryotic ribosome display with in situ DNA recovery, Nat. Methods 4 (2007) 281-288. https://doi.org/10.1038/nmeth1001.

[85] H. Ohashi, Y. Shimizu, B.W. Ying and T. Ueda, Efficient protein selection based on ribosome display system with purified components, Biochem. Biophys. Res. Commun. 352 (2007) 270-276. https://doi.org/10.1016/j.bbrc.2006.11.017.

[86] T. Ueda, T. Kanamori and H. Ohashi, Ribosome display with the PURE technology, Methods Mol. Biol. 607 (2010) 219-225. https://doi.org/10.1007/978-1-60327-331-2_18.

[87] L.A. Ryabova, D. Desplancq, A.S. Spirin and A. Plückthun, Functional antibody production using cell-free translation: Effects of protein disulfide isomerase and chaperones, Nat. Biotechnol. 15 (1997) 79-84. https://doi.org/10.1038/nbt0197-79.

[88] J. Hanes and A. Plückthun, *In vitro* selection and evolution of functional proteins by using ribosome display, Proc. Natl. Acad. Sci. U. S. A. 94 (1997) 4937-4942. https://doi.org/10.1073/pnas.94.10.4937.

[89] J. Hanes, C. Schaffitzel, A. Knappik and A. Plückthun, Picomolar affinity antibodies from a fully synthetic naive library selected and evolved by ribosome display, Nat. Biotechnol. 18 (2000) 1287-1292. https://doi.org/10.1038/82407.

[90] J. Hanes, L. Jermutus, S. Weber-Bornhauser, H.R. Bosshard and A. Plückthun, Ribosome display efficiently selects and evolves high-affinity antibodies *in vitro* from immune libraries, Proc. Natl. Acad. Sci. U. S. A. 95 (1998) 14130-14135. https://doi.org/10.1073/pnas.95.24.14130.

[91] H. Ohashi, T. Kanamori, E. Osada, B.K. Akbar and T. Ueda, Peptide screening using PURE ribosome display, Methods Mol. Biol. 805 (2012) 251-259. https://doi.org/10.1007/978-1-61779-379-0_14.

[92] C.L. Frankling, M.F. Downes, A.S. Kang and E.R.G. Main, Exploring the 'N-terminal arm' & 'convex surface' binding interfaces of the T3SS chaperone-translocator complexes from P. aeruginosa, J. Mol. Biol. 435 (2023) 168146. https://doi.org/10.1016/j.jmb.2023.168146.

[93] Y. Kawaguchi, M.S. Sarker, M. Yokoyama, M. Nakaya, T. Hosokawa, N. Kamiya and M. Goto, Development of dectin-1-binding peptides targeting dendritic cells for antigen delivery via ribosome display, J. Biosci. Bioeng. 141 (2026) 158-164. https://doi.org/10.1016/j.jbiosc.2025.11.005.

[94] Y. Kawaguchi, M.S. Islam, M. Yokoyama, T. Hosokawa, M. Nakaya, N. Kamiya and M. Goto, Directed evolution of Clec12a-binding peptides using mammalian-expressed recombinant protein, Biochem. Biophys. Rep. 45 (2026) 102531. https://doi.org/10.1016/j.bbrep.2026.102531.

[95] L.T. Dang, Y. Miao, A. Ha, K. Yuki, K. Park, C.Y. Janda, K.M. Jude, K. Mohan, N. Ha, M. Vallon, J. Yuan, J.G. Vilches-Moure, C.J. Kuo, K.C. Garcia and D. Baker, Receptor subtype discrimination using extensive shape complementary designed interfaces, Nat. Struct. Mol. Biol. 26 (2019) 407-414. https://doi.org/10.1038/s41594-019-0224-z.

[96] B. Seidelt, C.A. Innis, D.N. Wilson, M. Gartmann, J.P. Armache, E. Villa, L.G. Trabuco, T. Becker, T. Mielke, K. Schulten, T.A. Steitz and R. Beckmann, Structural insight into nascent polypeptide chain-mediated translational stalling, Science 326 (2009) 1412-1415. https://doi.org/10.1126/science.1177662.

[97] H.K. Binz, M.T. Stumpp, P. Forrer, P. Amstutz and A. Plückthun, Designing repeat proteins: well-expressed, soluble and stable proteins from combinatorial libraries of

consensus ankyrin repeat proteins, J. Mol. Biol. 332 (2003) 489-503. https://doi.org/10.1016/s0022-2836(03)00896-9.
[98] V.S. Devi, H.K. Binz, M.T. Stumpp, A. Plückthun, H.R. Bosshard and I. Jelesarov, Folding of a designed simple ankyrin repeat protein, Protein Sci. 13 (2004) 2864-2870. https://doi.org/10.1110/ps.04935704.
[99] S.K. Wetzel, G. Settanni, M. Kenig, H.K. Binz and A. Plückthun, Folding and unfolding mechanism of highly stable full-consensus ankyrin repeat proteins, J. Mol. Biol. 376 (2008) 241-257. https://doi.org/10.1016/j.jmb.2007.11.046.
[100] G. Interlandi, S.K. Wetzel, G. Settanni, A. Plückthun and A. Caflisch, Characterization and further stabilization of designed ankyrin repeat proteins by combining molecular dynamics simulations and experiments, J. Mol. Biol. 375 (2008) 837-854. https://doi.org/10.1016/j.jmb.2007.09.042.
[101] T. Merz, S.K. Wetzel, S. Firbank, A. Plückthun, M.G. Grütter and P.R. Mittl, Stabilizing ionic interactions in a full-consensus ankyrin repeat protein, J. Mol. Biol. 376 (2008) 232-240. https://doi.org/10.1016/j.jmb.2007.11.047.
[102] S.K. Wetzel, C. Ewald, G. Settanni, S. Jurt, A. Plückthun and O. Zerbe, Residue-resolved stability of full-consensus ankyrin repeat proteins probed by NMR, J. Mol. Biol. 402 (2010) 241-258. https://doi.org/10.1016/j.jmb.2010.07.031.
[103] M.A. Kramer, S.K. Wetzel, A. Plückthun, P.R. Mittl and M.G. Grütter, Structural determinants for improved stability of designed ankyrin repeat proteins with a redesigned C-capping module, J. Mol. Biol. 404 (2010) 381-391. https://doi.org/10.1016/j.jmb.2010.09.023.
[104] B. Virnekäs, L. Ge, A. Plückthun, K.C. Schneider, G. Wellnhofer and S.E. Moroney, Trinucleotide phosphoramidites: Ideal reagents for the synthesis of mixed oligonucleotides for random mutagenesis, Nucleic Acids Res. 22 (1994) 5600-5607. https://doi.org/10.1093/nar/22.25.5600.
[105] J. Schilling, J. Schöppe and A. Plückthun, From DARPins to LoopDARPins: novel LoopDARPin design allows the selection of low picomolar binders in a single round of ribosome display, J. Mol. Biol. 426 (2014) 691-721. https://doi.org/10.1016/j.jmb.2013.10.026.
[106] K.M. Schlinkmann, M. Hillenbrand, A. Rittner, M. Kunz, R. Strohner and A. Plückthun, Maximizing detergent stability and functional expression of a GPCR by exhaustive recombination and evolution, J. Mol. Biol. 422 (2012) 414-428. https://doi.org/10.1016/j.jmb.2012.05.039.
[107] C. Klenk, M. Scrivens, A. Niederer, S. Shi, L. Mueller, E. Gersz, M. Zauderer, E.S. Smith, R. Strohner and A. Plückthun, A Vaccinia-based system for directed evolution of GPCRs in mammalian cells, Nat. Commun. 14 (2023) 1770. https://doi.org/10.1038/s41467-023-37191-8.
[108] J. Van den Brulle, M. Fischer, T. Langmann, G. Horn, T. Waldmann, S. Arnold, M. Fuhrmann, O. Schatz, T. O'Connell, D. O'Connell, A. Auckenthaler and H. Schwer, A novel solid phase technology for high-throughput gene synthesis, Biotechniques 45 (2008) 340-343. https://doi.org/10.2144/000112953.
[109] P. Kuhn, K. Wagner, K. Heil, M. Liss and N. Netuschil, Next generation gene synthesis: From microarrays to genomes, Eng. Life Sci. 17 (2017) 6-13. https://doi.org/10.1002/elsc.201600121.
[110] A. Currin, N. Swainston, P.J. Day and D.B. Kell, SpeedyGenes: exploiting an improved gene synthesis method for the efficient production of synthetic protein libraries for directed evolution, Methods Mol. Biol. 1472 (2017) 63-78. https://doi.org/10.1007/978-1-4939-6343-0_5.
[111] A. Li, C.G. Acevedo-Rocha, Z. Sun, T. Cox, J.L. Xu and M.T. Reetz, Beating bias in the directed evolution of proteins: combining high-fidelity on-chip solid-phase gene synthesis with efficient gene assembly for combinatorial library construction, ChemBioChem 19 (2018) 221-228. https://doi.org/10.1002/cbic.201700540.
[112] C. Zahnd, E. Wyler, J.M. Schwenk, D. Steiner, M.C. Lawrence, N.M. McKern, F. Pecorari, C.W. Ward, T.O. Joos and A. Plückthun, A designed ankyrin repeat protein

evolved to picomolar affinity to Her2, J. Mol. Biol. 369 (2007) 1015-1028. https://doi.org/10.1016/j.jmb.2007.03.028.
[113] V.C. Epa, O. Dolezal, L. Doughty, X. Xiao, C. Jost, A. Plückthun and T.E. Adams, Structural model for the interaction of a designed Ankyrin Repeat Protein with the human epidermal growth factor receptor 2, PLoS One 8 (2013) e59163. https://doi.org/10.1371/journal.pone.0059163.
[114] C. Jost, J. Schilling, R. Tamaskovic, M. Schwill, A. Honegger and A. Plückthun, Structural basis for eliciting a cytotoxic effect in HER2-overexpressing cancer cells via binding to the extracellular domain of HER2, Structure 21 (2013) 1979-1991. https://doi.org/10.1016/j.str.2013.08.020.
[115] F. Andres, M. Schwill, Y.L. Boersma and A. Plückthun, High-throughput generation of bispecific binding proteins by sortase A-mediated coupling for direct functional screening in cell culture, Mol. Cancer Ther. 19 (2020) 1080-1088. https://doi.org/10.1158/1535-7163.MCT-19-0633.
[116] H.K. Binz, P. Amstutz, A. Kohl, M.T. Stumpp, C. Briand, P. Forrer, M.G. Grütter and A. Plückthun, High-affinity binders selected from designed ankyrin repeat protein libraries, Nat. Biotechnol. 22 (2004) 575-582. https://doi.org/10.1038/nbt962.
[117] F. Parmeggiani, R. Pellarin, A.P. Larsen, G. Varadamsetty, M.T. Stumpp, O. Zerbe, A. Caflisch and A. Plückthun, Designed armadillo repeat proteins as general peptide-binding scaffolds: consensus design and computational optimization of the hydrophobic core, J. Mol. Biol. 376 (2008) 1282-1304. https://doi.org/10.1016/j.jmb.2007.12.014.
[118] C.M. Kurylo, N. Alexander, R.A. Dass, M.M. Parks, R.A. Altman, C.T. Vincent, C.E. Mason and S.C. Blanchard, Genome sequence and analysis of Escherichia coli MRE600, a colicinogenic, nonmotile strain that lacks RNase I and the type I methyltransferase, EcoKI, Genome Biol. Evol. 8 (2016) 742-752. https://doi.org/10.1093/gbe/evw008.
[119] H.E. Wade and H.K. Robinson, Magnesium ion-independent ribonucleic acid depolymerases in bacteria, Biochem. J. 101 (1966) 467-479. https://doi.org/10.1042/bj1010467.
[120] G. Zubay, In vitro synthesis of protein in microbial systems, Annu. Rev. Genet. 7 (1973) 267-287. https://doi.org/10.1146/annurev.ge.07.120173.001411.
[121] J.M. Pratt, Coupled transcription-translation in prokaryotic cell-free systems in: B. D. Hemes and S. J. Higgins (Eds.), *Current Protocols*, IRL Press, Oxford, 1984, pp. 179-209.
[122] S.A. Lesley, Preparation and use of E. coli S-30 extracts, Methods Mol. Biol. 37 (1995) 265-278. https://doi.org/10.1385/0-89603-288-4:265.
[123] H.Z. Chen and G. Zubay, Prokaryotic coupled transcription-translation, Meth. Enzymol. 101 (1983) 674-690. https://doi.org/10.1016/0076-6879(83)01047-2.
[124] S.R. Kushner, mRNA decay in Escherichia coli comes of age, J. Bacteriol. 184 (2002) 4658-4665; discussion 4657. https://doi.org/10.1128/JB.184.17.4658-4665.2002.
[125] J. Hanes and A. Plückthun, In vitro selection methods for screening of peptide and protein libraries in: M. Famulok, E.-L. Winnacker and C.-H. Wong (Eds.), *Combinatorial Chemistry in Biology*, Vol. 243, Springer Verlag, Berlin Heidelberg, 1999, pp. 107-122.
[126] K.C. Keiler, P.R. Waller and R.T. Sauer, Role of a peptide tagging system in degradation of proteins synthesized from damaged messenger RNA, Science 271 (1996) 990-993. https://doi.org/10.1126/science.271.5251.990.
[127] A.A. Laminet and A. Plückthun, The precursor of *beta*-lactamase: Purification, properties and folding kinetics, EMBO J. 8 (1989) 1469-1477. https://doi.org/10.1002/j.1460-2075.1989.tb03530.x.
[128] C.H. O'Callaghan, A. Morris, S.M. Kirby and A.H. Shingler, Novel method for detection of beta-lactamases by using a chromogenic cephalosporin substrate, Antimicrob. Agents Chemother. 1 (1972) 283-288. https://doi.org/10.1128/AAC.1.4.283.

[129] A.F. Charvat, K. Mason-Chalmers and J.E. Gestwicki, A beginner's guide to differential scanning fluorimetry, The Biochemist 47 (2025) 11-15. https://doi.org/10.1042/bio_2024_921.
[130] L. Nieba, S.E. Nieba-Axmann, A. Persson, M. Hämäläinen, F. Edebratt, A. Hansson, J. Lidholm, K. Magnusson, A.F. Karlsson and A. Plückthun, BIACORE analysis of histidine-tagged proteins using a chelating NTA sensor chip, Anal. Biochem. 252 (1997) 217-228. https://doi.org/10.1006/abio.1997.2326.
[131] Z. Huang, P. Hwang, D.S. Watson, L. Cao and F.C. Szoka, Jr., Tris-nitrilotriacetic acids of subnanomolar affinity toward hexahistidine tagged molecules, Bioconjug. Chem. 20 (2009) 1667-1672. https://doi.org/10.1021/bc900309n.
[132] C. You and J. Piehler, Multivalent chelators for spatially and temporally controlled protein functionalization, Anal. Bioanal. Chem. 406 (2014) 3345-3357. https://doi.org/10.1007/s00216-014-7803-y.
[133] S. Lata, A. Reichel, R. Brock, R. Tampe and J. Piehler, High-affinity adaptors for switchable recognition of histidine-tagged proteins, J. Am. Chem. Soc. 127 (2005) 10205-10215. https://doi.org/10.1021/ja050690c.
[134] P.J. Schatz, Use of peptide libraries to map the substrate specificity of a peptide-modifying enzyme: a 13 residue consensus peptide specifies biotinylation in Escherichia coli, Biotechnology (N. Y.) 11 (1993) 1138-1143. https://doi.org/10.1038/nbt1093-1138.
[135] G. Petris, L. Vecchi, M. Bestagno and O.R. Burrone, Efficient detection of proteins retro-translocated from the ER to the cytosol by in vivo biotinylation, PLoS One 6 (2011) e23712. https://doi.org/10.1371/journal.pone.0023712.
[136] J. Schindelin, I. Arganda-Carreras, E. Frise, V. Kaynig, M. Longair, T. Pietzsch, S. Preibisch, C. Rueden, S. Saalfeld, B. Schmid, J.Y. Tinevez, D.J. White, V. Hartenstein, K. Eliceiri, P. Tomancak and A. Cardona, Fiji: an open-source platform for biological-image analysis, Nat. Methods 9 (2012) 676-682. https://doi.org/10.1038/nmeth.2019.
[137] B. Dreier, A. Honegger, C. Hess, G. Nagy-Davidescu, P.R. Mittl, M.G. Grütter, N. Belousova, G. Mikheeva, V. Krasnykh and A. Plückthun, Development of a generic adenovirus delivery system based on structure-guided design of bispecific trimeric DARPin adapters, Proc. Natl. Acad. Sci. U. S. A. 110 (2013) E869-877. https://doi.org/10.1073/pnas.1213653110.
[138] C. Zahnd, C.A. Sarkar and A. Plückthun, Computational analysis of off-rate selection experiments to optimize affinity maturation by directed evolution, Protein Eng. Des. Sel. 23 (2010) 175-184. https://doi.org/10.1093/protein/gzp087.
[139] E. Hajnsdorf, F. Braun, J. Haugel-Nielsen, J. Le Derout and P. Regnier, Multiple degradation pathways of the rpsO mRNA of Escherichia coli. RNase E interacts with the 5' and 3' extremities of the primary transcript, Biochimie 78 (1996) 416-424. https://doi.org/10.1016/0300-9084(96)84748-1.
[140] L. Jermutus, L.A. Ryabova and A. Plückthun, Recent advances in producing and selecting functional proteins by using cell-free translation, Curr. Opin. Biotechnol. 9 (1998) 534-548. https://doi.org/10.1016/s0958-1669(98)80042-6.
[141] F. Andres, L. Iamele, T. Meyer, J.C. Stuber, F. Kast, E. Gherardi, H.H. Niemann and A. Plückthun, Inhibition of the MET kinase activity and cell growth in MET-addicted cancer cells by bi-paratopic linking, J. Mol. Biol. 431 (2019) 2020-2039. https://doi.org/10.1016/j.jmb.2019.03.024.
[142] F. Radom, C. Vonrhein, P.R.E. Mittl and A. Plückthun, Crystal structures of HER3 extracellular domain 4 in complex with the designed ankyrin-repeat protein D5, Acta Crystallogr. F Struct. Biol. Commun. 77 (2021) 192-201. https://doi.org/10.1107/S2053230X21006002.
[143] P. Milovnik, D. Ferrari, C.A. Sarkar and A. Plückthun, Selection and characterization of DARPins specific for the neurotensin receptor 1, Protein Eng. Des. Sel. 22 (2009) 357-366. https://doi.org/10.1093/protein/gzp011.
[144] M. Schütz, A. Batyuk, C. Klenk, L. Kummer, S. de Picciotto, B. Gulbakan, Y. Wu, G.A. Newby, F. Zosel, J. Schöppe, E. Sedlak, P.R. Mittl, R. Zenobi, K.D. Wittrup and A.

Plückthun, Generation of fluorogen-activating designed ankyrin repeat proteins (FADAs) as versatile sensor tools, J. Mol. Biol. 428 (2016) 1272-1289. https://doi.org/10.1016/j.jmb.2016.01.017.

[145] L. Kummer, P. Parizek, P. Rube, B. Millgramm, A. Prinz, P.R. Mittl, M. Kaufholz, B. Zimmermann, F.W. Herberg and A. Plückthun, Structural and functional analysis of phosphorylation-specific binders of the kinase ERK from designed ankyrin repeat protein libraries, Proc. Natl. Acad. Sci. U. S. A. 109 (2012) E2248-2257. https://doi.org/10.1073/pnas.1205399109.

[146] P. Parizek, L. Kummer, P. Rube, A. Prinz, F.W. Herberg and A. Plückthun, Designed Ankyrin Repeat Proteins (DARPins) as novel isoform-specific intracellular inhibitors of c-Jun N-terminal kinases, ACS Chem. Biol. 7 (2012) 1356-1366. https://doi.org/10.1021/cb3001167.

[147] C. Zahnd, F. Pécorari, N. Straumann, E. Wyler and A. Plückthun, Selection and characterization of Her2 binding-designed ankyrin repeat proteins, J. Biol. Chem. 281 (2006) 35167-35175. https://doi.org/10.1074/jbc.M602547200.

[148] O. Scholz, S. Hansen and A. Plückthun, G-quadruplexes are specifically recognized and distinguished by selected designed ankyrin repeat proteins, Nucleic Acids Res. 42 (2014) 9182-9194. https://doi.org/10.1093/nar/gku571.

[149] C. Schaffitzel, I. Berger, J. Postberg, J. Hanes, H.J. Lipps and A. Plückthun, *In vitro* generated antibodies specific for telomeric guanine-quadruplex DNA react with *Stylonychia lemnae* macronuclei, Proc. Natl. Acad. Sci. U. S. A. 98 (2001) 8572-8577. https://doi.org/10.1073/pnas.141229498.

[150] L. Jermutus, A. Honegger, F. Schwesinger, J. Hanes and A. Plückthun, Tailoring *in vitro* evolution for protein affinity or stability, Proc. Natl. Acad. Sci. U. S. A. 98 (2001) 75-80. https://doi.org/10.1073/pnas.98.1.75.

[151] B. Luginbühl, Z. Kanyo, R.M. Jones, R.J. Fletterick, S.B. Prusiner, F.E. Cohen, R.A. Williamson, D.R. Burton and A. Plückthun, Directed evolution of an anti-prion protein scFv fragment to an affinity of 1 pM and its structural interpretation, J. Mol. Biol. 363 (2006) 75-97. https://doi.org/10.1016/j.jmb.2006.07.027.

[152] R.E. Hawkins, S.J. Russell and G. Winter, Selection of phage antibodies by binding affinity. Mimicking affinity maturation, J. Mol. Biol. 226 (1992) 889-896. https://doi.org/10.1016/0022-2836(92)90639-2.

[153] B. Dreier, G. Mikheeva, N. Belousova, P. Parizek, E. Boczek, I. Jelesarov, P. Forrer, A. Plückthun and V. Krasnykh, Her2-specific multivalent adapters confer designed tropism to adenovirus for gene targeting, J. Mol. Biol. 405 (2011) 410-426. https://doi.org/10.1016/j.jmb.2010.10.040.

[154] C. Zahnd, S. Spinelli, B. Luginbühl, P. Amstutz, C. Cambillau and A. Plückthun, Directed in vitro evolution and crystallographic analysis of a peptide binding scFv antibody with low picomolar affinity, J. Biol. Chem. 279 (2004) 18870-18877. https://doi.org/10.1074/jbc.M309169200.

[155] A. Mann, N. Friedrich, A. Krarup, J. Weber, E. Stiegeler, B. Dreier, P. Pugach, M. Robbiani, T. Riedel, K. Moehle, J.A. Robinson, P. Rusert, A. Plückthun and A. Trkola, Conformation-dependent recognition of HIV gp120 by designed ankyrin repeat proteins provides access to novel HIV entry inhibitors, J. Virol. 87 (2013) 5868-5881. https://doi.org/10.1128/JVI.00152-13.

[156] N. Stefan, P. Martin-Killias, S. Wyss-Stoeckle, A. Honegger, U. Zangemeister-Wittke and A. Plückthun, DARPins recognizing the tumor-associated antigen EpCAM selected by phage and ribosome display and engineered for multivalency, J. Mol. Biol. 413 (2011) 826-843. https://doi.org/10.1016/j.jmb.2011.09.016.

[157] M. Zaccolo, D.M. Williams, D.M. Brown and E. Gherardi, An approach to random mutagenesis of DNA using mixtures of triphosphate derivatives of nucleoside analogues, J. Mol. Biol. 255 (1996) 589-603. https://doi.org/10.1006/jmbi.1996.0049.

[158] M. Simon, U. Zangemeister-Wittke and A. Plückthun, Facile double-functionalization of designed ankyrin repeat proteins using click and thiol chemistries, Bioconjug. Chem. 23 (2012) 279-286. https://doi.org/10.1021/bc200591x.

[159] K. Friedrich, J.R. Hanauer, S. Prüfer, R.C. Münch, I. Volker, C. Filippis, C. Jost, K.M. Hanschmann, R. Cattaneo, K.W. Peng, A. Plückthun, C.J. Buchholz, K. Cichutek and M.D. Mühlebach, DARPin-targeting of measles virus: unique bispecificity, effective oncolysis, and enhanced safety, Mol. Ther. 21 (2013) 849-859. https://doi.org/10.1038/mt.2013.16.

[160] M. Simon, R. Frey, U. Zangemeister-Wittke and A. Plückthun, Orthogonal assembly of a designed ankyrin repeat protein-cytotoxin conjugate with a clickable serum albumin module for half-life extension, Bioconjug. Chem. 24 (2013) 1955-1966. https://doi.org/10.1021/bc4004102.

[161] A. Kohl, H.K. Binz, P. Forrer, M.T. Stumpp, A. Plückthun and M.G. Grütter, Designed to be stable: Crystal structure of a consensus ankyrin repeat protein, Proc. Natl. Acad. Sci. U. S. A. 100 (2003) 1700-1705. https://doi.org/10.1073/pnas.0337680100.

[162] F. Degorce, A. Card, S. Soh, E. Trinquet, G.P. Knapik and B. Xie, HTRF: A technology tailored for drug discovery - a review of theoretical aspects and recent applications, Curr. Chem. Genomics 3 (2009) 22-32. https://doi.org/10.2174/1875397300903010022.

[163] J.F. Jacobs, R.G. van der Molen, X. Bossuyt and J. Damoiseaux, Antigen excess in modern immunoassays: to anticipate on the unexpected, Autoimmun. Rev. 14 (2015) 160-167. https://doi.org/10.1016/j.autrev.2014.10.018.

[164] P. Heine, G. Witt, A. Gilardi, P. Gribbon, L. Kummer and A. Plückthun, High-throughput fluorescence polarization assay to identify ligands using purified G protein-coupled receptor, SLAS Discov. 24 (2019) 915-927. https://doi.org/10.1177/2472555219837344.

[165] A.S. Fahad, M.F. Gutierrez-Gonzalez, B. Madan and B.J. DeKosky, Antibody data analysis from diverse immune libraries, Cold Spring Harb. Protoc. 2025 (2025) doi:10.1101/pdb.prot108627. https://doi.org/10.1101/pdb.prot108627.

[166] D.K. Sell, B. Bakhshinejad, A.W. Sinkjaer, I.M. Dawoodi, M.N. Wiinholt, A.B. Sloth, C. Stavnsbjerg and A. Kjaer, Using NGS to uncover the corruption of a peptide phage display xelection, Curr. Issues Mol. Biol. 46 (2024) 10590-10605. https://doi.org/10.3390/cimb46090627.

[167] A.Q. Maranhao, H.M. Silva, W.M.C. da Silva, R.K.A. Franca, T.C. De Leo, M. Dias-Baruffi, R.T. Burtet and M.M. Brigido, Discovering selected antibodies from deep-sequenced phage-display antibody library using ATTILA, Bioinform. Biol. Insights 14 (2020) 1177932220915240. https://doi.org/10.1177/1177932220915240.

[168] R. Rouet, K.J.L. Jackson, D.B. Langley and D. Christ, Next-generation sequencing of antibody display repertoires, Front. Immunol. 9 (2018) 118. https://doi.org/10.3389/fimmu.2018.00118.

[169] F. Radom, E. Paci and A. Plückthun, Computational modeling of designed ankyrin repeat protein complexes with their targets, J. Mol. Biol. 431 (2019) 2852-2868. https://doi.org/10.1016/j.jmb.2019.05.005.

[170] J. Abramson, J. Adler, J. Dunger, R. Evans, T. Green, A. Pritzel, O. Ronneberger, L. Willmore, A.J. Ballard, J. Bambrick, S.W. Bodenstein, D.A. Evans, C.C. Hung, M. O'Neill, D. Reiman, K. Tunyasuvunakool, Z. Wu, A. Zemgulyte, E. Arvaniti, C. Beattie, O. Bertolli, A. Bridgland, A. Cherepanov, M. Congreve, A.I. Cowen-Rivers, A. Cowie, M. Figurnov, F.B. Fuchs, H. Gladman, R. Jain, Y.A. Khan, C.M.R. Low, K. Perlin, A. Potapenko, P. Savy, S. Singh, A. Stecula, A. Thillaisundaram, C. Tong, S. Yakneen, E.D. Zhong, M. Zielinski, A. Zidek, V. Bapst, P. Kohli, M. Jaderberg, D. Hassabis and J.M. Jumper, Accurate structure prediction of biomolecular interactions with AlphaFold 3, Nature 630 (2024) 493-500. https://doi.org/10.1038/s41586-024-07487-w.

[171] R. Evans, M. O'Neill, A. Pritzel, N. Antropova, A. Senior, T. Green, A. Žídek, R. Bates, S. Blackwell, J. Yim, O. Ronneberger, S. Bodenstein, M. Zielinski, A. Bridgland, A. Potapenko, A. Cowie, K. Tunyasuvunakool, R. Jain, E. Clancy, P. Kohli, J. Jumper and D. Hassabis, Protein complex prediction with AlphaFold-Multimer, bioRxiv (2022) 2021.2010.2004.463034. https://doi.org/10.1101/2021.10.04.463034.

[172] A. Harmalkar, S. Lyskov and J.J. Gray, Reliable protein-protein docking with AlphaFold, Rosetta, and replica-exchange, eLife 13 (2025) RP94029. https://doi.org/10.7554/eLife.94029.
[173] C.M. Berg, L. Liu, M. Coon, L.D. Strausbaugh, P. Gray, N.B. Vartak, M. Brown, D. Talbot and D.E. Berg, pBR322-derived multicopy plasmids harboring large inserts are often dimers in Escherichia coli K-12, Plasmid 21 (1989) 138-141. https://doi.org/10.1016/0147-619x(89)90057-7.
[174] T. Schmidt, K. Friehs, M. Schleef, C. Voss and E. Flaschel, Quantitative analysis of plasmid forms by agarose and capillary gel electrophoresis, Anal. Biochem. 274 (1999) 235-240. https://doi.org/10.1006/abio.1999.4291.
[175] E.A. Stephens, M.B. Ludwicki, B. Meksiriporn, M. Li, T. Ye, C. Monticello, K.J. Forsythe, L. Kummer, P. Zhou, A. Plückthun and M.P. DeLisa, Engineering single pan-specific ubiquibodies for targeted degradation of all forms of endogenous ERK protein kinase, ACS Synth. Biol. 10 (2021) 2396-2408. https://doi.org/10.1021/acssynbio.1c00357.
[176] M. Kawe, U. Horn and A. Plückthun, Facile promoter deletion in Escherichia coli in response to leaky expression of very robust and benign proteins from common expression vectors, Microb. Cell Fact. 8 (2009) 8. https://doi.org/10.1186/1475-2859-8-8.
[177] F.W. Studier, Stable expression clones and auto-induction for protein production in E. coli, Methods Mol. Biol. 1091 (2014) 17-32. https://doi.org/10.1007/978-1-62703-691-7_2.
[178] R.L. Rich and D.G. Myszka, Why you should be using more SPR biosensor technology, Drug Discov. Today Technol. 1 (2004) 301-308. https://doi.org/10.1016/j.ddtec.2004.09.009.
[179] J. Hartmann, R.C. Münch, R.T. Freiling, I.C. Schneider, B. Dreier, W. Samukange, J. Koch, M.A. Seeger, A. Plückthun and C.J. Buchholz, A library-based screening strategy for the identification of DARPins as ligands for receptor-targeted AAV and lentiviral vectors, Mol. Ther. Methods Clin. Dev. 10 (2018) 128-143. https://doi.org/10.1016/j.omtm.2018.07.001.
[180] D. Steiner, P. Forrer, M.T. Stumpp and A. Plückthun, Signal sequences directing cotranslational translocation expand the range of proteins amenable to phage display, Nat. Biotechnol. 24 (2006) 823-831. https://doi.org/10.1038/nbt1218.
[181] S.B. Ficarro, G. Adelmant, M.N. Tomar, Y. Zhang, V.J. Cheng and J.A. Marto, Magnetic bead processor for rapid evaluation and optimization of parameters for phosphopeptide enrichment, Anal. Chem. 81 (2009) 4566-4575. https://doi.org/10.1021/ac9004452.

Figures

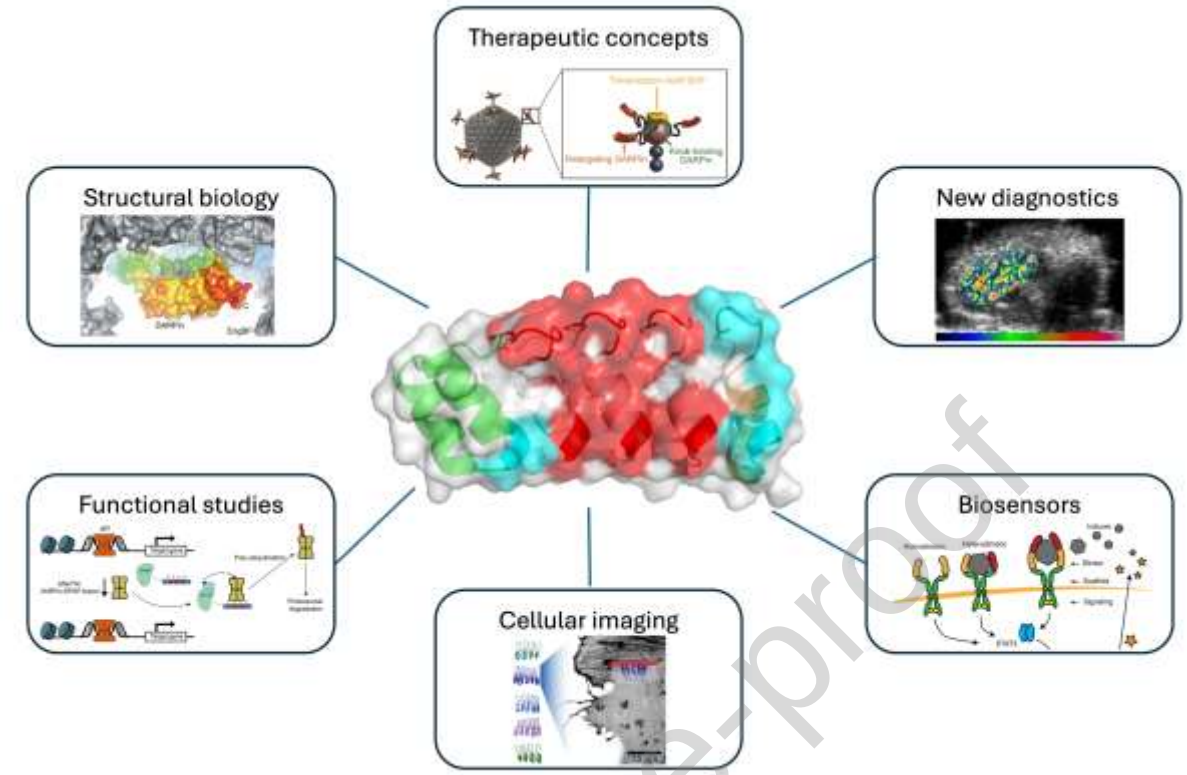

Figure 1: Pictorial overview of applications of DARPins generated by the HT Ribosome Display workflow described here. The symbolic pictures are taken from the cited references (clockwise starting from top) [179], [56], [54], [40], [37] and [51], We have grouped the targets according to the main motivation in the various projects, but in almost all cases the studies had more than one objective, and in many cases structures of the complexes were determined.

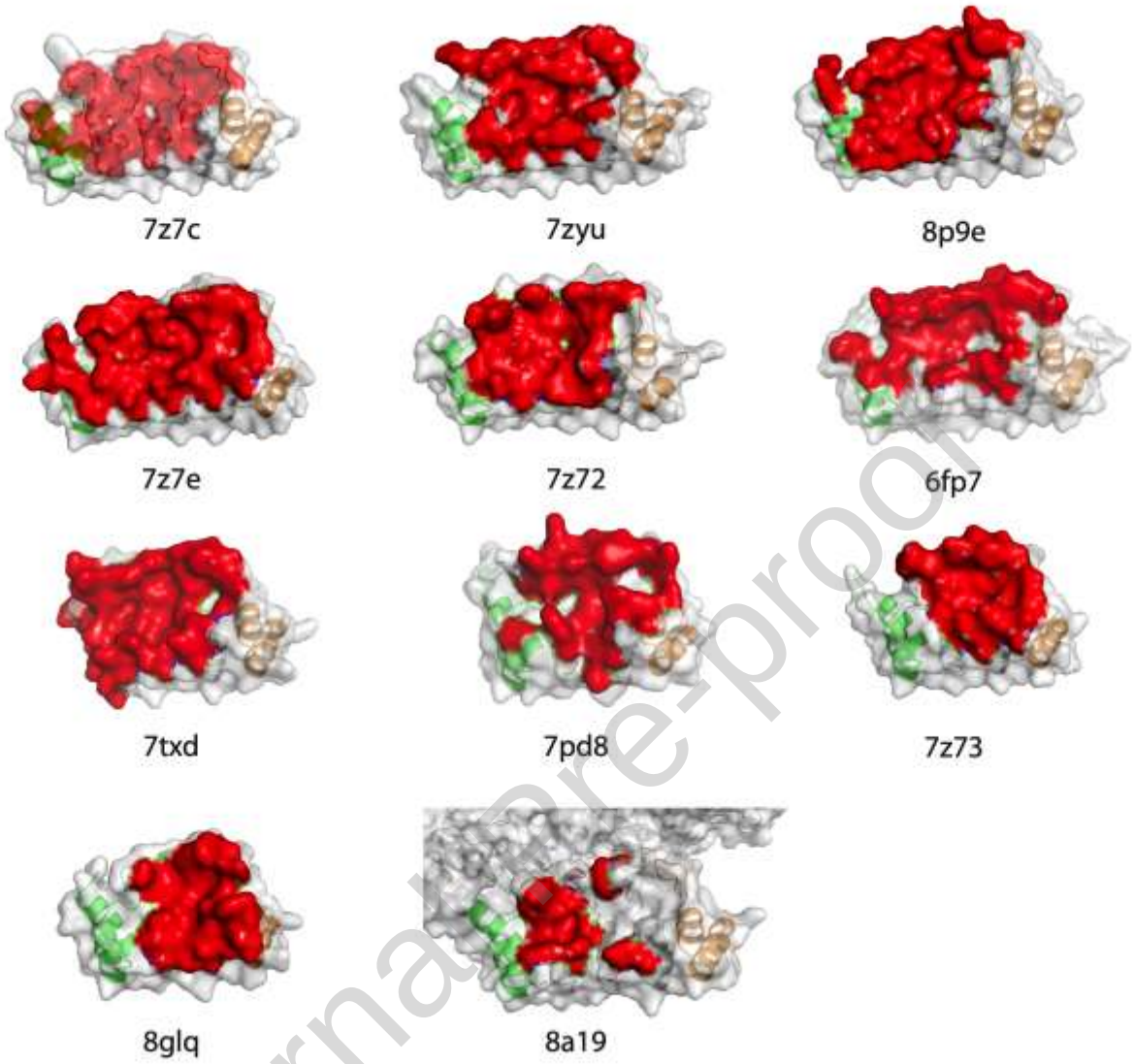

Figure 2: Structural alignment of the interaction interface of some of the DARPins selected by the HT-methods described in this review. They have been determined by x-ray crystallography or, in the case of 7pd8 and 7txd by cryo-EM and are labeled by their PDB IDs. The view is from the side of the target. The interaction surface is colored red, the DARPin is rendered as cartoon with the N-cap in green, the C-cap in orange and the internal repeats in white. The top two rows are N3C DARPins, the bottom two rows are N2C DARPins (where N2C and N3C denote having 2 or 3 internal repeats between the N-and C-capping repeats, respectively), while 8a19 is a special fusion protein of an N3C construct with EngBF, permitting stable crystal formation and host-guest crystallization (cf. **Figure 3 and 4**).

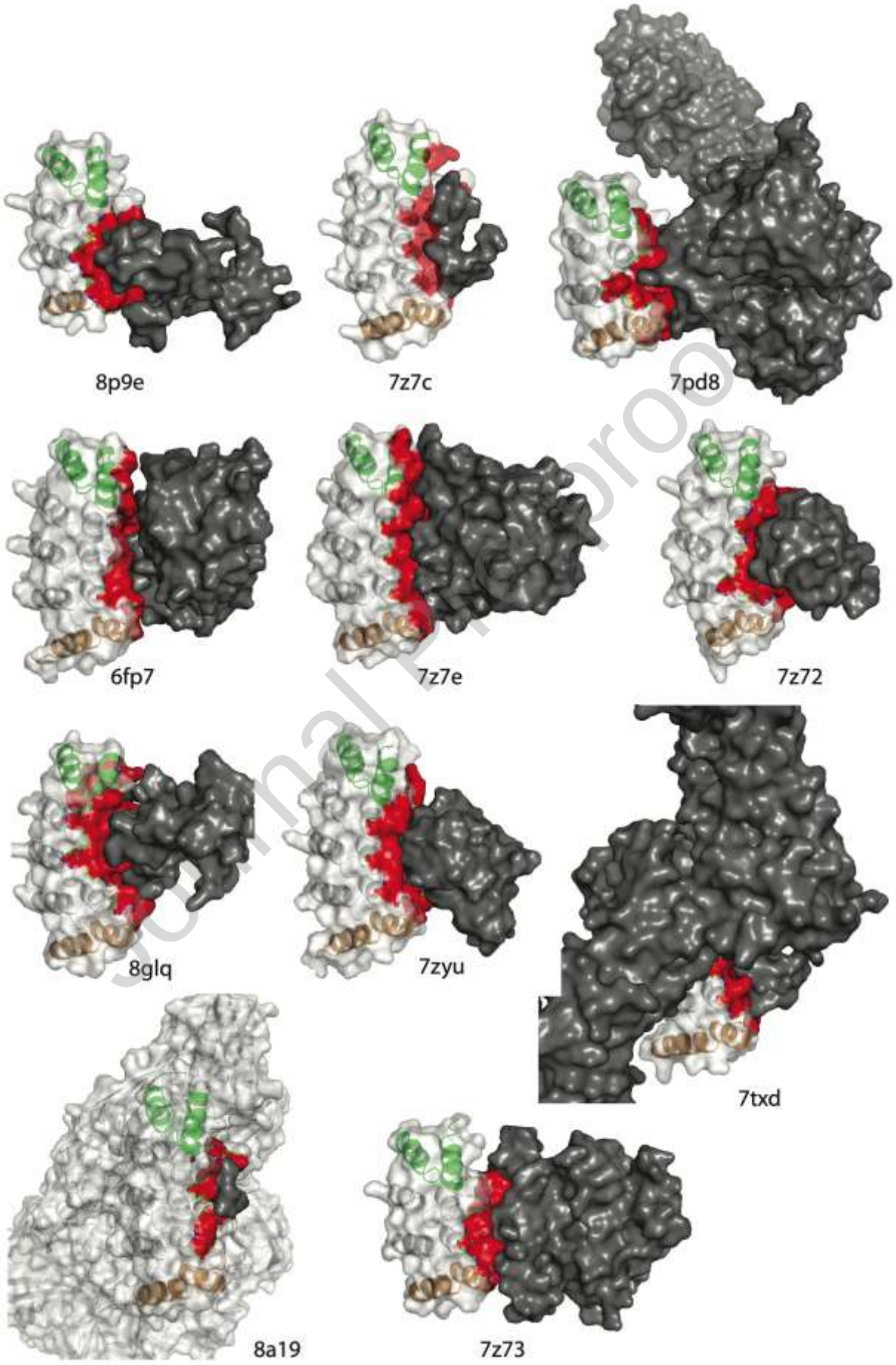

Figure 3: Structural alignment of the complexes of some of the DARPins selected by the HT-methods described in this review. The alignment is on the DARPin. They have been determined by x-ray crystallography or, in the case of 7pd8 and 7txd by cryo-EM and are labeled by their PDB IDs. The DARPin is on the left, with the interaction surface colored red, the DARPin rendered as cartoon with the N-cap in green, the C-cap in orange and the internal repeats in white. The target is rendered as a surface in dark grey. The structure 8a19 is a special fusion protein of an N3C construct with EngBF, permitting stable crystal formation and host-guest crystallization [51] (cf. **Figure 4**).

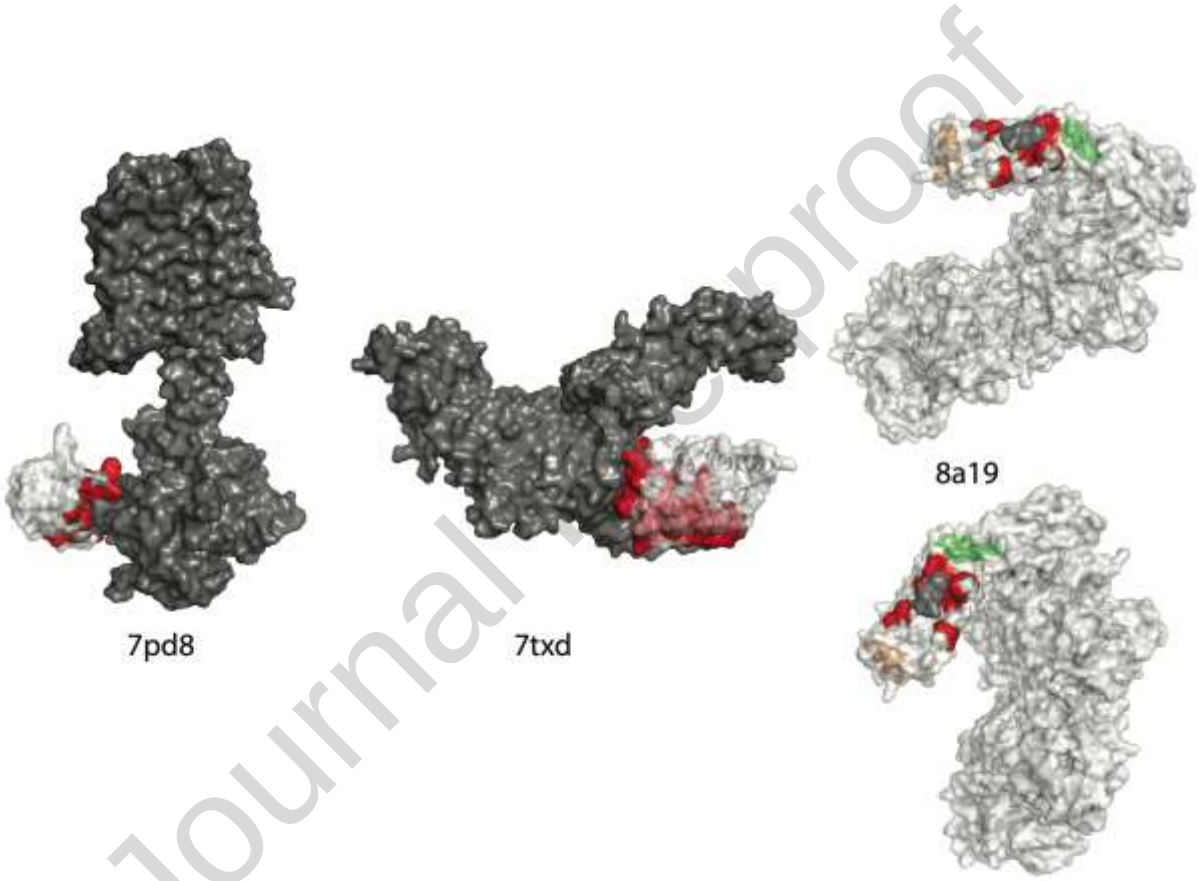

Figure 4: Some of the larger complexes structurally determined in a more optimal view. The structures of 7pd8 and 7txd have been determined by cryo-EM, while 8a19 has been determined by x-ray crystallography as a host-guest crystallization tool [51].

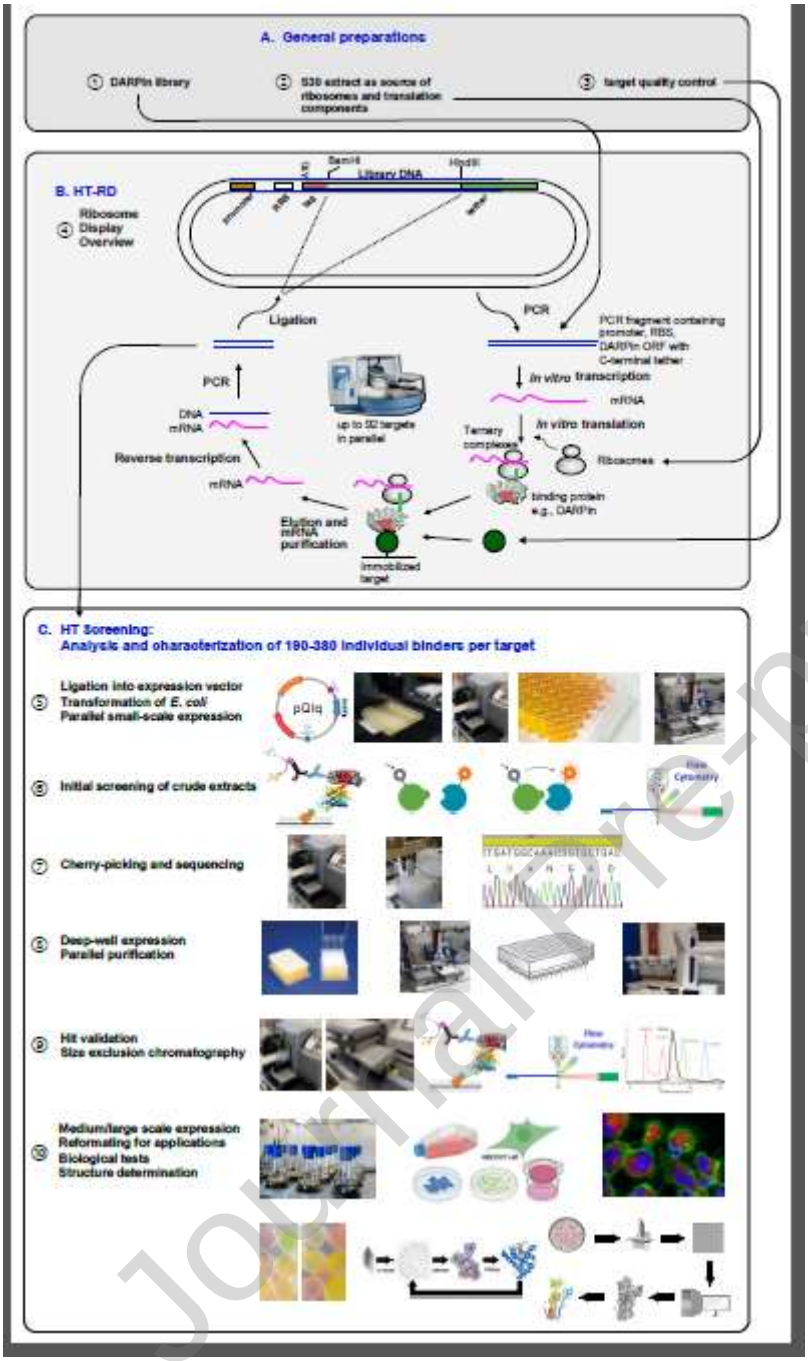

Figure 5: Overview of the High-Throughput Ribosome Display pipeline with subsequent screening of individual clones, as it has been applied for parallel DARPin selection. The circled numbers refer to the sections in which the various steps are described. **Sections 1-3** describe the general preparatory steps that are common to many selections, such as the library, the preparation of the S30 extract for in vitro translation and guidelines for target quality control (QC). **Section 4** is the actual Ribosome Display cycle that will be further subdivided in the respective Method sections and is also shown in more detail in **Figure 9**. The outcome is a pool of DNA encoding potential binders. **Sections 5 to 10** refer to the screening, i.e., the analysis and characterization of single clones after expression in *E. coli*.

Original N3C library

His tag	MRGSHHHHHHGS
N-cap	DLGKKLLEAARAGQDDEVRILMANGADVNA
1st int. rep.	XDXXGXTPLHLAAXXGHLEIVEVLLKHGADVNA
2nd int. rep.	XDXXGXTPLHLAAXXGHLEIVEVLLKNGADVNA
3rd int. rep.	XDXXGXTPLHLAAXXGHLEIVEVLLKYGADVNA
C-cap	QDKFGKTAFDISIDNGNEDLAEILQ**

Non-randomized caps: N3C nonrand

His tag	MRGSHHHHHHGS
N-cap	DLGKKLLEAARAGQDDEVRILMANGADVNA
1st int. rep.	XDXXGXTPLHLAAXXGHLEIVEVLLKHGADVNA
2nd int. rep.	XDXXGXTPLHLAAXXGHLEIVEVLLKNGADVNA
3rd int. rep.	XDXXGXTPLHLAAXXGHLEIVEVLLKYGADVNA
C-cap	QDKFGKTPFDLAIDNGNEDIAEVLQKAAKLN**

Randomized caps: N3C rand

His tag	MRGSHHHHHHGS
N-cap	DLGKKLLEAAXXGQDDEVRILMANGADVNA
1st int. rep.	XDXXGXTPLHLAAXXGHLEIVEVLLKHGADVNA
2nd int. rep.	XDXXGXTPLHLAAXXGHLEIVEVLLKNGADVNA
3rd int. rep.	XDXXGXTPLHLAAXXGHLEIVEVLLKYGADVNA
C-cap	QDXXGXTPFDLAAXXGNEDIAEVLQKAAKLN**

Figure 6: Sequences of the libraries typically used in HT RD selections. *Original N3C library* [97], with randomized residues shown with yellow highlight. These residues contain an equimolar mixture of all residues except Cys, Pro and Gly. The residues in red encode His, Asn or Tyr. *"N3C nonrand"*: Unrandomized caps, N3C library with stabilized C-cap "mut5" from [103]. *"N3C rand"*: Randomized caps, additional residues randomized shown with cyan highlight. In recent selections described in the Results section, the libraries *"N3C nonrand"* and *"N3C rand"* were mixed in a 1:1 ratio. The two stop codons (asterisks) at the end have been introduced into the expression vectors to prevent some readthrough due to the very strong expression observed [112, 180].

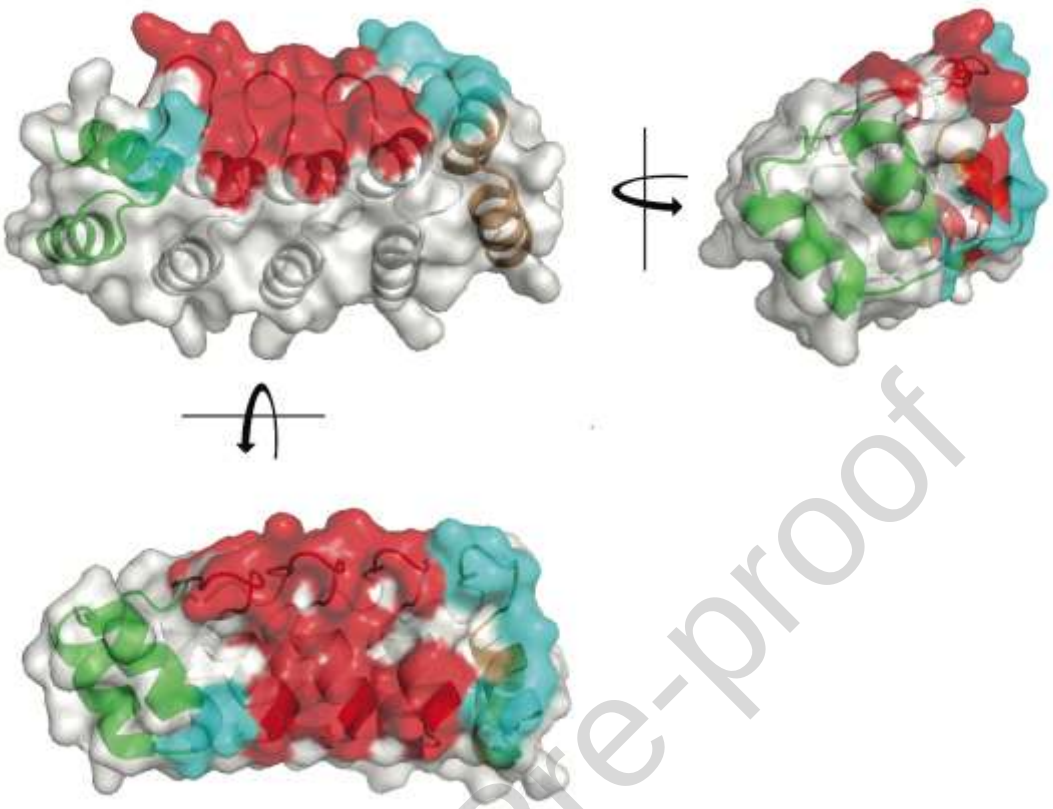

Figure 7: Depiction of the randomized region in the *NC3 rand* library. The randomized region within the internal repeats in both the *N3C nonrand* and *N3C rand* library are shown as a red surface. The additional randomized areas of the *N3C nonrand* library are in the caps and are shown as a cyan surface. The internal repeats are shown as a white cartoon, the N-cap as a green cartoon and the C-cap as an orange cartoon.

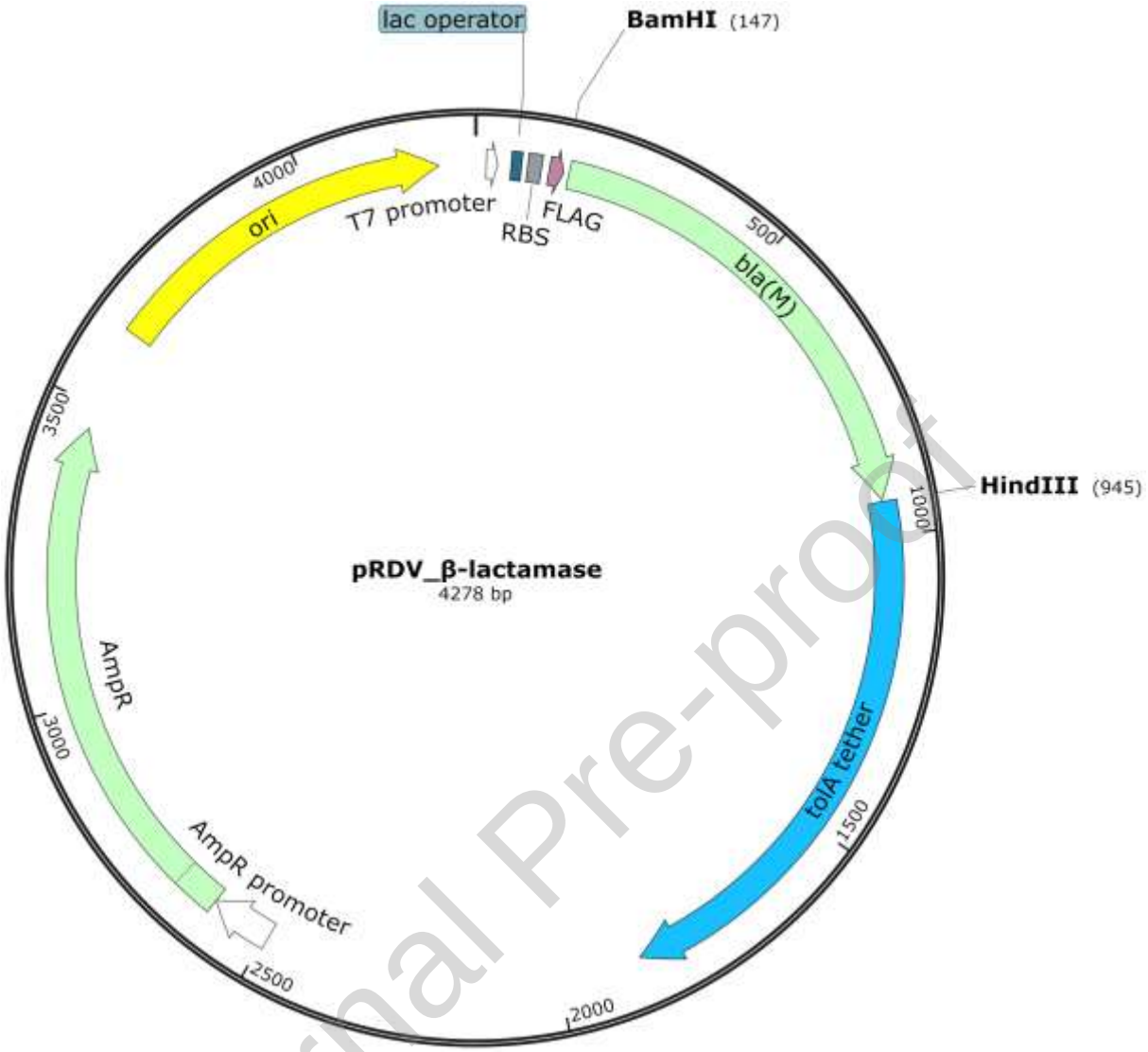

Figure 8: The pRDV_β-lactamase plasmid used in the β-lactamase assay to assess the activity of freshly prepared S30 extract and optimize the composition of PremixZ. The plasmid is adapted from the pRDV plasmid (GenBank accession code AY327136), but it contains two cysteine-to-alanine mutations in positions 51 and 97 of β-lactamase. The plasmid map was created using SnapGene software (https://www.snapgene.com/)

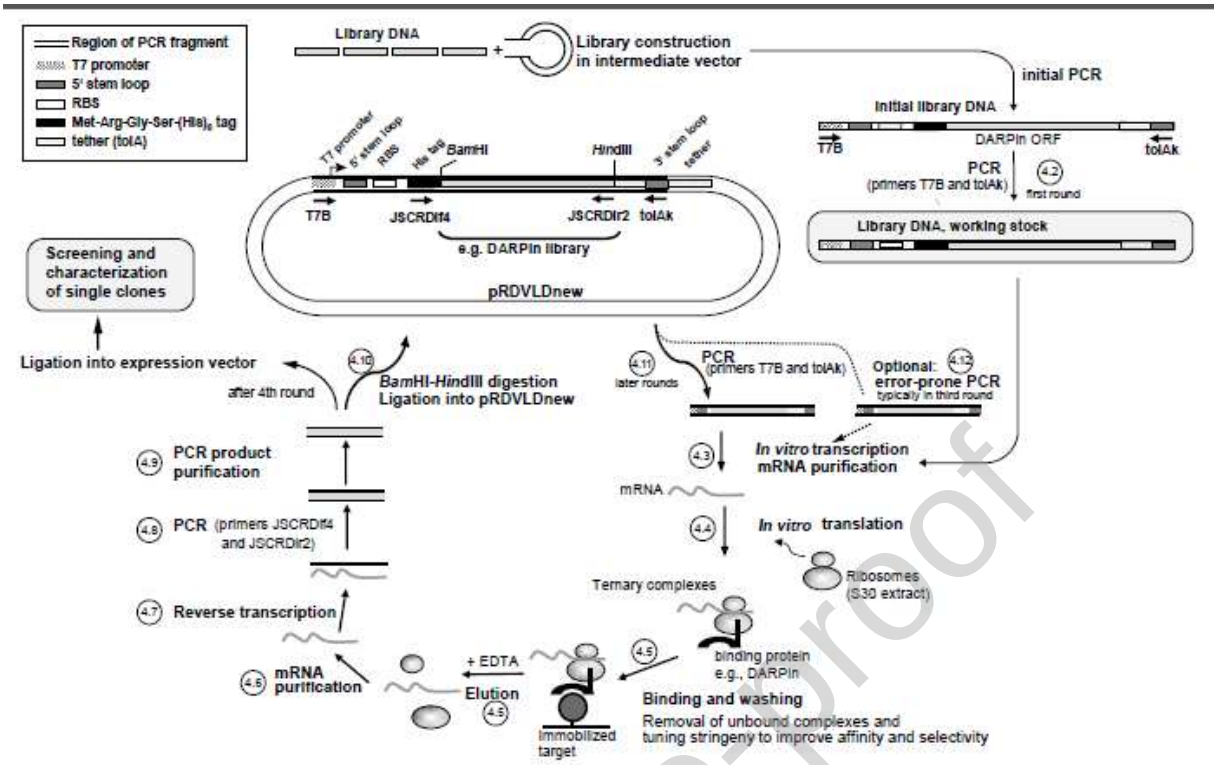

Figure 9: The circled numbers correspond to the numbered sections of the actual Ribosome Display workflow described in this section. This figure is a more detailed illustration of these steps than in **Figure 5**, but it simplifies the preparatory and screening steps. The figure is adapted from [32]. The cycle begins with the **working stock**, a PCR fragment encoding a library of the protein of interest, here the DARPins (the shaded elements are the same as within the vector drawing above). The ORF of interest (light grey) is fused to an additional protein region (the "spacer" or "tether", checkered white). This tether or spacer, used in our procedure as an unstructured region from the *E. coli* TolA protein, has the sole function of allowing the protein domain of interest (the DARPin) to emerge from the ribosomal tunnel. The **working stock** PCR fragment ranges from the T7 promoter (covering the rbs) to the middle of the tether using primers T7B and tolAk. Importantly, the PCR fragment does not encode a stop codon anywhere and can in principle be translated until the end. The process begins by transcribing the **working stock** from double-stranded DNA into mRNA (**Step 4.3**). It is subsequently translated by the ribosomes present in the added S30 extract (**Step 4.4**). This leads to ternary complexes consisting of ribosomes, mRNA and the DARPin. Each DARPin is encoded by its corresponding mRNA. Since there is no stop codon on the mRNA, the protein is not released from the ribosome. It is believed to be still covalently attached to the tRNA within the ribosome, with the tether in the tunnel, and the DARPin outside and already folded.

Selection is achieved by exposing the protein-ribosome-mRNA complexes in solution to the desired target immobilized on magnetic beads, followed by removal of unbound or non-specifically bound protein by stringent washing (**Step 4.5**).

The mRNA of the binders is recovered by destruction of the protein-ribosome-mRNA complex using EDTA (**Step 4.6**). Recovery of the genetic information of the binders is achieved by RT-PCR using the inner primers JSCRDif4 and JSCRDir2 (**Step 4.7**). This inner primer set is used to amplify the selected clones (**Step 4.8**), which often is not possible with the outer primer set due to incomplete synthesis or degradation of the mRNA. The PCR product is then purified (**Step 4.9**). For further selection rounds, the PCR product pool is subcloned into pRDVLDnew via the restriction endonucleases *Bam*HI and *Hin*dIII (**Step 4.10**). This in-vitro-ligated vector serves as template for a PCR with the outer primers T7B and tolAk (**Step 4.2** or **4.11,** respectively, as the conditions in the first round are slightly different). The primer T7B introduces the T7 promoter sequence and part of the mRNA-stabilizing 5' stem-loop and an N-terminal His tag, sequences that are part of the pRDVLDnew vector. The tolAk primer binds within the sequence of the *tolA* spacer (tether) region and also introduces a mRNA-stabilizing 3' stem-loop. The resulting PCR product then serves again as template for in vitro transcription, initiating the next round of selection. If further diversity is required, an error-prone PCR can be included at this step (**Step 4.12**), typically in round 3. At the end of the selection rounds (typically four rounds), the resulting PCR product pool is directly subcloned via the restriction endonucleases *Bam*HI and *Hin*dIII into an expression vector and *E. coli* are transformed in order to screen for individual binders and characterize them.

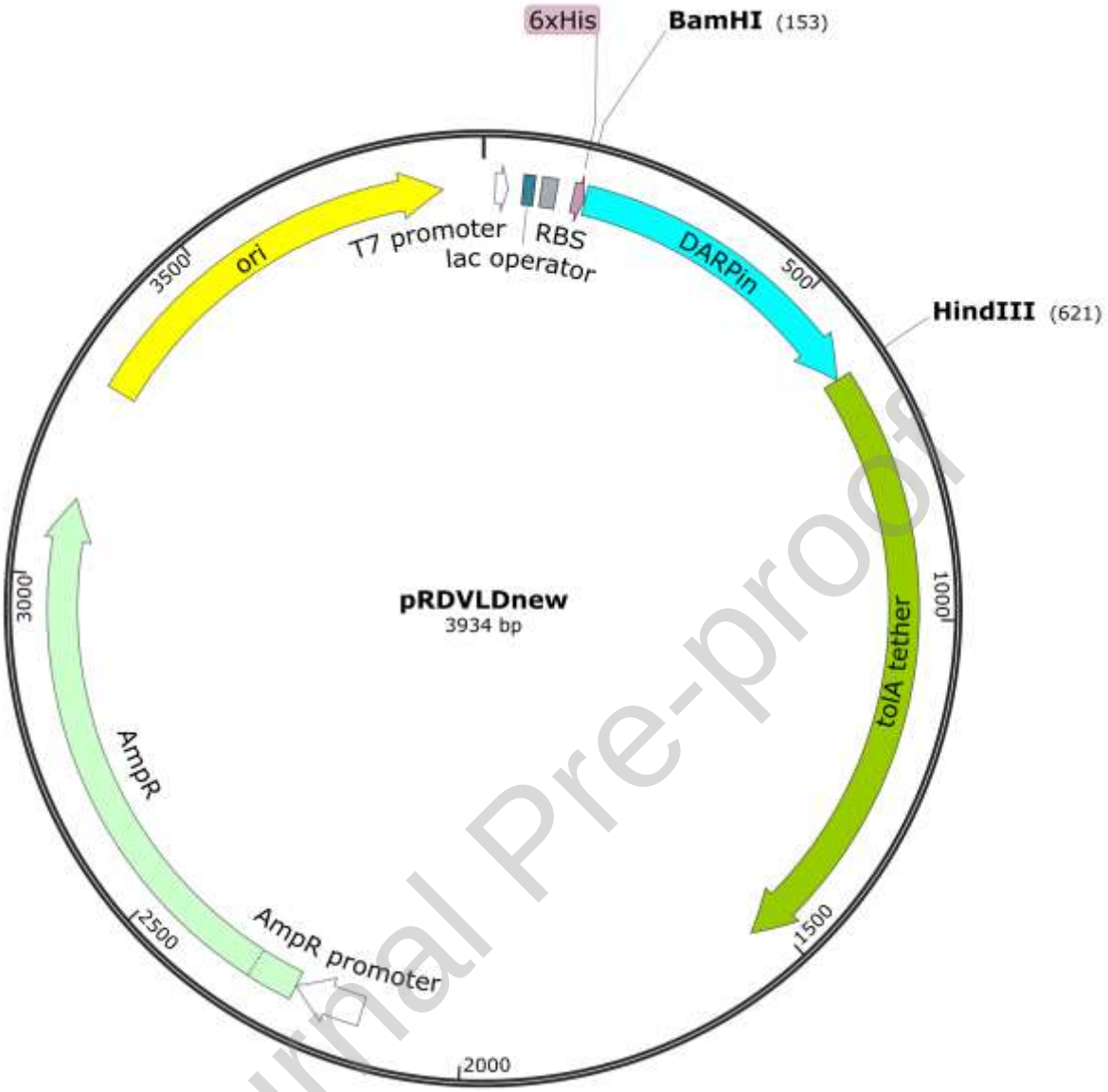

Figure 10: The pRDVLDnew plasmid used for HT RD (cf. Figure 10) drawn to scale. The DARPin library is preceded by a T7 promoter regulated by a lac operator, and a ribosome binding site (rbs). The plasmid map was created using SnapGene software (https://www.snapgene.com/)

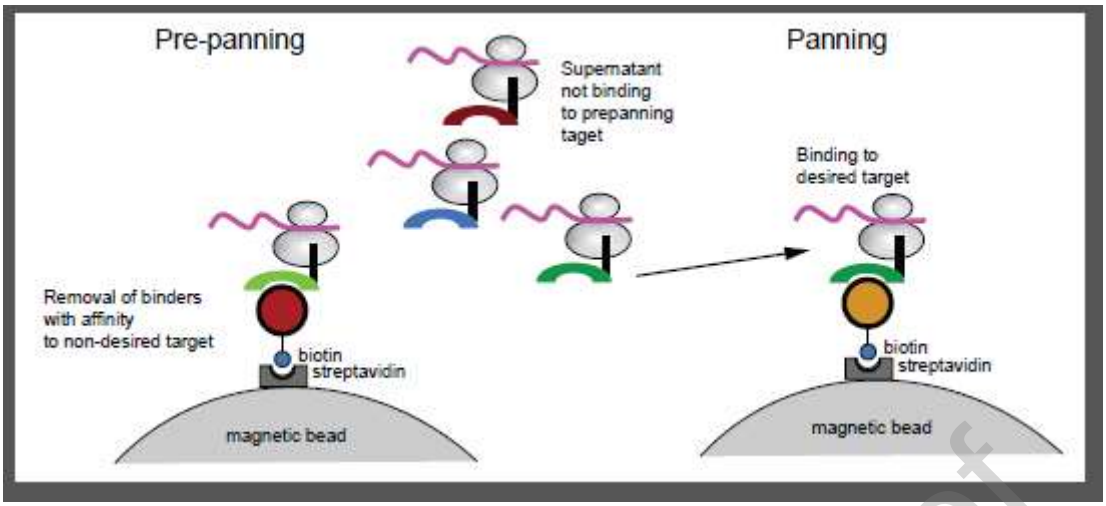

Figure 11. To counterselect against undesired target(s) (e.g. unwanted epitopes, isoforms, or fusion partners), a pre-panning step can be applied. Illustration of the pre-panning strategy using the unwanted biotinylated target(s) (dark red) in a first binding reaction. The supernatant containing the binders not engaged by the unwanted target are then exposed to the desired target (orange) immobilized on streptavidin-coated beads in a second binding reaction.

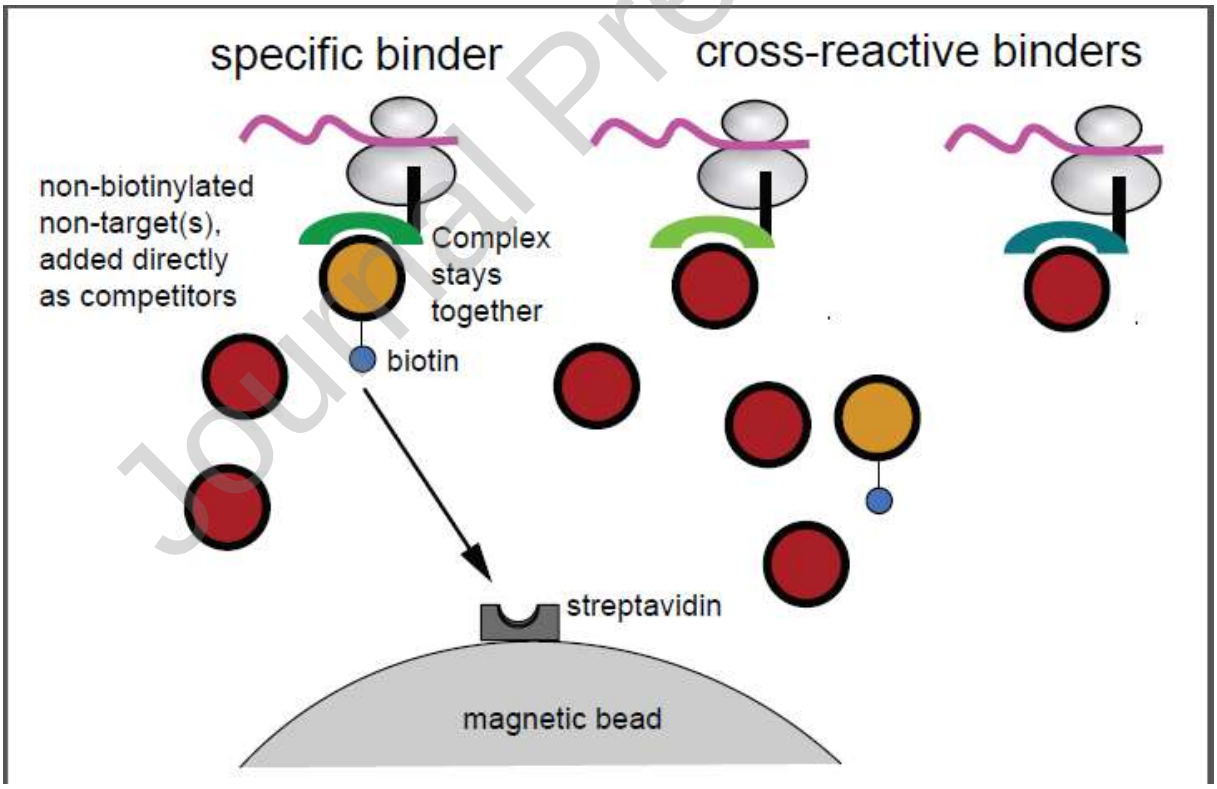

Figure 12. For competition, the undesired (non-)target(s) (dark red) are added as non-biotinylated competitors during the binding reaction in large excess, simultaneous with the biotinylated target (orange). The specific binders are enriched on the magnetic beads.

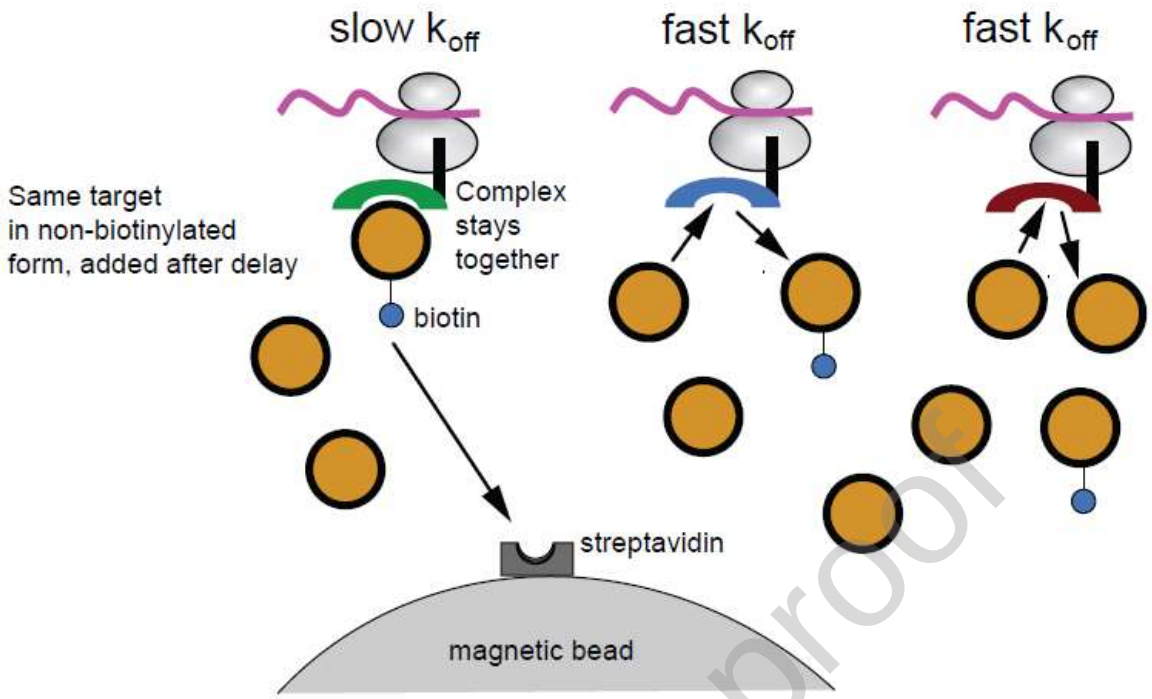

Figure 13. Illustration of off-rate selection increasing affinity. After a period of incubation (e.g. 1 h) with the biotinylated target, the same target is added in large excess in unbiotinylated form. Those ternary complexes with slow off-rates will retain the biotinylated target, those with faster off-rate will instead bind molecules from the large excess of non-biotinylated targets. When the population is exposed to the streptavidin-coated magnetic beads, only the ones with the retained target will bind, which are those with the slowest off-rate, and thus highest affinity.

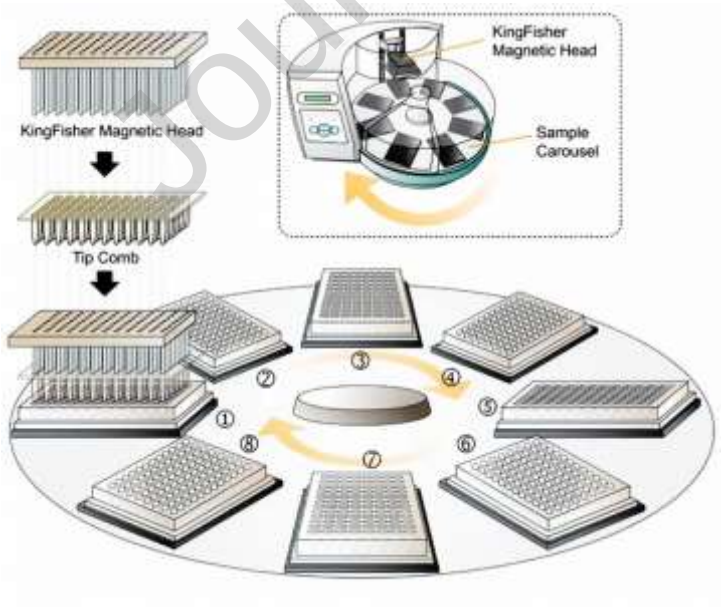

Figure 14: Illustration of the positioning of the plates on the KingFisher instrument. The content of the plates in the different rounds is summarized in **Table 2**. The figure is adapted from ref [181].

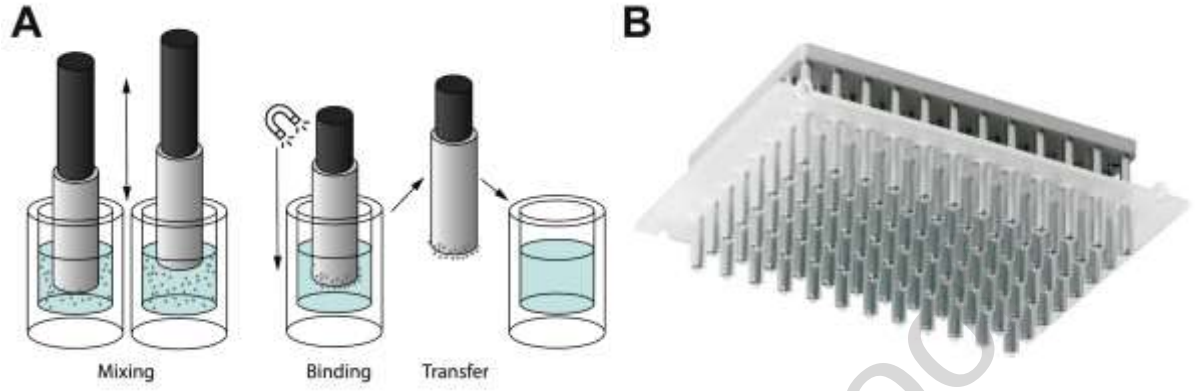

Figure 15: *Left*, operation of the KingFisher instrument explained on a single tip. With the magnet retracted, the up- and down movement mixes the magnetic beads. With the magnet entering the comb, the beads are binding, and can be transferred to the next well, e.g. for washing. For release, the magnet is retracted. *Right*, picture of the 96-well magnet and comb.

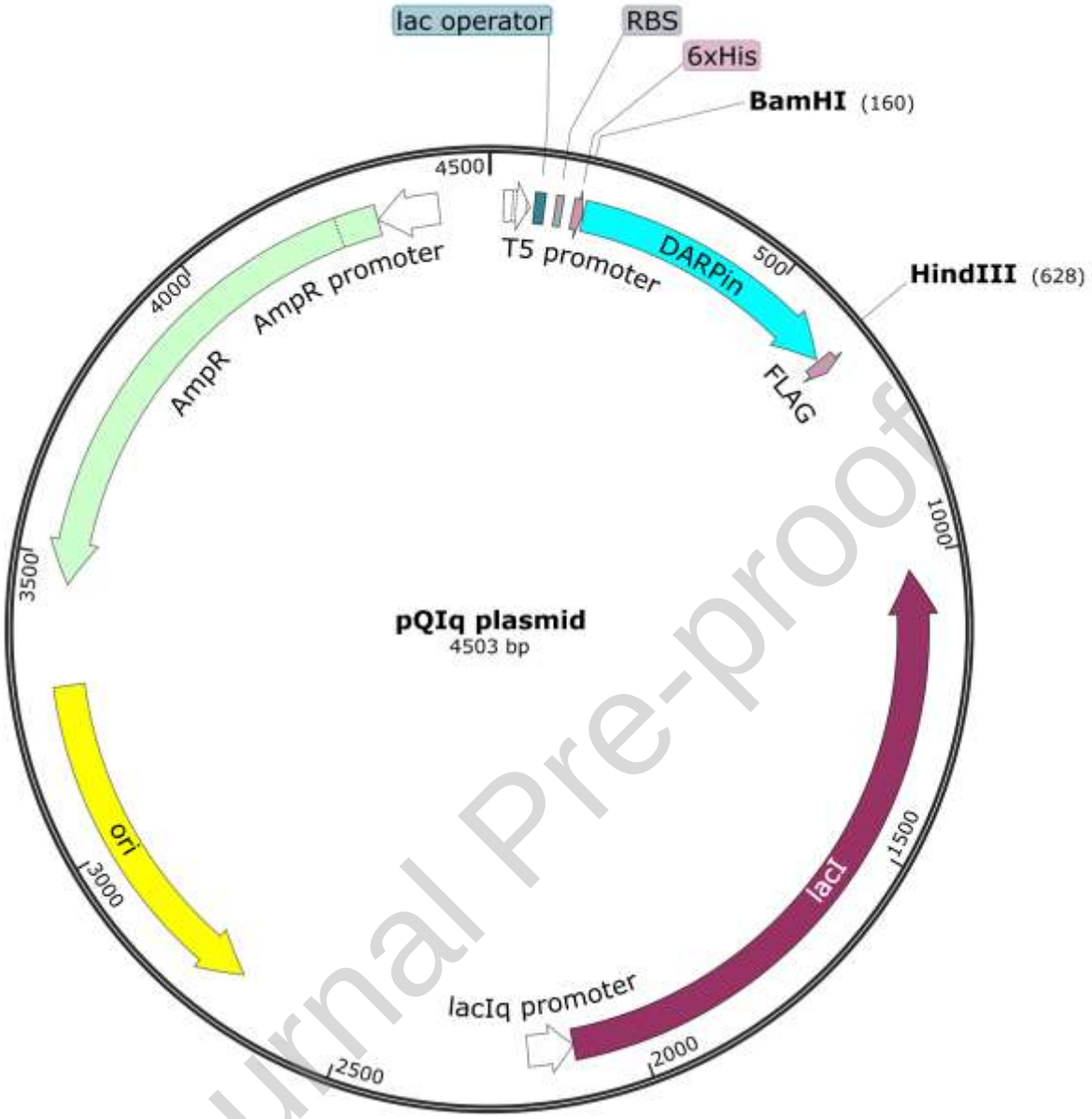

Figure 16: The pQIq plasmid is typically used for the expression of DARPins in *E. coli*. It is driving DARPin expression from the T5 promoter, which is controlled by a lac operator, and the lacI gene (under lacIq promoter control) on the same plasmid. Initially, most DARPins are produced with an N-terminal His tag ($MRGSH_6$), which is used for detection and purification, and a C-terminal FLAG tag for detection. Numerous derivatives of this vector for using different tags, fusions, chemical conjugation, etc. have been described in the respective publications. The plasmid map was created using SnapGene software (https://www.snapgene.com/)

Table 1: Parameters used in the different rounds of selection

	Round 1	Round 2	Round 3	Round 4
Target amount	250 pmol	125 pmol	5 pmol	50 pmol
Target binding	60 min	60 min	60 min	60 min
Panning	75 min	75 min	75 min	75 min
Washing	5 min	20 min	75 min	60 min
Elution	10 min	10 min	10 min	10 min

Table 2: Function of plates on the different positions in different rounds of RD

Position on Kingfisher Flex	Rd1	Rd2	Rd3	Rd4
1	Target plate	Target plate	Target plate	Target plate
2	pp-p-pd plate	pp-p-pd plate	pp-p-pd plate	pp-p-pd plate
3	Panning bead plate	Prepan bead / Wash4	Prepan bead / Wash4	Prepan bead / Wash4
4	Wash 2	Prepan / elution	Prepan / elution	Prepan / elution
5	Wash 3	Pan beads / Wash 5	Pan beads / Wash 5	Pan beads / Wash 5
6	Wash 4	Wash 1	Wash 1	Wash 1
7	Wash 5	Wash 2	Wash 2	Wash 2
8	Elution plate	Wash 3	Wash 3	Wash 3

Declaration of interests

☐ The authors declare that they have no known competing financial interests or personal relationships that could have appeared to influence the work reported in this paper.

☒ The authors declare the following financial interests/personal relationships which may be considered as potential competing interests:

Andreas Plueckthun reports a relationship with Molecular Partners AG that includes: equity or stocks. If there are other authors, they declare that they have no known competing financial

interests or personal relationships that could have appeared to influence the work reported in this paper.

Highlights

- High-throughput ribosome display enables parallel selection of DARPins to many targets
- Streamlined HT workflows support rapid screening and characterization of binders
- Methods are broadly applicable across diverse protein targets
- HT methods have generated DARPins suitable for research, diagnostics, and therapy
- Structural analysis reveals diverse DARPin–target interaction modes